AD-A168 685 PICOSECOND ELECTRONICS AND OPTOELECTRONICS HELD AT INCLINE VILLAGE NEVADA..(U) OPTICAL SOCIETY OF AMERICA WASHINGTON D C J W QUINN 04 FEB 86 AFOSR-TR-86-0157 1/2

UNCLASSIFIED AFOSR-85-0105 F/G 9/3 NL

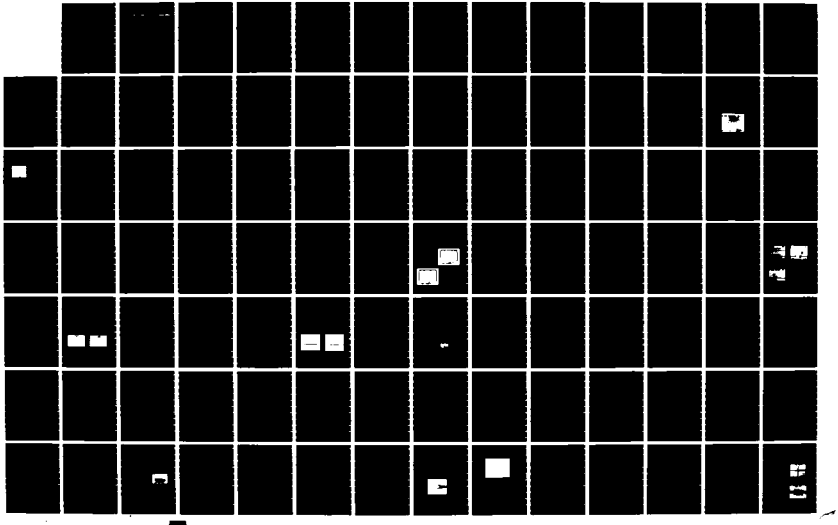

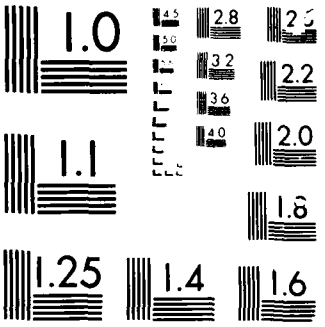

PICOSECOND ELECTRONICS AND OPTOELECTRONICS

Unclassified

SECURITY CLASSIFICATION OF THIS PAGE

REPORT DOCUMENTATION PAGE

1a REPORT SECURITY CLASSIFICATION Unclassified	1b RESTRICTIVE MARKINGS n/a
2a SECURITY CLASSIFICATION AUTHORITY n/a	3 DISTRIBUTION/AVAILABILITY OF REPORT Approved for public release - distribution unlimited
2b DECLASSIFICATION/DOWNGRADING SCHEDULE n/a	
4 PERFORMING ORGANIZATION REPORT NUMBER(S) ~~AFOSR-85-0165~~	5 MONITORING ORGANIZATION REPORT NUMBER(S) AFOSR-TR- 86-0157
6a NAME OF PERFORMING ORGANIZATION Optical Society of America 6b OFFICE SYMBOL (If applicable)	7a NAME OF MONITORING ORGANIZATION Air Force Office of Scientific Research
6c ADDRESS (City, State and ZIP Code) 1816 Jefferson Place, N.W. Washington, D.C. 20036	7b ADDRESS (City, State and ZIP Code) Building 410 Bolling, AFB, D.C. 20332
8a NAME OF FUNDING/SPONSORING ORGANIZATION 8b OFFICE SYMBOL (If applicable)	9 PROCUREMENT INSTRUMENT IDENTIFICATION NUMBER AFOSR-85-0165
8c ADDRESS (City, State and ZIP Code)	10 SOURCE OF FUNDING NOS PROGRAM ELEMENT NO: 61102F; PROJECT NO: 2305; TASK NO: B2; WORK UNIT NO:
11 TITLE (Include Security Classification) Topical Meeting on Picosecond Electronics and Optoelectronics	
12 PERSONAL AUTHOR(S) Quinn, Jarus W.	
13a TYPE OF REPORT Final	13b TIME COVERED FROM 85-02-01 TO 86-02-04
14 DATE OF REPORT (Yr, Mo, Day) 86-02-04	15 PAGE COUNT
16 SUPPLEMENTARY NOTATION	

17 COSATI CODES			18 SUBJECT TERMS (Continue on reverse if necessary and identify by block number)
FIELD	GROUP	SUB GR	

19 ABSTRACT (Continue on reverse if necessary and identify by block number)

The purpose of the meeting was to provide a forum for people working in the different areas of ultrafast electronics and optoelectronics and sharing a common interest in the understanding and improvements of the electronic properties of semiconductors and superconductors, the physics of ultrafast devices, their applications and methods of measurements.

20 DISTRIBUTION AVAILABILITY OF ABSTRACT UNCLASSIFIED/UNLIMITED ☒ SAME AS RPT ☐ DTIC USERS ☐	21 ABSTRACT SECURITY CLASSIFICATION Unclassified
22a NAME OF RESPONSIBLE INDIVIDUAL Jarus W. Quinn	22b TELEPHONE NUMBER (Include Area Code) 202/~~223~~-8130
	22c OFFICE SYMBOL

DD FORM 1473, 83 APR EDITION OF 1 JAN 73 IS OBSOLETE

Unclassified

SECURITY CLASSIFICATION OF THIS PAGE

TOPICAL MEETING ON PICOSECOND ELECTRONICS AND OPTOELECTRONICS

A digest of technical papers presented at the Topical Meeting on Picosecond Electronics and Optoelectronics, March 13–15, 1985, Incline Village, Nevada.

Cosponsored by:

Air Force Office of Scientific Research

Office of Naval Research

and

Optical Society of America

TUESDAY, MARCH 12, 1985

LOWER LOBBY

6:00 PM-9:00 PM REGISTRATION/REFRESHMENTS

WEDNESDAY, MARCH 13, 1985

SIERRA ROOM

8:00 AM-9:00 AM CONTINENTAL BREAKFAST

PROSPECTOR/RUBICON ROOM

8:45 AM-9:00 AM OPENING REMARKS

ULTRAFAST OPTICS AND ELECTRONICS I
Erich P. Ippen, *Massachusetts Institute of Technology, Presider*

9:00 AM WA1
Ultrafast Optical Electronics: from Femtoseconds to Terahertz, D. H. Auston, K. P. Cheung, J. A. Valdmanis, P. R. Smith, *AT&T Bell Laboratories.* The use of optical techniques for very high-speed electronic measurements of devices and materials is reviewed with emphasis on the properties of photoconducting and electrooptic materials. *(Invited Paper)*

9:30 AM WA2
Prospects of High-Speed Semiconductor Devices, H. Morkoc, *U. Illinois.* Issues facing the high speed FETs and heterojunction bipolar transistors are discussed. New high-performance heterojunction structures are evaluated and contrasted in the light of shrinking dimensions. As the switching speeds are increased (below 20 psec), the parasitics appear to play an important role making it difficult to harness the internal speed of devices. Concepts based on tunneling are also discussed. *(Invited Paper)*

10:00 AM WA3
The Role of Ultrashort Optical Pulses in High-Speed Electronics, C. V. Shank, *AT&T Bell Laboratories.* As the speed of electronic and optoelectronic devices moves into the picosecond time domain, optical techniques have the potential of an ever increasing importance in analyzing both device performance and the physical processes necessary for understanding high-speed operation. Optical methods have the advantage of ultrashort time resolution that exceeds all other high-speed measurement techniques. The state of ultrashort optical technology is reviewed and the areas where these methods promise to have an important impact are discussed. *(Invited Paper)*

SIERRA ROOM

10:30 AM-11:00 AM COFFEE BREAK

WEDNESDAY, MARCH 13, 1985—Continued

PROSPECTOR/RUBICON ROOM

ULTRAFAST OPTICS AND ELECTRONICS II
Paul T. Greiling, *Hughes Research Laboratories, Presider*

11:00 AM WB1
GaAs Integrated Circuit Technology for High Speed Analog and Digital Electronics, Gerard Nuzillat, *Thomson CSF, France. (Invited Paper)*

11:30 AM WB2
Hybrid Signal Processor for Wideband Radar, I. Yao, E. M. Hauser, C. A. Bouman, A. M. Chiang, *MIT Lincoln Laboratory.* A radar signal processor based on surface-acoustic-wave, optoelectronic, and charge-coupled-device technologies for processing radar signals with 200-MHz bandwidth is described.

11:45 AM WB3
Two-Dimensional E-Field Mapping with Subpicosecond Resolution, K. E. Meyer, G. A. Mourou, *U. Rochester.* A contactless technique to measure electrical signals with subpicosecond resolution and spatial resolution of 10 μm, using the electrooptic effect in reflection mode, is presented. This technique is well suited for the future characterization of very high-speed integrated circuits.

12:00 M WB4
Picosecond Electrooptic Sampling and Harmonic Mixing in GaAs, B. H. Kolner, K. J. Weingarten, D. M. Bloom, *Stanford U.* We describe an electrooptic sampling system, suitable for noncontact characterization of high-speed GaAs integrated circuits, and its implementation as a harmonic mixer.

12:15 PM WB5
Picosecond Pulse Generation in GaAlAs Lasers at a Repetition Rate of 18 GHz, K. Y. Lau, *Ortel Corporation,* A. Yariv, *CIT.* An ultrafast GaAlAs laser having a direct modulation bandwidth of 10 GHz is used to produce 12-psec optical pulses at 18 GHz by active mode locking in an external fiber cavity.

12:30 PM-1:30 PM BREAK

PROSPECTOR/RUBICON ROOM

HIGH-SPEED PHENOMENA IN SEMICONDUCTORS

D. [illegible] *École Polytechnique-ENSTA, Presider*

1:30 PM WC1
Picosecond Processes in Carrier Transport Theory, D. K. [illegible] Transport on the picosecond and subpicosecond timescale in semiconductors samples [illegible] comparable to the dominant [illegible] non-Markovian [illegible] equations for energy and [illegible] *Paper)*

2:00 PM WC2
Picosecond Time-Resolved Photoemission Study of the InP(110) Surface, [illegible] J. Stark, R. H. Storz, [illegible] *AT&T Bell Laboratories.* [illegible] time-resolved UV photoemission [illegible] dynamics in the picosecond [illegible] semiconductor [illegible]

2:15 PM WC3
Acoustic Phonon Generation in the Picosecond Dynamics of Dense Electron-Hole Plasmas in InGaAsP Films, [illegible] *Laboratories.* Picosecond [illegible] experiments are performed [illegible] behavior due to phonon [illegible] used to measure acoustic [illegible]

2:30 PM WC4
Carrier-Carrier Interaction and Picosecond Phenomena in Polar Semiconductors, [illegible] *Modena, Italy;* D. K. [illegible] of carrier-carrier interaction [illegible] studied using an [illegible] relaxation of monoenergetic [illegible] and the quasi-ballistic [illegible]

2:45 PM WC5
Subpicosecond Raman Spectroscopy of Electron-LO Phonon Dynamics in GaAs, [illegible] K. [illegible] J. C. Tsang, J. [illegible] *Center.* The rate at [illegible] and the dynamics [illegible] been directly [illegible] scattering

SIERRA ROOM

3:00 PM – 3:30 PM COFFEE BREAK

PROSPECTOR/RUBICON ROOM

PICOSECOND DIODE LASERS

Geoffrey L. Burdge, *Laboratory for Physical Sciences, Presider*

3:30 PM WD1
Semiconductor Lasers for Ultra High Speed Applications, Amnon Yariv, *CIT.* Semiconductor lasers have been modulated at rates exceeding 10 GHz and mode-locked to produce picosecond pulses. The talk reviews these developments as well as the fundamental laser material and structure parameters which are important for further progress. *(Invited Paper)*

4:00 PM WD2
Properties of GaAlAs/GaAs Quantum Well Heterostructures Grown by Metalorganic Chemical Vapor Deposition, R. D. Burnham, W. Streifer, T. L. Paoli, R. L. Thornton, D. L. Smith, *Xerox Palo Alto Research Center.* Major advances in growth of GaAlAs/GaAs quantum well heterostructures by metalorganic chemical vapor deposition have been achieved in recent years. This article reviews these advances and their impact on present and future devices. *(Invited Paper)*

4:30 PM WD3
InGaAsP 1.55-μm Mode-Locked Laser with a Single-Mode Fiber Output, G. Eisenstein, S. K. Korotky, U. Koren, R. M. Jopson, L. W. Stultz, J. J. Veselka, K. L. Hall, *AT&T Bell Laboratories.* We report the first 1.55-μm mode-locked laser in which pulses shorter than 5 psec and fiber coupled peak powers larger than 100 mW were obtained.

4:45 PM WD4
Fast Multiple Quantum Well Absorber for Mode Locking of Semiconductor Lasers, Y. Silberberg, P. W. Smith, *Bell Communications Research, inc.;* D. A. B. Miller, B. Tell, A. C. Gossard, W. Wiegmann, *AT&T Bell Laboratories.* Proton bombardment is shown to shorten the recovery time of GaAs/GaAlAs multiple quantum well saturable absorbers without substantially affecting the absorption or saturation characteristics.

SIERRA ROOM

5:30 PM-7:00 PM POSTER SESSION/REFRESHMENTS

WE1
Suppression of Timing and Energy Fluctuations in a Mode-Locked Semiconductor Laser by cw Injection, Finn Mengel, *Telecommunications Research Laboratory, Denmark;* Chinlon Lin, Niels Gade, *Technical U. Denmark, Denmark.* We demonstrate the suppression of pulse timing and energy fluctuations in an actively mode-locked 850 nm semiconductor laser by cw-injection locking. *(Poster Paper)*

WE2
Cross Modulation of Light in Si Semiconductor Materials in the Presence of Electric Fields, L. M. Walpita, W. S. C. Chang, H. H. Wieder, T. Van Eck, *UC-San Diego.* An optical AND gate is demonstrated by simultaneously transmitting two optical beams across the width of a Si semiconductor material. *(Poster Paper)*

WE3
Ultrafast Diffusion-Driven Detector, A. G. Kostenbauder, A. E. Siegman, *Stanford U.* We present the theory and experiments on a novel ultrafast photodetector whose dynamics are governed by diffusion and whose response time can be subpicosecond. *(Poster Paper)*

WE4
Optoelectronic Modulation of Millimeter Waves in a Silicon-on-Sapphire Waveguide, *Chi H. Lee, Aileen M. Yurek, M. G. Li, Eve Chauchard, R. P. Fischer, U. Maryland.* High-speed modulation of millimeter waves in a silicon-on-sapphire dielectric waveguide using an optoelectronic technique is described. Modulation bandwidth in excess of 1 GHz is achieved. *(Poster Paper)*

WE5
Kilovolt Sequential Waveform Generation by Picosecond Optoelectronic Switching in Silicon, C. S. Chang, M. J. Rhee, Chi H. Lee, *U. Maryland;* A. Rosen, H. Davis, *RCA Laboratories.* The generation of a sequential waveform by picosecond optoelectronic switching in silicon is described. By using a pulse bias, a square pulse of two and one half cycles has been obtained with a peak-to-peak voltage of 850 V. *(Poster Paper)*

WE6
Observation of Modulation Speed Enhancement and Phase Noise Reduction by Detuned Loading in a Coupled-Cavity Semiconductor Laser, Kerry Vahala, Joel Paslaski, Amnon Yariv, *Cal. Inst. Tech.;* Kam Lau, Nadav Bar Chaim, *Ortel Corporation.* Simultaneous direct modulation response enhancement and phase noise (linewidth) reduction are produced in a coupled-cavity semiconductor laser by a detuned loading mechanism. *(Poster Paper)*

WEDNESDAY, MARCH 13, 1985—Continued

WE7
Hot Electron Diffusion in Superlattices, J. Ho, R. O. Grondin, *Arizona State U.* Hot electron diffusion in superlattices is studied by Monte Carlo techniques. The diffusion coefficient falls as the field increases, with values comparable with those of the constitutent materials. *(Poster Paper)*

WE8
Time-Resolved Photoluminescence of GaAs/$Al_xGa_{1-x}As$ Quantum Well Structures Grown by Metalorganic Chemical Vapor Deposition, J. E. Fouquet, A. E. Siegman, *Stanford U.;* R. D. Burnham, T. L. Paoli, *Xerox Palo Alto Research Center.* Carrier dynamics in quantum well structures at temperatures from 16 K to 300 K and excitation photon energies above and below the barrier bandgap (300 K) are discussed. *(Poster Paper)*

WE9
Picosecond Pulse Production in the Semiconductor Laser with a 100-GHz Repetition Rate, J. McLean, D. Haas, J. Wurl, T. K. Gustafson, *UC-Berkeley.* The possibility of mode locking the semiconductor laser through nonlinear optical mixing is discussed. Numerical estimates show that 5-psec pulses with a repetition rate of 100 GHz should be possible. *(Poster Paper)*

WE10
Measurements of the Temperature and Intensity Dependence of Transient Photoconductivity in InP:Fe. D. R. Kania, R. J. Bartlett, R. B. Hammond, D. L. Smith, *Los Alamos National Laboratory.* We report our measurements of the temperature and intensity dependence of transient photoconductivity in InP:Fe photoconductors from 77 K to 300 K. *(Poster Paper)*

WE11
Pulse Waveform Standards for Electrooptics, Robert A. Lawton, *National Bureau of Standards.* The development of reference waveform generators for transfer of pulse measurement accuracy from the National Bureau of Standards to the electrooptic sampler is described. *(Poster Paper)*

WE12
Monte Carlo Investigation of Hot Carriers Generated by Subpicosecond Laser Pulses in Schottky Barrier Diodes, M. A. Osman, U. Ravaioli, D. K. Ferry, *Arizona State U.* The dynamics of carriers photoexcited by subpicosecond laser pulses in silicon submicron Schottky diodes is investigated by ensemble Monte Carlo simulation. Tunneling, band nonparabolicity, and hole transport are considered. *(Poster Paper)*

WEDNESDAY, MARCH 13, 1985—Continued

WE13
Hertzian Dipole Measurements with InP and InGaAs Photoconductors, P. M. Downey, J. R. Karin, *AT&T Bell Laboratories.* Experiments are described using ion-bombarded III-V photoconductors as radiating sources and receivers of picosecond electromagnetic pulses in two different configurations: back-to-back and face-to-face. *(Poster Paper)*

WE14
Modeling of Picosecond Pulse Propagation in Silicon Integrated Circuits, K. W. Goossen, *Princeton U.*; R. B. Hammond, *Los Alamos National Laboratory.* We performed time domain analyses of pulse propagation on silicon substrates. Geometric dispersion, conductor linewidth, conductor resistance, conductor skin effect, and substrate capacitance effects are included. *(Poster Paper)*

WE15
Femtosecond Nonlinearities of Standard Transparent Optical Glasses, J. Etchepare, I. Thomazeau, G. Grillon, A. Migus, A. Antonetti, *Ecole Polytechnique-ENSTA, France.* Nonlinearities with a temporal behavior on the femtosecond time scale are measured on transparent optical glasses. Their values are related to the content and nature of the modifier silica networks ions. *(Poster Paper)*

THURSDAY, MARCH 14, 1985

SIERRA ROOM

7:30 AM–8:00 AM CONTINENTAL BREAKFAST

PROSPECTOR/RUBICON ROOM

OPTOELECTRONICS
John Whinnery, *UC-Berkeley, Presider*

8:00 AM ThA1
Picosecond Integrated Optics, R. C. Alferness, S. K. Korotky, G. Eisenstein, R. S. Tucker, *AT&T Bell Laboratories.* We review the principles, current status, and potential applications of high-speed Ti:$LiNbO_3$ optical waveguide switch/modulators as well as the use of such devices as intracavity elements for semiconductor laser mode-locking. *(Invited Paper)*

8:30 AM ThA2
Study of Exciton and Carrier Dynamics and Demonstration of 1-psec Optical NOR Gate Operation of a GaAs/AlGaAs Device, N. Peyghambarian, H. M. Gibbs, J. L. Jewell, *U. Arizona;* A. Migus, A. Antonetti, *Ecole Polytechnique-ENSTA, France;* D. Hulin, A. Mysyrowicz, *Ecole Normale Superieure, France.* Dynamics of exciton screening by either free carriers or excitons in a GaAs/AlGaAs superlattice is investigated. The speed of a GaAs/AlGaAs optical logic gate is time resolved.

8:45 AM ThA3
22-GHz Bandwidth InGaAs/InP PIN Photodiodes, J. E. Bowers, C. A. Burrus, R. S. Tucker, *AT&T Bell Laboratories.* We describe the fabrication and characterization of an improved back-illuminated PIN mesa photodiode composed of InGaAs absorbing layers on an InP substrate. The measured 3-dB bandwidth is 22 GHz.

9:00 AM ThA4
Ultrafast Traveling-Wave Light Modulators with Reduced Velocity Mismatch, Masayuki Izutsu, Hiroshi Haga, Tadasi Sueta, *Osaka U., Japan.* The velocity mismatch between light and modulating waves was reduced to build efficient ultrafast traveling-wave light modulators. Fabrication and modulation experiments are also reported.

THURSDAY, MARCH 14, 1985—Continued

9:15 AM ThA5
Direct dc to rf Conversion by Impulse Excitation of a Resonant Cavity. Ming G. Li, Chi H. Lee, A. Caroglanian, E. A. Sovero, C. Mazzeno, C. Y. She, P. Polak-Dingles, *Laboratory for Physical Sciences*; A. Rosen, *RCA Laboratories*. Conversion of dc energy to rf pulses has been demonstrated with an impulse excitation of a coaxial resonant structure using a picosecond optoelectronic switching technique. A single excitation pulse is capable of generating more than a hundred rf pulses with an energy conversion efficiency better than 50.

9:30 AM ThA6
Subpicosecond Response Times from Ion-Bombarded InP. P. M. Downey, *AT&T Bell Laboratories*. The limiting speed of response of Fe-doped InP photoconductors irradiated with high doses of He ions has been empirically investigated. Fe-implanted samples with response times as short as [illegible] have been fabricated.

SIERRA ROOM

9:45 AM–10:15 AM COFFEE BREAK

PROSPECTOR/RUBICON ROOM

CRYOELECTRONICS
[illegible]

10:15 AM ThB1
***High-Speed Analog Signal* Processing with Superconductive Circuits.** R. [illegible] C. [illegible], *MIT Lincoln Laboratory*. Analog superconductive circuits are described which process high-speed signals. Experimental results on a 4-bit Fabry-Perot [illegible] and a 2-GHz bandwidth, 5-bit flash [illegible] are presented. *Invited Paper*.

10:45 AM ThB2
Picosecond Sampling with Josephson Junctions. Peter [illegible], *IBM Zurich Research Laboratory, Switzerland*. A new type of high-speed sampling gate using Josephson tunnel junctions is described. Results of operation of sampling systems and [illegible] are presented. *Invited Paper*.

11:15 AM ThB3
Transmission Line Designs with a Measured Step Response of 3 psec/cm. Charles J. Kocak, Sudeep M. Bandyopadhyay, Kevin F. Meyer, George A. Mourou, *U. Rochester*. [illegible] attributed to the generation and propagation of [illegible] are presented. Pulses [illegible] with [illegible] GHz. [illegible] are [illegible].

THURSDAY, MARCH 14, 1985—Continued

11:30 AM ThB4
Development of a 1-psec Cryosampler Using Electrooptic Techniques. D. R. Dykaar, T. Y. Hsiang, G. A. Mourou, *U. Rochester*. A cryogenic, electrooptic sampler is being developed. An initial version with room temperature signal source and cryogenic sampling crystal had a rise-time of 16.4 psec.

11:45 AM ThB5
Picosecond Josephson Logic Gates for Digital LSIs. Junichi Sone, Jaw-Shen Tsai, Hiroyuki Abe, *NEC Corporation, Japan*. This paper discusses the realized and projected picosecond logic speed of resistor-coupled Josephson logic for LSI applications.

12:00 M BREAK

PROSPECTOR/RUBICON ROOM

ULTRAFAST ELECTRONICS
James Harris, *Stanford U., Presider*

7:30 PM ThC1
Picosecond Switching Speed GaAs Circuits. Raymond [illegible], *Rockwell International*. *Invited Paper*.

8:00 PM ThC2
Characterization of TEGFETs and MESFETs Using the Electrooptic Sampling Technique. K. E. Meyer, D. R. Dykaar, G. A. Mourou, *U. Rochester*. Electrooptic sampling has been used to measure the transient response of GaAs TEGFETs and MESFETs. Rise times of 16 psec and 25 psec, respectively, have been obtained.

8:15 PM ThC3
Picosecond Optoelectronic Diagnostics of Field Effect Transistors. Donald E. Cooper, *Aerospace Corporation*. Impulse response measurements of a submicron FET are presented. Scattering matrix parameters for the millimeter wave region can be calculated from these data.

8:30 PM ThC4
High Electron Mobility Transistors—Their Evolution and Ultimate Speed. H. Sakaki, *Tokyo U., Japan*. Physical mechanisms governing the ultimate speed of high-purity heterojunction FETs (HEMTs) are discussed together with experimental experiments on hot-electron modulation [illegible]. *Invited Paper*.

SIERRA ROOM

9:00 PM–9:15 PM COFFEE BREAK

THURSDAY, MARCH 14, 1985—Continued

9:15 PM ThC5
Time-Domain Measurements for Silicon Integrated Circuit Testing Using Photoconductors. W. R. Eisenstadt, *U. Florida*; R. B. Hammond, *Los Alamos National Laboratory*; D. Bowman, R. W. Dutton, *Stanford U.* We developed ion-beam-damaged photoconductors on silicon integrated circuits for picosecond pulsing and sampling. Measurement bandwidths of 20 GHz were achieved and studies of interconnections are reported.

9:30 PM ThC6
Molecular Beam Epitaxy Materials for High-Speed Digital Heterostructure Devices. D. L. Miller, *Rockwell International Corporation.* Molecular beam epitaxy material has been used in nearly all the recent advanced high-speed heterostructure digital devices. The reasons for this and the prospects for eventual circuit production are discussed. *(Invited Paper)*

FRIDAY, MARCH 15, 1985

SIERRA ROOM

7:30 AM–8:00 AM CONTINENTAL BREAKFAST

PROSPECTOR/RUBICON ROOM

QUANTUM STRUCTURES
Claude Weisbuch, *Thomson CSF, Presider*

8:00 AM FA1
New High-Speed Optoelectronic and Electron Superlattice and Heterojunction Devices. Federico Capasso, *AT&T Bell Laboratories.* Very recent advances in heterojunction and superlattice structures for high-speed optoelectronic and electron device applications are discussed. *(Invited Paper)*

8:30 AM FA2
Semiconductor Quantum Wells: Physics and Applications. D. S. Chemla, *AT&T Bell Laboratories.* We review the physical properties and the applications to high-speed optoelectronics of the room temperature excitonic resonances observed at 0.85 μm in GaAs and at 1.6 μm in GaInAs quantum wells. *(Invited Paper)*

9:00 AM FA3
Electric Field-Induced Decrease of Exciton Lifetimes in GaAs Quantum Wells. J. A. Kash, E. E. Mendez, *IBM T. J. Watson Research Center*; H. Morkoc, *U. Illinois at Urbana Champaign.* Electric fields perpendicular to the quantum-well plane quench exciton photoluminescence lifetimes. Fowler-Nordheim tunneling is responsible. Exciton screening reduces the quenching at high pump intensities.

9:15 AM FA4
Reduction of Electron-Phonon Scattering Rates by Total Spatial Quantization. M. A. Reed, R. T. Bate, W. M. Duncan, W. R. Frensley, H. D. Shih, *Texas Instruments, Inc.* Photoluminescence of laterally patterned multiple quantum-well structures exhibits spectra best explained by a reduced electron-phonon scattering rate produced by total spatial quantization.

9:30 AM FA5
High-Speed Phenomena in Resonant Tunneling. T. C. L. G. Sollner, C. A. Correa, P. E. Tannenwald, W. D. Goodhue, *MIT Lincoln Laboratory*; H. Q. Le, *MIT Francis Bitter National Magnet Laboratory.* Resonant tunneling processes, shown to respond in times < 100 fsec, have revealed new photoconductive effects with time constants from femtoseconds to days.

SIERRA ROOM

9:45 AM–10:15 AM COFFEE BREAK

PROSPECTOR/RUBICON ROOM

ELECTRONICS AND OPTOELECTRONICS

Gerald Witt, *Air Force Office of Scientific Research, Presider*

10:15 AM FB1
Heterojunction Bipolar Transistor Technology for High-Speed Integrated Circuits, Peter M. Asbeck, *Rockwell International Corporation.* Heterojunction bipolar transistors combine the high transconductance of bipolar structures with the high-speed characteristic of III-V devices. Cutoff frequency, f_t, up to 40 GHz and frequency divider operation up to 8.5 GHz have been achieved to date. *(Invited Paper)*

10:45 AM FB2
Permeable Base Transistor, R. A. Murphy, *MIT Lincoln Laboratory.* The development and current status of the permeable base transistor (PBT) is reviewed. Both silicon and GaAs PBTs have been fabricated and have demonstrated high frequency performance. *(Invited Paper)*

11:15 AM FB3
Picosecond Photoconductivity in Polycrystalline CdTe Films Prepared by UV-Enhanced OMCVD, A. M. Johnson, D. W. Kisker, W. M. Simpson, *AT&T Bell Laboratories.* Photodetectors with oscilloscope-limited response times of 35 psec and carrier mobilities of 11 cm^2/V sec are reported in thin polycrystalline CdTe films with a 200-Å grain size.

11:30 AM FB4
High-Speed Internal Photoemission Detectors Enhanced by Grating Coupling to Surface Plasma Waves, S. R. J. Brueck, V. Diadiuk, T. Jones, W. Lenth, *MIT Lincoln Laboratory.* The response of AlInP internal photoemission detectors to [illegible] wavelength enhanced (~30 ×) by grating coupling to surface plasma [illegible]

11:45 AM FB5
Submicron Gap Photoconductive Switching in Silicon, G. [illegible] *Department of* [illegible] With sub[illegible] have [illegible]

WEDNESDAY, MARCH 13, 1985

WA, ULTRAFAST OPTICS AND ELECTRONICS I

Erich P. Ippen, Massachusetts Institute of Technology, *Presider*

ULTRAFAST OPTICAL ELECTRONICS: FROM FEMTOSECONDS TO TERAHERTZ

D. H. Auston, K. P. Cheung,
J. A. Valdmanis and P. R. Smith

AT&T Bell Laboratories
600 Mountain Avenue, Room 1C-424
Murray Hill, New Jersey 07974
(201) 582-3188

SUMMARY

The use of optical techniques to generate and measure fast electronic events is a challenging approach to high speed electronics with many important potential advantages relative to conventional electronic instrumentation.

This talk will review this subject with specific emphasis on the optimum choice of materials and transmission structures for picosecond and sub-picosecond applications. Two classes of materials have emerged as valuable building blocks for picosecond optical electronic measurement systems. These are photoconductors and electro-optic materials. Each have found important applications for both generating and detecting very high speed electrical transients. This talk will present a unified description of the properties of photoconducting and electro-optic materials stressing their similarities and differences. Specific properties will be illustrated by experiments in which they have been applied to the measurement of high speed devices and materials.

As a guide to the optimum choice of materials, we have examined three criteria: speed, sensitivity, and versatility. By representing their response as a

generalized nonlinear polarization current it is possible to make quantitative comparisons of the sensitivity and speed of photoconducting and electro-optic materials. When used as sources of electrical transients, we find that photoconductors[1] are generally preferred for their greater sensitivity when the response time is greater than one picosecond. For sub-picosecond applications, however, the inverse electro-optic effect has proven to be more effective[2]. When used as sampling gates, similar conclusions apply, with photoconductors having greater sensitivity for the slower apertures ($\geq 3ps$) and electro-optic materials being preferred for faster measurements[3]. For sub-picosecond measurements we have also found it more expedient to treat these electromagnetic transients as free waves rather than to confine them to transmission lines or other guiding structures. For this reason, sub-picosecond electrical techniques are at present best suited for measurements of materials rather than devices. As an illustration, we will describe recent experiments in which sub-picosecond electrical transients have been used to develop a novel approach to far-infrared spectroscopy in the spectral range from 0.1 to 3 THz. These results illustrate how the ultimate speed limit of electro-optic materials is determined by lattice vibrational resonances.

[1] for a recent review see: D. H. Auston, "Picosecond Photoconductors: Physical Properties and Applications," in *Picosecond Optoelectronic Devices*, ed. C. H. Lee, Academic Press (1984).

[2] D. H. Auston, K. P. Cheung, J. A. Valdmanis, and D. A. Kleinman, Phys. Rev. Lett., *53*, 1555 (1984).

[3] J. A. Valdmanis, G. A. Mourou, and C. W. Gabel, IEEE J. Quant. Electr., *QE-19*, 664 (1983).

Prospects of High Speed Semiconductor Devices

by

H. Morkoç

1101 W. Springfield Avenue

University of Illinois

Urbana, IL 61801

Abstract

Search for high speed has over the years focussed on miniturization and high performance semiconducting materials. Scaling up in speed reaches a saturation as the dimensions are reduced because parasitics do not entirely scale down, particularly in integrated circuits. As a result new material systems e.g. GaAs/AlGaAs modulation doped structures with enhanced transport properties have received a great deal of attention. The propagation delay in Si devices (both bipolars and FETs) appear to have reached a limit at around 30 ps while the bulk GaAs FETs operate around 15 ps. Near 10 ps and sub 10 ps switching speeds however belong to modulation doped GaAs/AlGaAs FETs with $\sim 0.5\mu$ gate lengths. Heterojunction GaAs/AlGaAs bipolar transistors are expected to reach the 10ps range in a few years being at $\sim$ 30 ps at the present time. It is becoming very clear that the progress below 10 ps in a given material system is very difficult because of parasitics. The 10 ps switchings time obtained for an individual device (gate) can not be maintained in a real circuit where a chain of gates are used, again because of parasitics and interconnects causing delays. If it were not for the delays associated with the input capacitance changing time and other parasitic effects, intrinsic delays of about 1 ps should be possible. In field effect transistors for example, it is fair to assume that a great portion of the delay arises from input and output charging times. Obviously lowering the lateral dimension (e.g. gate) alone does not necessarily lead to expected improvements in speed. This is even more so in heterojunction bipolar transistors where the input charging time accounts for about 75% of the total delay time: therefore, reducing the base width further, well under 0.1μm may not necessarily lead to faster operation.

Devices relying on current transport, without scattering which limits the intrinsic speed process to about 1 ps, through tunneling may be of value. However the devices demonstrated so far are of the two terminal type and do not have wide ranging applications that could be possible with three terminal devices having gain and isolation between the input and output. Even though tunneling process is extremely fast ($\sim 10^{-16}$s), the parasitics slow the device considerably.

In this pressentation an overview of FETs, HBT's will be given along with preliminary results on heterojunction tunnel devises. The limiting factors which are traceable to the parasitics will be alluded to. Finally speculations for some future directions will be addressed.

The Role of Ultrashort Optical Pulses in High Speed-Electronics

C. V. Shank
AT&T Bell Laboratories
Crawfords Corner Road, Room 4E-436
Holmdel, NJ 07733

As the speed of electronic and optoelectronic devices moves into the picosecond time domain, optical techniques have the potential of an ever increasing importance in analyzing both device performance and the physical processes necessary for understanding high-speed operation. Optical methods have the advantage of ultrashort time resolution that exceeds all other high-speed measurement techniques. The state of ultrashort optical techniques is reviewed and the areas where these methods are likely to have an important impact are discussed.

WEDNESDAY, MARCH 13, 1985

WB, ULTRAFAST OPTICS AND ELECTRONICS II

Paul T. Greiling, Hughes Research Laboratories,
Presider

GaAs Integrated Circuit Technology for High Speed Analog and Digital Electronics

Gerard Nuzillat and Rene Castagne
Thomson-CSF
Laboratoire Central de Recherche
Domaine de Corbeville
BP 10
91401 Orsay Cedex
France

Some guidelines for the understanding of the technological trends in GaAs IC'S can be found in a brief recall of device and interconnect behaviour under scaling down. Let us recall that the device control parameters are the internal charge Q_t carried by the electrons in the control region end the electron transit time t_t. When N identical devices are driven by N interconnexions, each having the same length and carrying the same charge Q_L, the switching time is aproximately given by $t_{pd} = N\ t_t\ (1+Q_L/Q_t)$. The local speed will then be improved by reducing both t_t and Q_L/Q_t. As long as Q_L/Q_t is greater than one, a common practice is to increase the control region width (say the gate width). Here Q_t is increased, t_t remaining constant. But it is well known that the counterpart of such an improvement for the current driving capabilities of the device is poundered by an increase in power dissipation. Cn the other hand, reducing the length of the control region (for instance the gate length of a MESFET) leads to a reduction of t_t and Q_t. So that in order to be effective. one should also scale down the interconnects width of the same quantity.

This is no longer the case when Q_L/Q_t becomes smaller than one. The intrinsic qualities of the device, and more precisely the transport properties of the material prevail. Both high electron concentrations and high electron velocities are then required. Electron mobility is reduced by Coulomb Scattering on ionized impurities. In MISFET and Heterojunction TEGFET, it is possible to confine high densities

of electrons along an interfacial barrier in a very low doped material. Conditions are then met for high density - high velocity electron flow. However MISFET is not a high mobility transistor because of scattering by interfacial charges in the insulating material. In a TEGFET structure on the other hand, high electron mobilities are achieved through the high quality of the epitaxial interface : This is a technological improvement.

Access resistance and especially the gate-source resistance R_{sg} can drastically reduce the charge Q_t which is effectively controlled. Given an input voltage swing ΔV_i, only a fractionnal part $V_{eff} = \Delta V_i/(1+k)$ is, in effect, applied to the control region. k is the serie feed back factor, proportional to the access resistance R_{sg}. The Q_I, Q_t ratio is then multipled by (1+k) which can easily reach a value of ten. It is then obvious that access resistances have to be reduced.

During the past few years, a very important effort has been done in GaAs technology along must of these guidelines. A general geometrical scaling down have been reached through the generalization of direct EB writting. In the same time, a decisive improvement was obtained in the semi insulating material quality by industrial use of CZ crystals giving very low residual doping level and high temperature stability during annealing. These crystals allow direct channel and access zone ion implantation, reducing both the source access resistance and the dispersion in gate threshold voltage V_T. A self aligned refractory gate technology then brings GaAs MESFET to a nearly perfect technological quality and open the way to DCFL gates.

Various examples will be presented illustrating the fact that GaAs IC'S technology has reached an industrial maturity in Digital Circuitry. So that it is now in a position to tackle high speed analog or analog to digital problems.

GaAs devices and circuits have then demonstrated their capability to switch or drive interconnexion pattern more fastly than their silicon homologues. A further reduction in line width should the theoretically bring circuits performance towards device intrinsic speed limits and then set the GaAs superiority over Silicon. But switching times of the order of 10 ps would then be in the range of propagation times along the distributed microstrip interconnexion lines.

In digital circuits, an impedance desadaptation is necessary for saving power dissipation so that multiple reflexions and inter connexion cross-talk noise could become the source of the ultimate limitations. Circuit architecture could then be the field of the next generation researchs with the usual seek for circuits density giving place to new principles, pushing design of new C A D tools forwards.

Hybrid Signal Processor For Wideband Radar*

I. Yao, E. M. Hauser, C. A. Bouman, and A. M. Chiang

Lincoln Laboratory, Massachusetts Institute of Technology,
P. O. Box 73
Lexington, Massachusetts 02173-0073

The signal processing task for radar systems with large instantaneous bandwidth and wide range coverage stresses the throughput rate of conventional digital processors. In this paper, a hybrid analog signal processor for wideband pulse-Doppler radar[1] is described. It offers the potential of a compact, high-throughput processor. In the processor, three types of analog signal processing devices are incorporated. They are: (1) a surface-acoustic-wave (SAW) convolver[2] to perform programmable pulse compression for radar signals with 200-MHz instantaneous bandwidth in order to provide target range information with 0.75-m resolution, (2) optoelectronic sample-and-hold (S/H) circuits[3] to perform the range gating function and the buffering of the sampled data into the Doppler processor, and (3) charge-coupled-device (CCD) matrix-matrix-product (MMP) chips[4] to perform Doppler Fourier analysis in order to provide target velocity information.

The processor is flexible enough to accommodate a wide variety of radar waveforms. This work features nonrepeating pseudonoise-encoded burst waveforms with large instantaneous bandwidth. These have the desirable traits of high range resolution, no range ambiguity, and robust performance against interference. Fig.1 shows the block diagram of the analog portion of the proposed signal processor. It consists of 1 SAW convolver and its reference waveform generator, 8 optoelectronic S/H circuits, and 80 CCD-MMP chips. The radar return signal with 200-MHz bandwidth is first pulse-compressed in the SAW convolver. Because of the frequency doubling effect in the convolver, the bandwidth of the compressed pulse is 400 MHz. After video demodulation, this signal is split into in-phase (I) and quadrature (Q) channels. There are 4 optoelectronic S/H circuits operating at a 100-MHz sampling rate in each channel to provide a 800-MHz effective sampling rate. Since the CCD-MMP chips are to be clocked at 10 MHz, the output of each S/H feeds 10 CCD-MMP chips. However, because the input stage of each CCD-MMP chip is capable of capturing data samples in 10 ns, no additional S/H circuits are necessary. As the signal reaches the CCD-MMP chips, Doppler processing is performed on each range bin based on the discrete Fourier transform (DFT) algorithm to derive the target velocity information. Finally, the Doppler processor output would feed the digital post processor for further processing. With this architecture, 1280 range bins by 32 Doppler bins would be provided in real time and it is therefore useful for search, track, and imaging applications.

Under development is a demonstration system using a thinned version of this processor for proving the validity of the concept. In this thinned processor, one SAW convolver, two optoelectronic S/H circuits, and two CCD-MMP chips will be incorporated. All analog elements exist, and currently this demonstration system has been integrated up through the optoelectronic S/H circuits. Fig.2 shows a range-Doppler plot of two targets, one stationary and one moving, produced by the demonstration system where the Doppler processing was simulated in a host computer. The CCD-MMP chip is currently being optimized for higher dynamic range; it will then be integrated into the system. Functionally, it performs a 32-point DFT for 32 different range bins at the same time and thus provides 32 Doppler bins for each of 32 range bins. At its peak load, each CCD-MMP chip executes 640 million real arithmetic operations per second.

* This work was supported by the Department of the Army and the Defense Advanced Research Projects Agency.

Because of their throughput-rate, power, and size advantages, these analog signal processing devices are well suited for computationally intensive, real-time signal-processing applications. This processor, when fully populated, will be capable of handling 1280 range bins and 32 Doppler bins per range bin for radar signals with bandwidths more than an order of magnitude beyond those handled with conventional digital technologies.

References

1. I. Yao, E. M. Hauser, C. A. Bouman, G. T. Flynn, and J. H. Cafarella, "Wideband Radar Signal Processor Based On SAW Convolvers," 1984 IEEE Ultrasonics Symposium, Dallas, Texas, 1984. Proceedings to be published.
2. I. Yao and S. A. Reible, "Wide Bandwidth Acoustoelectric Convolvers," *1979 Ultrasonics Symposium Proceedings*. New York: IEEE, 1979, pp. 701-705.
3. C. H. Cox,III, V. Diadiuk, I. Yao, F. J. Leonberger, and R. C. Williamson, "InP Optoelectronic Switches and Their High-Speed Signal Processing Applications," Proc. Soc. Photo-Opt. Inst. Eng., vol. 439, pp. 164-168, 1983.
4. A. M. Chiang, R. W. Mountain, D. J. Silversmith, and B. J. Felton, "CCD Matrix-Matrix-Product Parallel Processor," *Tech. Dig. 84 Int. Solid-State Circ. Conf.* San Fransisco: IEEE, 1984, pp. 110-111.

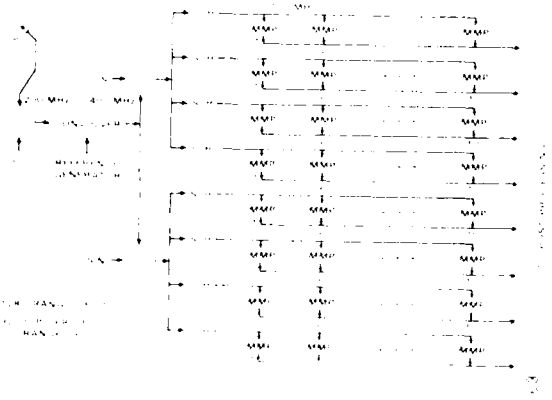

Fig.1 Analog portion of the hybrid signal processor architecture.

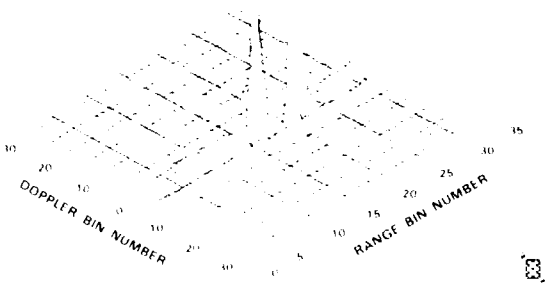

Fig.2 Range-Doppler plot for two targets, one moving and one stationary, generated by the demonstration system using a computer-simulated Doppler processor.

Two-dimensional E-Field Mapping with Subpicosecond Resolution

K.E. Meyer and G.A. Mourou
Laboratory for Laser Energetics, University of Rochester, 250 East River Road
Rochester, New York 14623-1299

With the development of very high speed GaAs devices such as heterojunction bipolar transistors, GaAs MESFETs, TEGFETs and MODFETs, with response well into the picosecond regime, comes the need for new instrumentation to directly characterize these ultrafast devices. Requirements of such instrumentation include good spatial resolution, i.e., a few micrometers, a temporal response of few ps, and minimum interference with the circuit being tested.

We have demonstrated a technique which is a variation of the electro-optic sampler, developed at our laboratory,[1-3] which is capable of characterizing the response of microstructures in two dimensions with a temporal resolution of a fraction of a picosecond.

The reflection-mode electro-optic sampler is shown in Fig. 1. A thin slab of $LiTaO_3$ is located near the surface of a coplanar transmission line built on Cr:GaAs. The electrode widths as well as the distance between electrodes are 50 μm. The bottom face of the $LiTaO_3$ is covered with a high reflectivity coating. A fast electrical signal is generated by laser-induced photoconductivity in a gap interrupting one of the electrodes. The gap is 50 μm wide and biased with a few tens of volts. As the signal propagates down the transmission line, its fringing field penetrates into the thin slab of $LiTaO_3$ and slightly modifies the crystal birefringence according to the signal strength. This electrically-induced change is detected by a probe pulse, which is reflected by the dielectric coating. Presently the spatial resolution is 10-15 μm and can be improved to .5 μm by focusing the probe beam more tightly. Figure 2 shows the experimental results when 100 fs optical pulses are used to generate and probe the electrical pulses. The temporal resolution of .75 ps is limited by the double pass transit time of the probe pulse across the region of induced birefringence and is a function of the electrode spacing. Because the spatial extent of the fringing field scales down with the distance between electrodes, this effect should be minimized and consequently the temporal resolution improved for integrated circuits.

This technique will be tested in the near future on very high speed GaAs integrated circuits.

Acknowledgment

This work was supported by the Laser Fusion Feasibility Project at the Laboratory for Laser Energetics which has the following sponsors: Empire State Electric Energy Research Corporation, General Electric Company, New York State Energy Research and Development Authority, Northeast Utilities Service Company, Ontario Hydro, Southern California Edison Company, The Standard Oil Company, the University of Rochester and the United States Air Force Office of Scientific Research. Such support does not imply endorsement of the content by any of the above parties.

References

1. J.A. Valdmanis, G.A. Mourou and C.W. Gabel, **Appl. Phys. Lett.** 41, 211 (1982).
2. J.A. Valdmanis, G.A. Mourou and C.W. Gabel, **IEEE J. Quantum Electron.** QE-17, 664 (1983).
3. G.A. Mourou and K.E. Meyer, **Appl. Phys. Lett.** 45, 492 (1984).

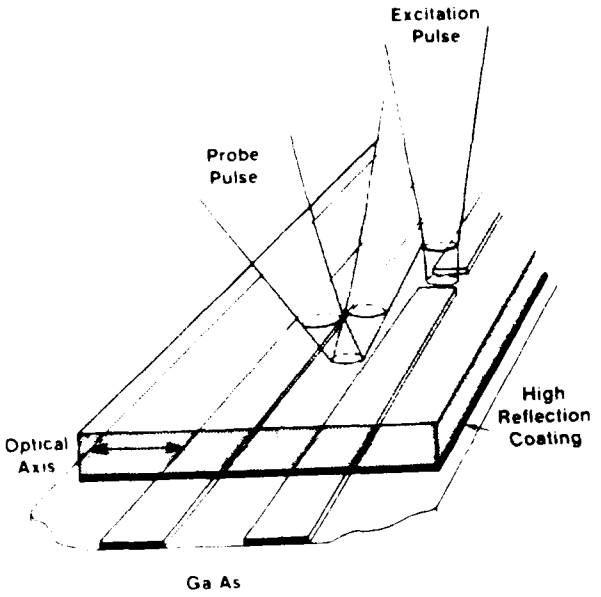

Fig. 1 Reflection-mode electro-optic sampler configuration.

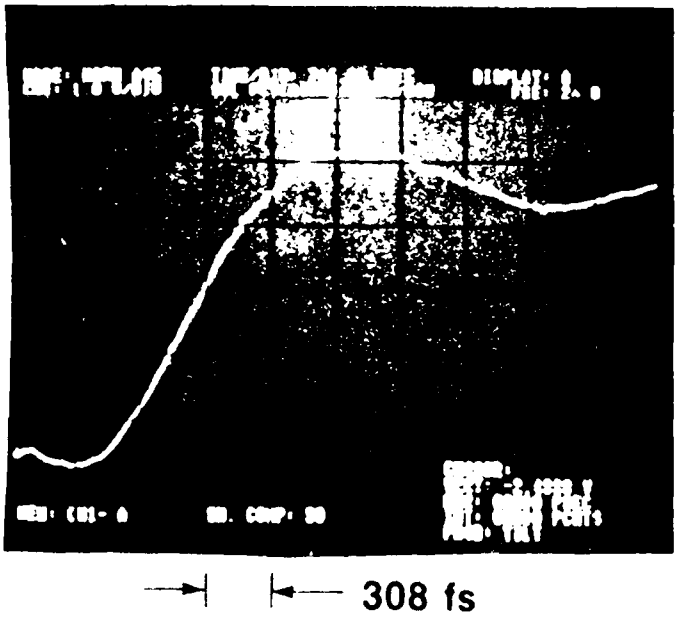

Fig. 2 Temporal response of the reflection-mode sampler with coplanar line dimensions of 50 μm. The 10%-90% rise time is .75 ps.

Picosecond Electro-Optic Sampling and Harmonic Mixing in GaAs

B.H. Kolner, K.J. Weingarten and D.M. Bloom

Edward L. Ginzton Laboratory
Stanford University
Stanford, California
94305

In recent years, the performance of high speed electronic and optoelectronic devices has surpassed the measurement capabilities of conventional instrumentation. At the same time, progress in ultrashort light pulse generation has continued to evolve and today subpicosecond laser systems are not uncommon. By combining very short optical pulses with the electro-optic effect in GaAs, we have developed a sampling probe suitable for non-contact characterization of high speed monolithic GaAs integrated circuits.[1] The circuits can be excited either by on-board photodetectors for impulse response measurements or by external signal generators, phaselocked to the laser pulse train, for swept frequency measurements.

Previous electro-optic sampling systems relied on connecting the device under test to a microstrip transmission line deposited on $LiTaO_3$.[2,3] Although $LiTaO_3$ does have a high electro-optic coefficient, this hybrid approach is a compromise when very wide bandwidth measurements are anticipated. Fortunately, GaAs is electro-optic and devices and circuits made in this material can be probed directly with sub-bandgap radiation without degrading circuit performance.

Of the various possible geometries for electro-optic modulation in GaAs, the longitudinal case illustrated in Figure 1a is the most attractive. In this configuration, the optical sampling beam passes through the wafer at a point adjacent to the upper conductor of a microstrip transmission line and is reflected back by the ground plane. For $\langle 100 \rangle$ cut GaAs (the most common orientation for integrated circuits), the electric field lines along the $\langle 100 \rangle$ axis induce birefringent axes along the $\langle 011 \rangle$ and $\langle 01\bar{1} \rangle$ directions. This birefringence, proportional to the signal being measured, is converted to an amplitude modulation of the sampling light pulses with a polarizer. The sensitivity, or minimum detectable voltage, is independent of the characteristic impedance of the transmission line and for a 50Ω system is nearly 10 times better than that of the transverse $LiTaO_3$ sampler (Fig. 1b).

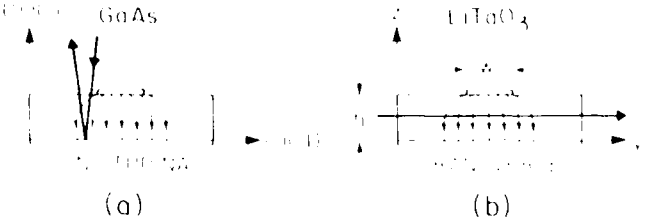

Fig. 1) Microstrip sampling geometries with indicated crystallographic axes.

A new aspect of this approach is the need for a two-wavelength picosecond source. A short wavelength pulse is required to excite the photodetector while a long wavelength pulse is needed to probe the fields. A Nd:YAG laser is ideal for this application. The fundamental output at 1.06 μm is used for sampling while frequency doubling to .532 μm yields a synchronized excitation

source. We used a cw mode-locked Nd:YAG laser in conjunction with a fiber-grating pulse compressor[4] to reduce the pulsewidth to 5 ps. The .532 μm beam was attenuated and used to excite a GaAs photodiode. The remaining 1.06 μm beam was passed through a variable delay line before sampling the GaAs transmission line. As the delay line was adjusted, the 1.06 μm sampling pulses mapped out the impulse response of the photodiode (Fig. 2).

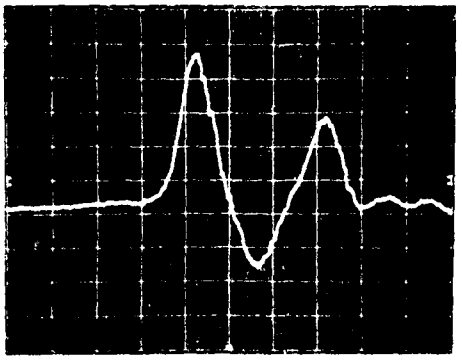

Fig. 2) Impulse response of 50 um diameter GaAs photodiode measured by electro-optic sampling of a GaAs microstrip transmission line (Vert: 10mV/div, Hor: 50 ps/div).

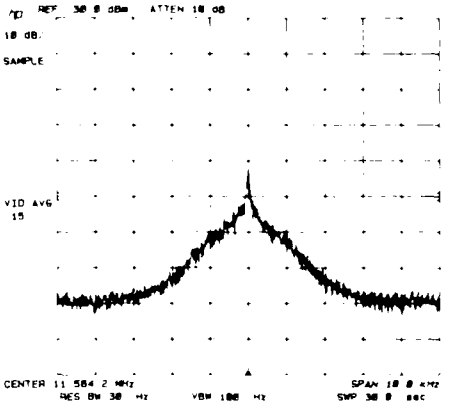

Fig. 3) Spectrum of 199th harmonic of laser pulse train mixed down to 11.58 MHz by electro-optic mixing with a 16 GHz cw signal. Phase noise sidebands predominate.

Because the sampler measures the product of the optical intensity and the electrical signal on the transmission line, it can be viewed as a mixer. Any signal on the transmission line will appear as sidebands on all of the harmonics of the fundamental sampling rate, ω_0. Therefore, if the transmission line is driven with a pure microwave signal, the nearest harmonic will mix with it and appear between DC and $\omega_0/2$ where it can be conveniently viewed on a spectrum analyzer. This spectrum contains a delta-function component and a phase noise continuum arising from the pulse to pulse jitter of the laser. The relative intensity of the phase noise contribution can be shown to vary as the square of the harmonic number while the area under the phase noise spectrum can be related to the r.m.s. jitter.[5] We performed this experiment by driving the microstrip line with frequencies up to 16 GHz (n=199) from a microwave synthesizer phaselocked to the laser mode-locker driver (Fig. 3). We found good agreement with the square law dependence and estimate the r.m.s. jitter to be less than 6 ps in a 33 ms integration time.

The electro-optic sampling and harmonic mixing techniques discussed in this paper provide the basis for non-invasive characterization of high speed GaAs integrated circuits in the time and frequency domains.

REFERENCES

1) B.H. Kolner and D.M. Bloom, Electron. Lett., 20, 818 (1984)
2) J.A. Valdmanis, G.A. Mourou and C.W. Gabel, Appl. Phys. Lett., 41, 211, (1982)
3) B.H. Kolner, D.M. Bloom and P.S. Cross, Electron. Lett., 19, 574 (1983)
4) J.D. Kafka, B.H. Kolner, T. Baer and D.M. Bloom, Optics Lett.,9,505(1984)
5) J. Kluge, Ph.D. Thesis, Universistat Essen, Fed. Rep. of Germany (1984)

Picosecond Pulse Generation in GaAlAs Lasers at a Repetition Rate of 18GHz

K.Y. Lau

Ortel Corporation, 2015 W. Chestnut St., Alhambra, Calif. 91803.

A. Yariv

California Institute of Technology, Pasadena, Calif. 91125.

Significant progress has been made recently in operating semiconductor laser diodes at very high frequencies. The development of ultrafast semiconductor laser diodes [1] have extended the -3dB direct modulation bandwidth to above 10GHz. It will be shown in this paper that in addition to being useful as optical transmitters of microwave signals up to X-band frequencies, the recently developed ultra-high speed laser can be used to generate picosecond pulses at a frequency of 18GHz. The laser used is a window buried heterostructure laser on semi-insulating substrate[1]. The presence of the window near the end facet alleviates the problem of catastrophic damage and enable the laser to operate at very high optical power densities. The tight optical and electrical confinement along the length of the laser cavity (except at the window region) enables maximum interaction between the photon and electrons to take place and results in a very high direct modulation bandwidth. The -3dB direct modulation bandwidth of this device operating at 14mW is 12GHz. The intrinsic modulation response at 18GHz is approximately 13dB below the midband value. This loss in modulation efficiency can be compensated by coupling the laser to an external cavity of the appropriate length. The external cavity is composed of a short length of standard graded index multimode fiber of 50 μm core diameter, with a high refractive index hemispherical lens attached to one end of the fiber to facilitate coupling. The far end of a fiber is cleaved and is butted to a gold mirror. This

induces a very sharp resonance in the modulation response of the laser. When the laser is driven on resonance by a microwave source whose power output is > 10dBm the optical modulation depth approaches unity and the optical waveform becomes pulse-like. Using an optical second harmonic generation autocorrelator the optical pulse width is found to be 12ps(FWHM). This, in effect, is active mode-locking of a laser diode at a repetition rate of 17.5GHz.

References

1. K.Y. Lau, N. Bar-Chaim, I. Ury and A. Yariv, Appl. Phys. Lett., **45**, 316 (1984).

WEDNESDAY, MARCH 13, 1985

WC, HIGH-SPEED PHENOMENA IN SEMICONDUCTORS

D. Hulin, Ecole Polytechnique-ENSTA, ***Presider***

Picosecond Processes in Carrier Transport Theory*

D. K. Ferry

Center for Solid State Electronics Research
Arizona State University, Tempe, AZ 95287

Summary

High-electric-field transport has been studied for some three decades. In recent years it has become of much more interest due to the advent of semiconductor devices on the micrometer and submicrometer dimensional scale. Theoretically, such hot-carrier transport has been discussed primarily in terms of the Boltzmann equation. However, semiconductor transport in high electric fields is a classical example of a far-from-equlibrium system. On the short-time scales appropriate to the submicrometer dimensions, the Boltzmann equation ceases to have general validity, and more exact approaches have been sought.

In general, we are concerned with the evolution of the average velocity and energy of the carrier ensemble in the presence of the high electric field. Previous approaches tend to be centered on either solving the Liouville equation or on developing appropriate generalized Langevin equations for the macrovariables of interest, as replacements for the Boltzmann equation. In either case retarded relaxation integrals are encountered, and these in turn involve kernels which lead to the evaluation

of a set of correlation functions. While these correlation functions do not normally appear in in simpler formulations of transport, it has been recognized for some time that parameters such as the differential mobility and diffusion constant are related to these functions. However, these correlation functions for high-field transport have been previously treated only by Green's functions based upon the Boltzmann equation. Since these same parameters are of considerable importance in evaluating transport and noise properties of submicrometer devices, a more general derivation of these correlation functions from first principles is possible.

As is known for other far-from-equilibrium systems, we show that the transport parameters of interest, the differential mobility and diffusion constant, can be readily obtained through a unique set of Green's functions to which we add proper knowledge of all relevant moments of the nonequilibrium statistical distribution (NESD) that are required. We can analyze the differential mobility and the diffusion constant for an ensemble of electrons in the presence of a steady, high electric field. These terms are evaluated in the high-temperature (classical) limit, although the derivations are more general. In these sections we discuss the appropriate Green's functions and the relevant initial values of the correlation functions, where the latter are intimately related to the distribution function n_k.

We also discuss a method to calculate the nonequilibrium density by Zubarev, but differ somewhat in approach. The results are used to evaluate the distribution function n_k. The evolution equations for the Green's functions developed here clearly show the role of memory effects and the intracollisional field effect.

---

* Supported by the Office of Naval Research

Picosecond Time Resolved Photoemission Study of the InP (110) Surface

J. Bokor, R. Haight, J. Stark, and R. H. Storz
AT&T Bell Laboratories, Holmdel, NJ 07733

R. R. Freeman and P. H. Bucksbaum
AT&T Bell Laboratories, Murray Hill, NJ 07974

Angle resolved ultraviolet photoemission spectroscopy (ARUPS) is a powerful and well established tool for the study of bulk and surface electron states in solids. We report the first demonstration of picosecond time-resolved ARUPS. The technique was used to study the dynamics of electrons photoexcited by a 50 picosecond visible laser pulse on a cleaved InP (110) surface.

On the (110) surface of InP, an unoccupied surface state lies at an energy slightly above the conduction band minimum (CBM).[1] During excitation of carriers into the bulk conduction band, this surface state becomes populated and rapidly comes into equilibrium with the bulk. Using time-resolved ARUPS, we have observed the transient population of this surface state, located its energy minimum at $\bar{\Gamma}$, the center of the surface Brillouin zone, and measured the surface band dispersion along two surface symmetry directions.

Clean InP (110) surfaces, produced by cleavage in ultra-high vacuum, were excited by 50 psec pulses of 532 nm laser radiation at a fluence level of 0.5 mJ/cm^2. The excited surface was probed by measuring the energy and angular distributions of electrons photoemitted by a 50 psec pulse of 118 nm (10.5 eV) laser harmonic radiation. A time-of-flight electron spectrometer with energy resolution of 100 meV, and angular resolution of $\pm 2.5°$ was used.

Figure 1 shows the energy spectra for electrons emitted along the surface normal direction obtained in this experiment. The zero of energy is chosen as the valence band maximum (VBM). Figure 1(a) displays a spectrum for the unexcited material where the probe pulse arrives at the sample before the pump pulse (t=-133 psec). When the pump and probe pulses overlap in time as in Fig. 1(b), a new feature appears centered at +1.3 eV. The insets in Figs. 1(b and c) show a magnified view of this feature. If the probe is delayed relative to the pump by 266 psec the spectrum in Fig. 1(c) is observed. Note that the 1.3 eV peak is significantly reduced both in intensity and width. Finally, Fig. 1(d) displays a spectrum obtained with coincident pump and probe pulses following submonolayer coverage of the surface with chemisorbed hydrogen. The -0.2 eV, -1 eV, and +1.3 eV peaks have essentially disappeared. Such sensitivity to hydrogenation is a generally accepted signature of surface states on semiconductor and metal surfaces. We assign the shoulder at -0.2 eV and the broad peak centered at - 1 eV to occupied surface states. The 1.3 eV peak is attributed to a normally unoccupied surface state.

The time dependence of the 1.3 eV signal is displayed in Fig. 2. The integrated intensity of the 1.3 eV signal is plotted as a function of relative time delay between the pump and probe pulses. A nonexponential decay is observed with the intensity dropping to half maximum within 100 psec. Since the surface state lies so close to the CBM (the band gap in InP is 1.35 eV), a quasi-equilibrium may be established between the surface and the bulk bands. Then the data shown in Fig. 3 represents the time dependence of the bulk carrier density *at the surface*. The expected evolution of the bulk plasma was calculated using a one-dimensional model including the temporal and spatial dependence of the carrier photoexcitation rate, radiative and Auger recombination, and ambipolar carrier diffusion away from the surface. The results of this calculation are shown as the solid line in Fig. 2. The fact that the surface state signal follows the expected behavior of the bulk carrier density in the near-surface region is taken as evidence that the surface state population is strongly coupled to the bulk plasma.

The insets in Fig. 1 show that the energy width of the surface state peak varies with time. The full width at half maximum (FWHM) drops from its maximum of 154 meV at t=0 to the

instrumental limit of 105 meV by 260 psec. Broadening is only observed on the high energy side of the peak. We attribute this result to bandfilling. With this interpretation, and assuming equilibrium between the surface and bulk electrons, we can estimate the peak bulk electron density as 7×10^{18} cm^{-3}

Information about the electron momentum distribution in the 1.3 eV surface state was obtained by measuring the peak intensity as a function of electron exit angle. This data combined with the peak width data has been used to obtain the energy dispersion of the surface state (effective mass) near $\bar{\Gamma}$ along the two surface symmetry directions.

In summary, we have used picosecond time-resolved ARUPS to study the energy and momentum of excited electrons on the InP (110) surface. A normally unoccupied surface state was directly observed to be populated via coupling to bulk photoexcited electrons. Measurements of the angular distribution of photoemitted electrons and the energy width of the surface state peak show that the surface band minimum must lie at $\bar{\Gamma}$, and allow a determination of the energy dispersion (effective mass) along two surface symmetry directions.

References

1 J. van Laar, A. Huijser, and T. L. van Rooy, J. Vac. Sci. Technol. *14*, 894 (1977).

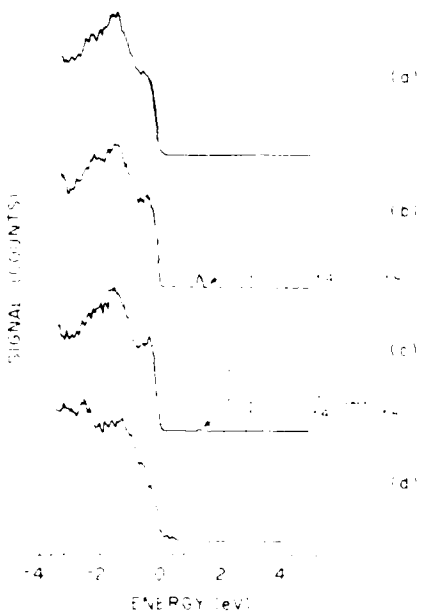

Fig. 1: Pump-probe photoelectron spectra from InP (110) for a) t = -133 psec; b) t = 0; c) t = 266 psec; and d) t = 0 where the surface has been hydrogenated. The insets in b) and c) have the vertical scale magnified by a factor of 10 and 60, respectively.

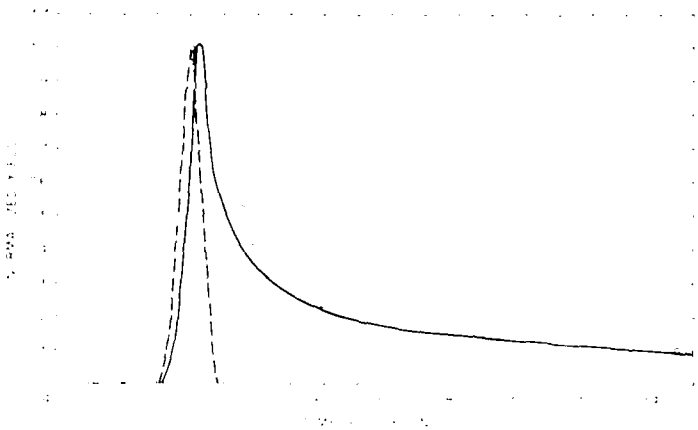

Fig. 2: Integrated transient surface state signal intensity as a function of time delay. The dashed curve represents the system time resolution function. The solid curve is a fit to the data as described in the text.

ACOUSTIC PHONON GENERATION IN THE PICOSECOND DYNAMICS OF DENSE ELECTRON-HOLE PLASMAS IN InGaAsP FILMS

Jay M. Wiesenfeld
AT&T Bell Laboratories
Crawford Hill Laboratory
Holmdel, New Jersey 07733

Semiconductor alloys of InGaAsP are of great importance for the technology of optical communication. Relatively few experiments which measure the ultrafast response of photoexcited carriers in these materials have been reported. In this contribution, the dynamics of dense electron-hole plasmas in InGaAsP films subsequent to ultrashort optical pulse excitation are examined by probing transient transmission and reflection. Typical results are shown in Fig. 1. From the transmission data one sees short-time bleaching or gain, long-time induced absorption, and regular oscillations of the induced absorption. The oscillations are due to coherent acoustic phonon generation subsequent to relaxation of the hot, photo-excited carriers, a phenomonon that has been observed and described by Thomsen, et al, for films of a-As_2Te_3 and cis-polyacetylene.[1] From the observation and analysis of the oscillations for the InGaAsP films, it is possible to deduce acoustic velocities and acoustic deformation potentials for these materials.

Pump and probe experiments in transmission and reflection are performed using 0.5 ps pulses at .625 μm from a cavity-dumped CPM laser. Pulse energies up to 2 nJ at a rate of 200 kHz are used. The samples are films of $In_{0.70}Ga_{0.30}As_{0.66}P_{0.34}$ ($\lambda_g \sim 1.3$ μm), $In_{0.58}Ga_{0.42}As_{0.93}P_{0.07}$ ($\lambda_g \sim 1.55$ μm), InP, and GaAs, thicknesses from 0.2 to 1.0 μm, grown by LPE on a [100] InP surface, and are the same films used in semiconductor film lasers.[2] Excitation densities are 1.5 mJ/cm^2 or less, which implies transient carrier densities of up to 1.5×10^{20} cm^{-3}.

Transient transmission and reflection data for a 0.2 ± .02 μm thick film of $In_{0.70}Ga_{0.30}As_{0.66}P_{0.34}$ are shown in Fig. 1. The oscillations seen in transmission and reflection are out of phase, and have a period of 120 ps. The acoustic wave generated is the standing wave with wavelength equal to twice the film thickness. Hence, the velocity of sound for propagation in the [100] direction in InGaAsP ($\lambda_g \sim 1.3$ μm) is measured to be 3.3×10^5 cm/s. For a 0.6 ± .06 μm thick film of this material, the oscillation period is 360 ps, yielding the same value for the velocity of sound. For a GaAs film, thickness of 0.5 ± 0.1 μm, the oscillation period is 185 ps, which yields a velocity of sound for [100] propagation of 5.4×10^5 cm/s (literature value [3] is 4.7×10^5 cm/s).

The fractional modulation of transmission, $\Delta T/T$, has been shown by Thomsen, et al. to be proportional to the energy density deposited in the sample by the pump pulse.[1] A plot of $\Delta T/T$ vs energy density for the 0.2 μm thick InGaAsP film is shown in Fig. 2. The slope is proportional to many material parameters, including the acoustic deformation potential. Using values for the other parameters,[4] the acoustic deformation potential for InGaAsP ($\lambda_g \sim 1.3$ μm) derived from the data in Fig. 2 is 8.5 eV. This parameter is important in carrier-acoustic phonon scattering.

The short-time and long-time transmission and reflection data are related to the relaxation dynamics of dense, hot electron-hole plasmas, and are also being studied.

[1] C. Thomsen, J. Strait, Z. Vardeny, H. J. Maris, J. Tauc, and J. J. Hauser, Phys. Rev. Lett., 53, 989 (1984).

[2] J. Stone, J. M. Wiesenfeld, A. G. Dentai, T. C. Damen, M. A. Duguay, T. Y. Chang, and E. A. Caridi, Opt. Lett., 6, 534 (1981).

[3] J. S. Blackmore, J. Appl. Phys., 53, R-123 (1982)

[4] S. Adachi, J. Appl. Phys., 53, 8775 (1982).

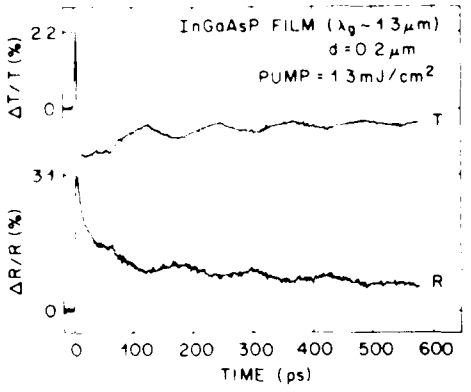

Fig. 1: Time-resolved transmission and reflection changes for the 0.2 μm InGaAsP film.

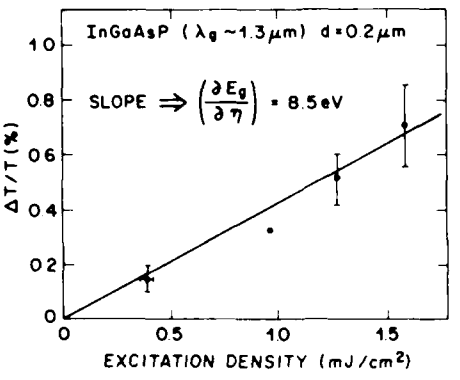

Fig. 2: Magnitude of oscillatory transmission changes for the 0.2 μm thick InGaAsP film.

CARRIER-CARRIER INTERACTION AND PICOSECOND PHENOMENA IN POLAR SEMICONDUCTORS

P. Lugli

Dipartimento di Fisica, Università di Modena, Modena, Italy

D. K. Ferry

Center for Solid State Electronics Research, A.S.U., Tempe, AZ, USA

The effect of carrier-carrier interaction in semiconductors becomes important when high concentrations and short characteristic times are reached. By going to submicron dimensions and picosecond resolutions we are often in such situations. The details of energy and momentum relaxation are then crucial and can be stongly affected by the coulombic scattering among carriers and by the onset of collective phenomena.

We first present an analysis of the conditions under which plasma effects can be of importance in polar semiconductors, through a study of the wave-vector and frequency dependent dielectric function. The calculation includes both Landau and collisional damping. It is found that, even under non-degenerate conditions, the excitation spectrum presents peaks characteristic of plasma modes. As the concentration increases, the coupling of plasmon and phonon modes drastically modifies the transport properties of those materials.

An Ensemble Monte Carlo simulation is then performed for n-GaAs, that includes electron-electron and electron-plasmon interaction. It is shown

that the time evolution of the electron distribution function from an initial δ-like function, is strongly modify by coulombic scatterings. A Maxwellian shape is obtained on times much shorter than the characteristic times of the e-phonon interaction. The Ensemble Monte Carlo technique has been also used for a situation very similar to the base of a Planar Doped Base transistor. A non-energetic beam of electrons with initial energy E_o is injected into a low field region with a concentration of cold electrons of 10^{17} cm^{-3}. Fig. 1 shows that the addition of e-e and e-plasmon interactions(solid line) to the usual e-phonon and e-impurity scatterings(dashed line) further reduces the possibility of ballistic transport, both at room and nitrogen temperature. The possibility that a uniform electric field might improve this picture is also investigated.

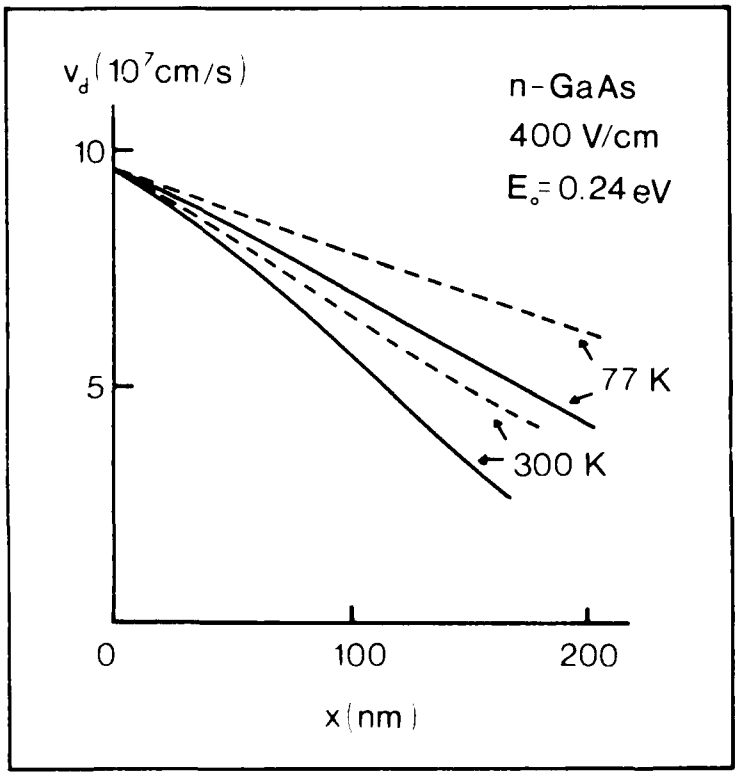

Fig.1 Average drift velocity versus distance with (solid curve) and without (dashed curve) e-e and e-plasmon interaction , for two different temperatures.

Sub-picosecond Raman Spectroscopy of Electron - LO Phonon Dynamics in GaAs

J.A. Kash, J.C. Tsang, and J. Hvam
IBM Thomas J. Watson Research Center
Yorktown Heights, New York 10598

Highly excited ("hot") conduction band electrons in GaAs lose their energy primarily by the emission of zone center LO phonons[1]. The quantitative study of this emission process requires the ability to measure the vibrational spectrum of GaAs on a sub-picosecond time scale. We have combined a sync-pumped dye laser with a filtered fiber optic pulse compressor to obtain spectrally clean 600 femtosecond pulses for wavelengths between 580 nm and 610 nm. A pump pulse generates excited carriers and a weaker, delayed probe pulse measures the Raman scattering from the phonons created by these carriers. Because the average probe beam power is of the order of 1 milliwatt and has a spectral full width at half maximum of about 30 cm^{-1}, the weak Raman scattered spectrum is detected by a cooled, microchannel plate photomultiplier with a position sensitive resistive anode. Changes of less than 10% from the equilibrium room temperature phonon population can be observed using this system. Spectral shifts of the order of 10 cm^{-1} can be resolved.

As shown in figure 1, we observe that the non-equilibrium LO phonon population rises in 2 psec. With an initial excess carrier energy of 700 meV the phonon emission is a 19 phonon cascade here. Because of wavevector conservation, the Raman backscattering monitors only phonons near the middle of the cascade. Thus, the time for a "hot" carrier to emit a single LO phonon is about 200 fsec. This is the first direct measure of the emission rate, although previous work[2] at 3 psec time resolution has measured the 77K decay of these phonons to be 7 psec.

In addition, since for the first time we report spectral shape as well as Raman intensity, we can observe changes in the shape of the Raman emission with time. As seen in figure 2, the spectrum shifts to a lower energy peak on a time scale of 2-4 psec. This shift results from electrons relaxing to the conduction band minimum. As the electrons relax, their ability to screen LO phonons increases, so the LO phonons become degenerate with the Raman forbidden TO phonons.

In conclusion, we have made the first direct measurements of both the phonon emission rate and the dynamics of the electron screening for optically excited electrons in GaAs.

REFERENCES

1. E.M. Conwell and M.O. Vassel, IEEE Trans. on Elec. Devices ED-13, 22 (1966).
2. D. von der Linde, J. Kuhl, and H. Klingenburg, Phys. Rev. Lett. 44, 1505 (1980).

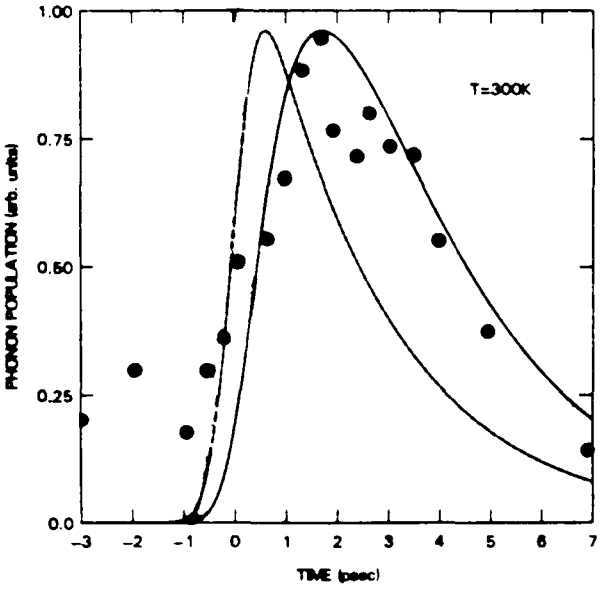

Figure 1. Change in the room temperature LO phonon population in GaAs as a function of time after the pump pulse. The laser wavelength in 589 nm; pump pulse energy is 0.1 njoule, corresponding to a peak electron concentration of about 3×10^{18} cm^{-3}. The solid curve is the predicted response for a 2 psec rise and a 2.5 psec decay time. The dashed curve is the predicted response for an infinitely fast rise time and a 2.5 psec decay time

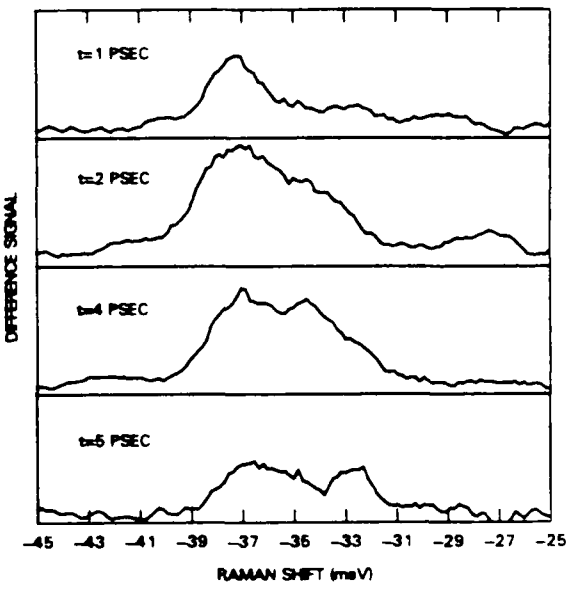

Figure 2. Anti-stokes Raman spectra at several times after the pump pulse under the same conditions as in figure 1. The spectra shown are difference spectra, as the background due to the 300K thermal phonons has been subtracted.

NOTES

WEDNESDAY, MARCH 13, 1985

WD, PICOSECOND DIODE LASERS

Geoffrey L. Burdge, Laboratory for Physical Sciences, *Presider*

Semiconductor Lasers for Ultra High Speed Applications

Amnon Yariv
California Institute of Technology
Pasadena, California 91125

SUMMARY

There exist two important modes of modulation of semiconductor lasers: (1) direct current sinusoidal or pulse modulation, and (2) mode locking.

Direct modulation of GaAs/GaAlAs semiconductor lasers was accomplished at rates exceeding 11 GHz[1]. The uppermost limit for this modulation is conventionally taken as the relaxation resonance frequency[1,2]

$$\omega_R = \frac{1}{2\pi}\sqrt{\frac{AP_0}{\tau_p}}$$

where A is the differential optical gain constant of the optical mode, P_0 is the steady state photon density at the active region, and τ_p is the photon lifetime.

The increase of ω_R requires separate optimization of A, P_0, and τ_p. We will describe the basic limitations to each one of these parameters with special emphasis on recently derived quantum mechanical expressions[3] for the differential gain parameter A in quantum well and in quantum wire lasers.

Direct current modulation of quaternary GaInAsP/InP looms as an important application area. Initial results in this area will be reviewed.

Mode locking of semiconductor lasers[4,5,6] can give rise to subpicosecond optical pulses because of the large available gain linewidths. Some of the recent experiments in this area will be reviewed.

References:

1. K. Lau, Ch. Harder, and A. Yariv, Appl. Phys. Lett., 44, 273 (1984).
2. K. Lau, N. Bar-Chaim, I. Ury and A. Yariv, Appl. Phys. Lett., 43, (1983).
3. Y. Arakawa, K. Vahala and A. Yariv, submitted to Appl. Phys. Lett.
4. P. T. Hol, L. A. Glasser, E. P. Ippen, and H. A. Haus, Appl. Phys. Lett., 33, (1978).
5. J. P. van der Ziel, R. A. Logan, and R. M. Mikulyak, Appl. Phys. Lett., 39, (1981).
6. J. C. AuYeung, and A. R. Johnston, Appl. Phys. Lett., 40, (1982).

Properties of GaAlAs/GaAs Quantum Well Heterostructures Grown by Metalorganic Chemical Vapor Deposition

R. D. Burnham, W. Streifer, T. L. Paoli, R. L. Thornton, and D. L. Smith
Xerox Palo Alto Research Center, Palo Alto, CA 94304

The existence of the heterojunction and the recent development of methods for growing a variety of epitaxial ultrathin III-V semiconductor layers (wider-gap or narrower-gap, doped or undoped, abrupt or graded) enables the fabrication of sophisticated quantum-well heterostructures. In the past few years, one of these techniques, metalorganic chemical vapor deposition (MO-CVD), has become increasingly popular as a consequence of its versatility and economy. The chemistry of MO-CVD growth of III-V compounds was pioneered by Manasevit as early as 1968[1]; however, it was Dupuis and Dapkus in 1977[2] who demonstrated that high quality GaAlAs/GaAs heterostructure lasers can be grown by MO-CVD.

MO-CVD growth is an extremely complex combination of chemical reactions and mass transfer kinetics. The basic mechanism of GaAs growth by combination of single trimethyl gallium (TMGa) and arsine molecules to form GaAs plus three methane molecules[3] is almost certainly made more complex by the importance of intermediate reaction steps.

In addition to understanding the basic physical processes, the impact of materials quality and growth parameters on device quality continues to be a subject for careful investigation.[4] The availability of high purity AsH_3 has been identified as particularly important. Experiments[4] indicate that variations in electroluminescent intensity by four orders of magnitude can be related to variability in the purity of the AsH_3 source, with the variation being correlated with cylinder preparation as opposed to AsH_3 source preparation.[4] One of the main causes of this variability is the H_2O and O_2 adsorbed and/or possibly chemisorbed on the inner wall of an AsH_3 cylinder due to variable surface preparation.[4,5] Purity of AsH_3 sources is vital, since desorption of the volatile As from the crystal itself requires that the growth of these compounds occur in an excess of AsH_3.[3] The critical molar ratio $(AsH_3)/(TMGa + TMAl)$ at which p- to n-type conversion occurs decreases with increasing growth temperature but increases with an increase of Al fraction.[4] Also n_D-n_A varies by about four orders of magnitude (10^{13} to 10^{17} cm^{-3}) as the growth temperature is increased from 660°C to 800°C.[4] To make matters even more confusing, about an order of magnitude increase in photoluminescent intensity is achieved if $Ga_{.85}Al_{.15}As$ is grown at 850°C instead of 700°C.[6] It is therefore quite remarkable that significant advances in devices have been made in spite of an inadequate understanding of the MO-CVD growth process.

The impact of MO-CVD on device research has perhaps been greatest in the growth of structures utilizing ultrathin layers with thicknesses less than ~500 Å, where the quantum size effect is responsible for producing unique properties.[7,8] There are two techniques which allow for the growth of such ultrathin layers. One technique uses interrupted growth sequences to achieve square wells with interfaces that are smooth to less than ±1 monolayer even though growth rates of 20 Å/sec are used.[11] The other technique uses slow growth rates on the order of 3.5 Å/sec, high flow velocities and an optimized reactor design to eliminate the need for the interruption of growth.[12] To date, MO-CVD has produced quantum well heterostructure (QWH) lasers with both the lowest threshold current densities and highest output powers measured for diode lasers in the visible and near infrared regions. QWH lasers exhibit long life even at cw output powers of 100 mW.[13] The wavelength tuning range in an external cavity is more than three times that of conventional double heterostructure lasers.[14] By thermally annealing a crystal containing

a QWH, it is possible to change the shape of a quantum well from an initially square well of GaAs to a rounded shallower AlGaAs well, thus shifting the confined particle electrons and hole states to higher energy. This is a convenient method for adjusting the wavelength of a QWH laser without significantly increasing the lasing threshold.[10] Perhaps the most exciting capability of QWH's is the variation in energy gap which can be obtained either laterally or vertically via impurity-induced disordering (*n* or *p*).[10,14] This process has produced a simple form of buried heterostructure laser[10,15] and suggests how QWH's and impurity-induced disordering can serve as the basis for fabricating new forms of integrated electrical and optoelectronic circuits.

To date, MO-CVD has not produced high-electron mobility transistor (HEMT) structures that are of the same quality as those grown by moleculear beam epitaxy (MBE).[16] However, this is not thought to be a fundamental limitation of the MO-CVD process. Progress has been made on inelastic and resonant tunneling in AlAs/GaAs heterostructures.[17] These structures might be extremely promising as a high speed tunneling transistor.[18]

Considering that only about five years have elapsed in which extensive research has been performed on MO-CVD, the achievements thus far are remarkable, and the future potential is excellent.

References

1. H. M. Manasevit, Appl. Phys. Lett. 12 (1968) 146.
2. R. D. Dupuis and P. D. Dapkus, Appl. Phys. Lett. 31 (1977) 466.
3. H. M Manasevit and W. I. Simpson, J. Electrochem. Soc. 118 (1971) 647.
4. T. Nakanisi, J. Crystal Growth 68 (1984) 282.
5. P. D. Dapkus, H. M. Manasevit, K. L. Hess, T. S. Low and G. E. Stillman, J. Crystal Growth 55 (1981) 10.
6. E. E. Wagner, G. Hom and G. B. Stringfellow, J. Electron. Mater. 10 (1981) 239.
7. E. J. Thrush and J. E. A. Whiteaway, Inst. Phys. Conf. Ser. 56 (1981) 337.
8. J. P. André, M. Boulou and A. Micrea-Roussel, J. Crystal Growth 55 (1981) 192.
9. N. Holonyak, Jr., R. M. Kolbas, R. D. Dupuis and P. D. Dapkus, IEEE J. Quantum Electron. QE-16 (1980) 170.
10. R. D. Burnham, W. Streifer, T. L. Paoli and N. Holonyak, Jr., J. Crystal Growth 68 (1984) 370.
11. R. D. Dupuis, R. C. Miller, and P. M. Petroff, J. Crystal Growth 68 (1984) 398.
12. M. R. Leys, C. van Opdorp, M. P. A. Viegers, and H. J. Talen van der Mheen, J. Crystal Growth 68 (1984) 431
13. G. L. Harnagel, T. L. Paoli, R. L. Thornton, R. D. Burnham, and D. L. Smith, to be published in Appl. Phys. Lett.
14. K. Meehan, N. Holonyak,Jr., J. M. Brown, M. A. Nixon, P. Gavrilovic and R. D. Burnham, Appl. Phys Lett. 45 (1984) 549.
15. K. Meehan, P. Gavrilovic, N. Holonyak, Jr., R. D. Burnham and R. L. Thornton, to be published in Appl. Phys. Lett.
16. J. P. André, A. Brière, M. Rocchi, and M. Riet, J. Crystal Growth 68 (1984) 445.
17. R. T. Collins, A. R. Bonnefoi, J. Lambe, T. C. McGill and R. D. Burnham, Proceedings of the International Conference on Superlattices, Champaign-Urbana, Illinois, 1984.
18. N. Yokoyama, K. Imamura, T. Ohshima, H. Nishi, S. Muto, K. Kondo, and S. Hiyamizu, Jpn. J. Appl. Phys. 23 (1984) L311.

An InGaAsP 1.55 μm Mode-Locked Laser With a Single-Mode Fiber Output

G.Eisenstein S.K.Korotky R.S.Tucker U.Koren
R.M.Jopson L.W.Stulz J.J.Veselka K.L.Hall

AT&T AT&T Bell Laboratories
Crawford Hill Laboratory
Holmdel, New Jersey 07733

Active mode-locking of semiconductor lasers[1] is a useful technique for the generation of short,high peak-power optical pulses. For communication purposes, these pulse trains may subsequently be encoded by a modulator, which can either be integrated with the mode-locked laser[2] or external and coupled to it using an optical fiber[3]. The external cavity of mode-locked lasers can take various forms[4]. In all reported schemes however, the output is from a cleaved laser chip facet.Coupling to an output fiber consequently incurrs a coupling loss of 3-5dB. In this paper we describe the first mode-locked 1.55 μm InGaAsP-optical -fiber composite-cavity laser with a single-mode fiber output.The laser output is coupled to a fiber of the same type as used for the cavity with a coupling loss of less than 0.5dB.

The InGaAsP-optical fiber-composite-cavity laser is shown schematically in Fig.1. It consists of a 1.55 μm TCBC[4] laser chip with both facet reflectivities modified by dielectric coatings, and a 5cm single-mode fiber resonator. Mirror R_1 is a multilayer dielectric mirror with reflectivity $R_1>0.9$.Facet R_2 is antireflection coated with a residual reflectivity $2X10^{-4}$. Mirror R_3 is a partially reflecting multilayer dielectric mirror with reflectivity R_3=0.6 measured through the fiber using an optical time domain reflectometer. The laser cavity is formed between mirrors R_1 and R_3 with the output taken from the partially transparent mirror R_3. The cavity fiber is spliced to a connectorized output fiber using a silicon V grooved chip.The splice loss is 0.1-0.2dB.

Mode-locking is achieved by superimposing a dc bias and an ac current at the fundamental resonance frequency (1.97GHz) or a harmonic. Fig.2a shows a generated pulse train at the second harmonic (3.94GHz). Fig.2b shows a single pulse obtained at the fundamental frequency, measured with a fast InGaAs PIN detector and a sampling oscilloscope. The displayed pulse width 36.6ps FWHM is indistinguishable from the detection system impulse response. The pulse width is estimated to be 1-5ps FWHM based on the detector response and the spectral width. Second harmonic generation measurements are in progress to accurately determine the pulse width. These are the shortest reported pulses from an InGaAsP mode-locked laser.These lasers operate in the 1.3-1.55 μm wavelength range where no suitable saturable absorber has been demonstrated and all mode- locking experiments rely on active mode-locking. Typical pulses obtained in the past were in the 20ps FWHM range. The drastic decrease in the pulse width reported here is assumed to be due to the high Q cavity and due to the fast response of the TCBC laser chip. The average output power of these pulses is measured to be 0.9mW resulting in a pulse peak power larger than 100mW *delivered in the output single mode fiber.*

REFERENCES

1) R.S.Tucker, G.Eisenstein, I.P.Kaminow, Elect. Lett.19 No.14 1983 and references therein.
2) G.Eisenstein, R.S.Tucker, I.P.Kaminow, T.P.Lee, C.A.Burrus, Elect. Lett.20 No.15 1984.
3) S.K.Korotky, G.Eisenstein, B.L.Kasper, R.C.Alferness, J.J.Veselka, L.L.Buhl, Elect. Lett. 20 No.20 1984.
4) G.Eisenstein, U. Koren, R.S.Tucker, B.I.Kasper, A.H.Gnauck, P.K.Tien App. Phys. Lett. 45 No.4 1984.

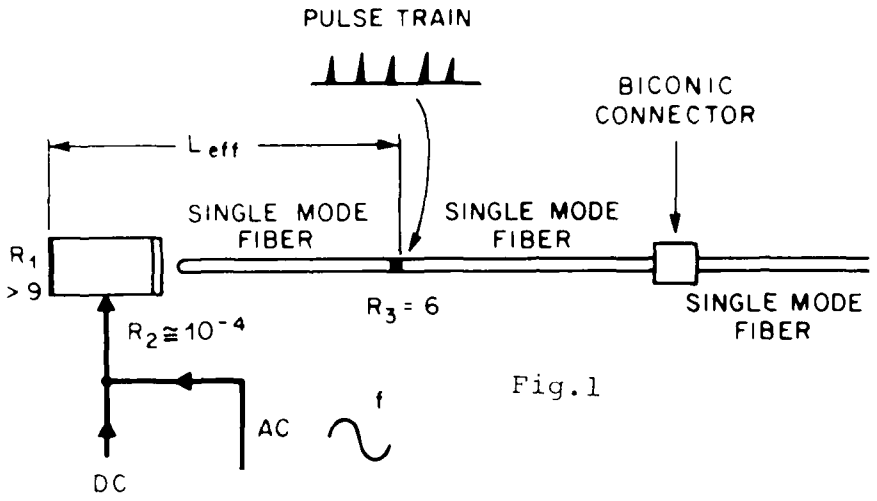

Fig.1

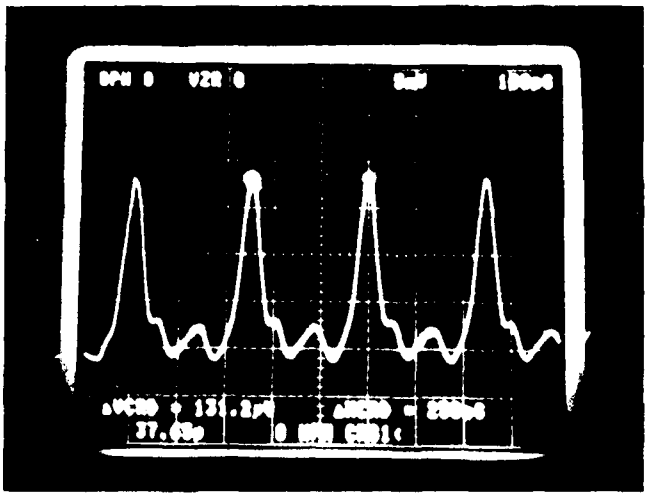

Fig.2a

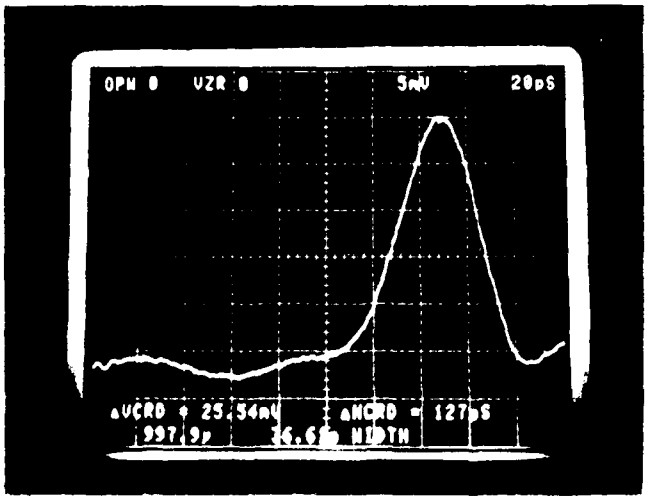

Fig.2b

FAST MULTIPLE QUANTUM WELL ABSORBER FOR MODE LOCKING OF SEMICONDUCTOR LASERS

Y. Silberberg and P. W. Smith,
Bell Communications Research, Inc.,
Holmdel, N. J. 07733

D. A. B. Miller and B. Tell,
AT&T Bell Laboratories,
Holmdel, N. J. 07733

A. C. Gossard and W. Wiegmann,
AT&T Bell Laboratories,
Murray Hill, N. J. 07974

SUMMARY

Passive mode locking of a semiconductor laser using GaAs/GaAlAs multiple quantum well (MQW) material as a saturable absorber has been reported recently[1]. The MQW material exhibits clear and easily-saturable room-temperature exciton absorption resonances. The mode locked laser produces a train of pulses as short as 1.6 psec. Such lasers are potentially important sources for future high-capacity optical communications systems.

In order to obtain good mode locking, the relaxation time of the absorber must be faster than that of the gain. The relaxation time of the gain in a GaAs diode was recently measured to be 375 psec[2]. The absorption recovery time is normally governed by the carrier recombination time[3]. For our MQW samples this time was measured to be 30 nsec. For mode locking, we previously focussed the light tightly on the MQW sample so that the absorption recovery was instead determined by carrier diffusion out of the excited region. This method, however, requires operating the laser just above threshold, since at high light powers the absorber becomes totally bleached. It would be much better to find a method to speed up the intrinsic carrier recombination time. Ion bombardment is well known to reduce carrier lifetimes but can also severely perturb the bandedge absorption.

In this paper we report on our studies of proton bombardment of MQW samples. This proves to be a practical method of obtaining a fast-responding saturable absorber without destroying the exciton resonances. We have bombarded MQW samples with various doses of 200 KeV protons, and measured the absorption relaxation times, spectra, and saturation characteristics. Our results are summarised in Table I and in Fig 1. We have found that the relaxation time can be reduced to <150 psec before a significant change is observed in the absorption spectrum or the nonlinear properties of the absorber. The bombardment dosage at which excitons dissapear agrees with a simple probabilistic model.

Table I

Absorption Recovery time for proton-bombarded MQW Samples

Dose (protons/cm^2)	Recovery Time (psec)	
	Annealed	Unannealed
10^{10}	-	530
10^{11}	>3000	450
10^{12}	560	200
10^{13}	150	(27)
10^{14}	(33)	(<10)

(The times in brackets are for samples for which the nonlinear absorption was appreciably reduced)

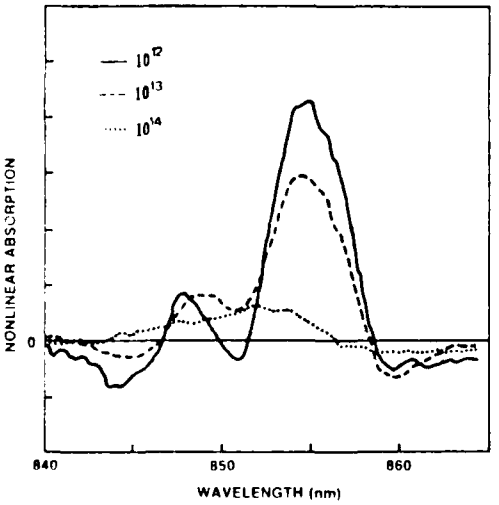

FIG.1 Nonlinear spectra for annealed samples.

Samples bombarded with 10^{13} protons/cm^2 were used as a saturable absorber in an external cavity mode locked diode laser. Stable mode locked operation was obtained over a wide range of operating parameters. We will describe details of this laser operation.

The usefulness of fast-response MQW material is by no means limited to mode locking applications. This material will find wide use for fast, low power optical devices for a variety of signal-processing applications.

REFERENCES

(1) Y. Silberberg, P. W. Smith, D. J. Eilenberger, D. A. B. Miller, A. C. Gossard, and W. Wiegmann, Opt Lett 9, (1984)

(2) W. Lenth, Opt Lett 9, 396 (1984)

(3) D. S. Chemla, D. A. B. Miller, P. W. Smith, A. C. Gossard, and W. Wiegmann, IEEE J. Quantum Electron QE 20, 265 (1984)

NOTES

WEDNESDAY, MARCH 13, 1985

WE, POSTER SESSION

SUPPRESSION OF TIMING AND ENERGY FLUCTUATIONS IN A MODELOCKED SEMICONDUCTOR LASER BY cw-INJECTION

Finn Mengel
Telecommunications Research Laboratory, Borups Alle 43, 2200 Copenhagen Denmark

Chinlon Lin* and Niels Gade
Electromagnetics Institute, Technical University of Denmark, 2200 Lyngby, Denmark

Introduction: Active modelocking of semiconductor diode lasers in an external cavity by synchronous electrical pumping is a simple and attractive method for generation of short optical pulses in the wavelength region of interest for optical communication [1]. Up to now, most attention has been paid to the time-averaged behaviour of pulse width, optical spectrum and time-bandwidth product, but pulse intensity fluctuations are of major importance in communications and logic applications. In this paper we investigate this type of noise and demonstrate a partial suppression by cw injection locking. Similar results have previously been demonstrated in a CO_2 laser [2].

Experiment: A Hitachi 850 nm CSP laser with AR-coating giving residual reflectivity in the 0.5-1% range was placed in an external cavity with an objective and a grating and synchronously pumped by a 1 GHz pulse train and dc bias. A similar uncoated laser was used as master oscillator with injected power around -10 - -20 dBm. The master frequency could be current tuned to any of a large number of slave laser external cavity modes, but extreme frequency stability was required to maintain locking to any particular mode. The optical signal was detected with a Si Pin-diode of 8 GHz bandwidth or an intensity correlation interferometer.

Results and discussion: In fig. 1, we show a single sweep of 100 pulses on a 1 GHz real-time oscilloscope (a) without and (b) with injection. Pulse energy fluctuations are clearly decreased by injection, while the pulse width increases from 30 ps to 37 ps. Quantitative noise measurements can be obtained by baseband spectral analysis [3]. In figs. 2 and 3 we show the spectra around the first and seventh harmonic of the pulse repetition frequency (a) without and (b) with injection. We observe a symmetric low-pass noise band of bandwidth ~20 MHz increasing with harmonic number n approximately as n^2, indicating pure pulse timing jitter [3]. The broadband structure with a bandwidth of ~100 MHz becomes progressively more asymmetric with increasing harmonic number in contrast to the results of ref. 3 for Argon and dye lasers. This can be explained by a correlation between timing jitter of characteristic frequency f and energy fluctuations of frequency 2f. Both types of noise are decreased by ~10 dB by injection. Fabry-Perot spectra suggest a stabilisation of the optical spectrum as well.

The noise is caused by spontaneous emission [4] and enhanced by the internal (imperfectly AR-coated) laser mirror and the amplitude/phase coupling [5]. The above mentioned noise correlation is qualitatively expected, since pulses arriving at the laser too early and too late will both experience less gain than perfectly timed pulses. Preliminary results of a numerical simulation of an extended version of the laser rate equations [5] support this explanation. Fig. 4 shows calculated pulses from a coated, detuned laser. Numerical studies of the effect of AR-coating quality, detuning and injection locking are in progress.

* Permanent address: AT&T Bell Laboratories, Holmdel, NJ 07733 USA.

... Injection locking is an attractive way to improve the noise performance of mode-... semiconductor lasers with imperfect AR-coating. A simple servo loop using derivative ... is used to lock the master frequency to the slave laser cavity.

... Bass, Appl. Phys. 26, 1007 (1981).

... Van der Ziel, Opt. Commun. 45, 404 (1983).

... Linde, D. Meinhart and D. von der Linde, Opt. Commun. 51, 271 (1984).

... New and C.M. Cotterill, Proc. CLEO 84, Anaheim, 82 (1984).

... Yariv and P. Yeh, IEEE J. Quantum Electron. QE-16, 347 (1980).

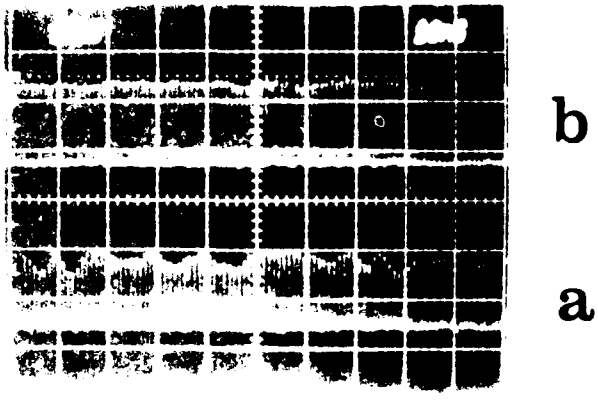

... 1 GHz

...

...

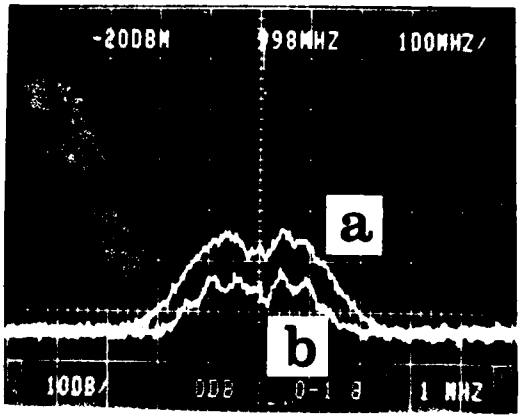

Fig. 2: Baseband spectrum of (a) unlocked and (b) locked pulse train around 1 GHz (n=1).

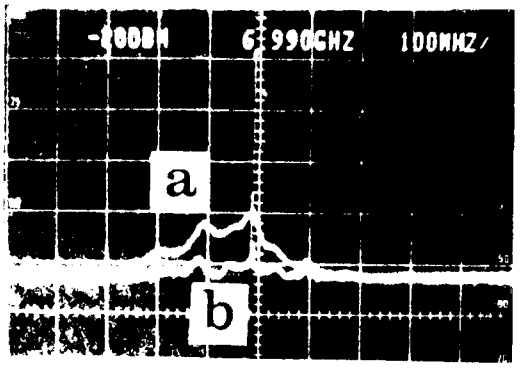

...

...

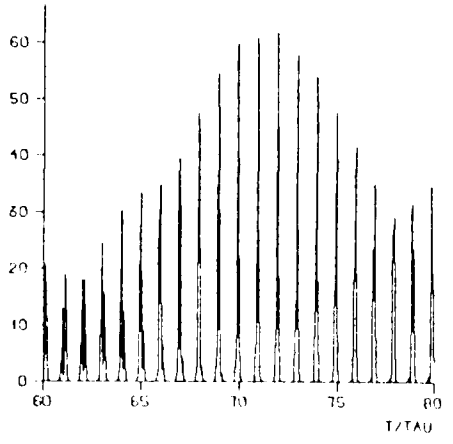

Fig. 3: ... pulse train ... ... external cavity ...

Cross Modulation of Light in SI Semiconductor Materials In the presence of Electric fields

L. M. Walpita, W. S. C. Chang, H. H. Wieder and T. Van Eck
Department of Electrical Engineering and Computer Sciences,
Mail Code C-014
University of California, San Diego
La Jolla, California 92093

Various optical devices are currently being investigated for optical signal processing and communication[1,2]. In this paper we will discuss cross modulation of light observed in semiconductor materials. This effect could potentially be used to obtain optical logic functions such as AND gate.

In the initial experiments, we have used an undoped Semi-Insulating (SI) GaAs sample of which both sides are polished. The sample has InSnO and Al electrodes deposited on both surfaces and a window is left in the Al electrode for light to pass through. A beam of light from a LED source (10 mwatts) centered at λ = 0.88 μm is transmitted through a 400 micron thick sample (figure 1). Some part of the LED light spectrum fell below the absorption edge (figure 2). When a voltage pulse of few tens of μ sec. duration at 300 volts (corresponding to an electric field of 7.5kV/cm) is applied to the InSnO/Al electrodes the light is absorbed as shown in figure 3. Our data agrees only roughly with other available electro-absorption data[3], because the LED has an extended spectral width and because the absorption edge of SI GaAs is not very abrupt.

When another optical pulse (λ = 8850 Å ± 100 Å) of maximum intensity 1 kwatt/cm^2 is transmitted through the sample, the absorption of the LED light is instantaneously reduced. Within the limits of the switching speed established by the RC time constant of the pulse voltage circuit, the cross modulation effect is instantaneous. Thus, we have demonstrated a new optical cross modulation effect. This effect performs essentially the function of an optical 'AND' gate. Our explanation of the cross modulation is that the photo current generated by the laser pulse has reduced the electric field and the electro-absorption in the SI GaAs. A change of absorption due to photo current of an incident light beam, was also described in relation to the self electro-optic effect[4] (SEED).

A number of side effects have also been observed. After the optical pulse the electro-absorption continues to increase beyond what is possible with a simple voltage pulse alone (figure 4). A non-linear dependence of the cross modulation on the laser pulse intensity is also observed; at optical pulse intensity 8 watt/cm^2 and voltage 200v, a 7% absorption modulation is seen, while at 600 watt/cm^2 for the same voltage only 20% absorption modulation is seen. These effects are now being investigated further.

It is interesting to note that the optical power needed for cross modulation may be reduced to less than 200 mwatts/cm^2 for 10% modulation if the LED is replaced by a laser source. This effect might also be applied to obtain two dimensional spatial light modulation at a speed much faster than the liquid crystal devices. The effect might be present in the vicinity of the bandgaps of other direct semiconductors. This work is supported in part by AFOSR grant 80-0057.

References
1. P. W. Smith, Bell Sys. Tech. J., vol. 61, p. 1975, 1982.
2. D. S. Chemla, et al., IEEE J. of Quan. Elec., vol. 20, p. 265, 1984.
3. G. E. Stillman, et. al., Appl. Phys. Lett., vol. 28, p. 544, 1976.
4. D. A. B. Miller, et. al., Appl. Phys. Lett. vol. 45, p. 13 , 1984.

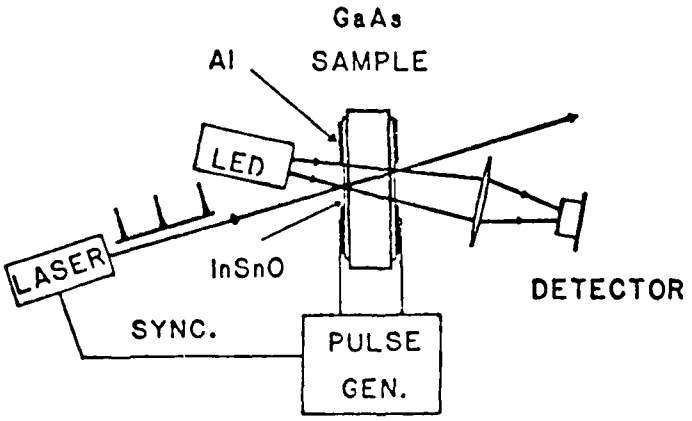

Fig. 1. Schematic of the optical 'AND' gate.

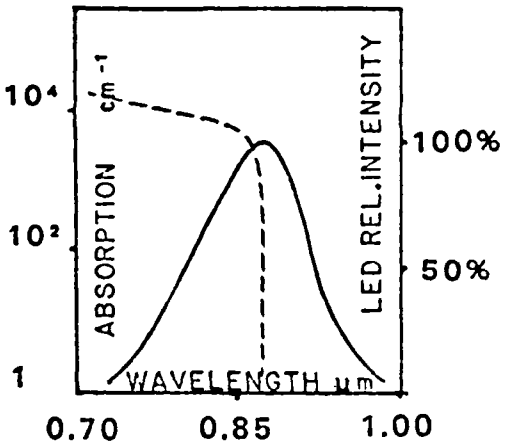

Fig. 2. The wavelength spectrum of the LED in relation to the absorption edge of GaAs in the ideal situation[3] is shown. The LED spectrum was obtained from the RCA data sheet.

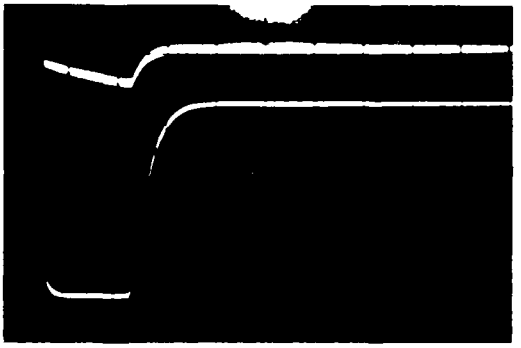

Fig. 3. The absorption of LED caused by a voltage pulse is shown. The bottom trace is the voltage pulse with horizontal scale 15μsec./cm and vertical scale 150v/cm. The upper trace represents the absorption with vertical scale 10%/cm.

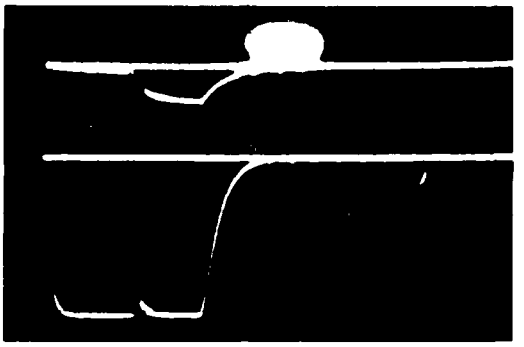

Fig. 4. The effect of the optical pulse of 1 kwatt/cm^2 on the LED absorption is shown. The bottom trace is the voltage pulse with horizontal scale 15μsec./cm and vertical scale 150v/cm. The upper trace represents the absorption caused by both optical and voltage pulse, with vertical scale 75%/cm.

AN ULTRAFAST DIFFUSION-DRIVEN DETECTOR

A.G. Kostenbauder and A.E. Siegman
Edward L. Ginzton Laboratory
Stanford University
Stanford, California 94305

Numerous fast semiconductor photodetectors have been developed in the last decade. These devices have used short carrier lifetimes[1,2] or large electric fields and small geometries[3,4] to produce fast impulse responses. In contrast to these methods of making fast photodetectors, we propose a photovoltaic device whose operating speed is due to *diffusion* of carriers. This device involves interfering light waves to form a grating of photoexcited carriers with a $\sin Kx$ spatial dependence. Such a distribution will decay with a time constant of $(DK^2)^{-1}$, where D is the material's diffusion constant. Because K can be made very large, the response time can be extremely short. If the grating is formed in silicon, for example, with optical beams of 1 μm wavelength having antiparallel k-vectors, then the diffusion-driven detector response time will be 0.25 psec.

As shown in Fig. 1, the diffusion-driven detector consists of a thin slab of semiconductor, illuminated through both the front and back faces, and with (transparent) electrodes on these two sides. Solving the well known equations of motion[5] for the carrier densities and the generated current yields a relatively large quantum efficiency of about $(K\ell)^{-2}$, and an impulse response proportional to $\exp(-D_a K^2 t)$ where $D_a = 2D_n D_p/(D_n + D_p)$.

The achievement of 0.25 picosecond impulse responses in a conventional photodiode would require the use of a very thin depleted region (to reduce the transit time to $\lesssim 0.25$ psec) which would in turn require a very small collecting area ($\lesssim 0.25$ μm^2) in order that the RC time constant associated with the device not exceed 0.25 psec. On the other hand, the diffusion-driven detector's transit time is the time required for a carrier to move from a peak to a trough (which is the $(DK^2)^{-1}$ time constant), while the capacitance depends only upon the electrode spacing. Thus, one can fix the collecting area and K (thus determining the transit time) and vary ℓ to achieve the required capacitance. This existence of two characteristic lengths (K^{-1} and ℓ) allows the previously impossible combination of large collecting area and high speed.

We have performed a low frequency test of a diffusion-driven detector. Instead of using counterpropagating optical beams to produce the nonuniform carrier density, we have used a Gaussian beam focused to 50 μm. The equations of motion used to derive the $\exp(-D_a K^2 t)$ impulse response also predict that a gap that is illuminated with an intensity that varies linearly from I_1 at one electrode to I_2 at the other will produce current with a quantum efficiency of $\eta = (2(D_n - D_p)\tau/\ell^2)((I_1 - I_2)/(I_1 + I_2))$, where τ is the carrier lifetime and ℓ is the gap width. This behavior has been observed, and both the magnitude and shape of the current versus relative position curve is in good agreement with theory (see Fig. 2). We will also present experimentally measured impulse responses on both silicon and indium phosphide structures. The silicon devices have 100 μm gaps and are configured in the geometry shown in Fig. 1, while the indium phosphide devices have both electrodes on one face of the crystal with a 25 μm gap. These experiments employed the output of a mode-locked YAG laser and show the K^{-2} dependence of the response time.

References

1. A.M. Johnson, A.M. Glass, D.H. Olson, W.M. Simpson, and J.P. Horbison, *Appl. Phys. Lett.* **44**, 450 (1984).
2. R.B. Hammond, N.G. Paulter, R.S. Wagner, and T.E. Springer, *Appl. Phys. Lett.* **44**, 620 (1984).
3. S.Y. Yang and D.M. Bloom, *Elec. Lett.* **19**, 554 (1983).
4. B.H. Kolner, D.M. Bloom, and P.S. Cross, *Elec. Lett.* **19**, 574 (1983).
5. R.S. Muller and T.I. Kamins, *Device Electronics for Integrated Circuits*, Wiley, New York, 1977.

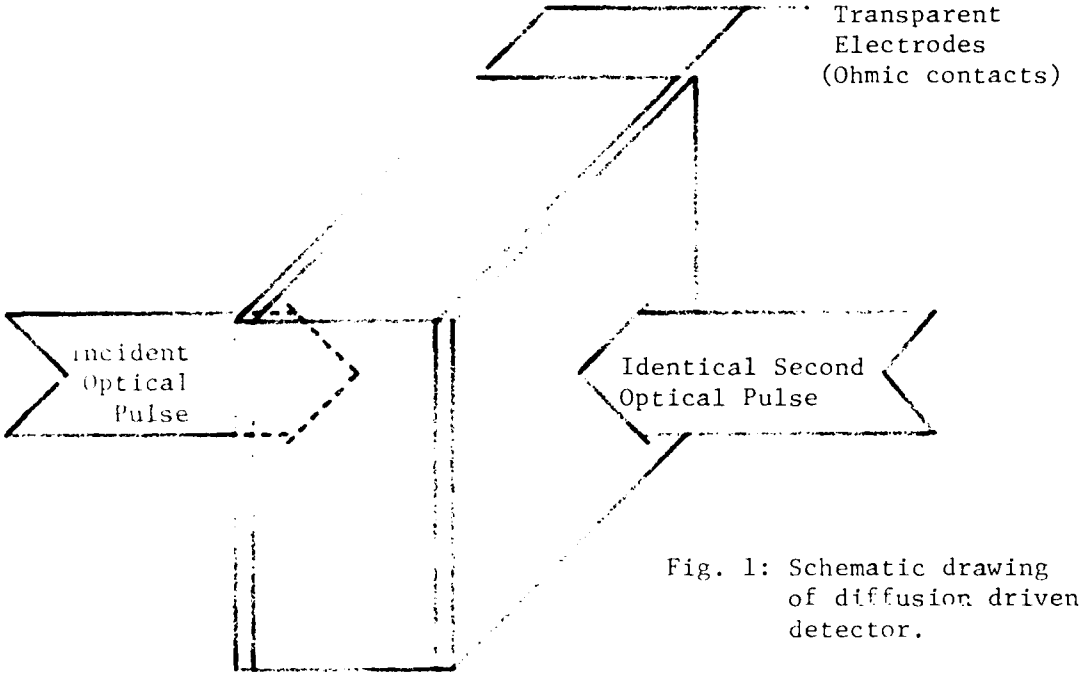

Fig. 1: Schematic drawing of diffusion driven detector.

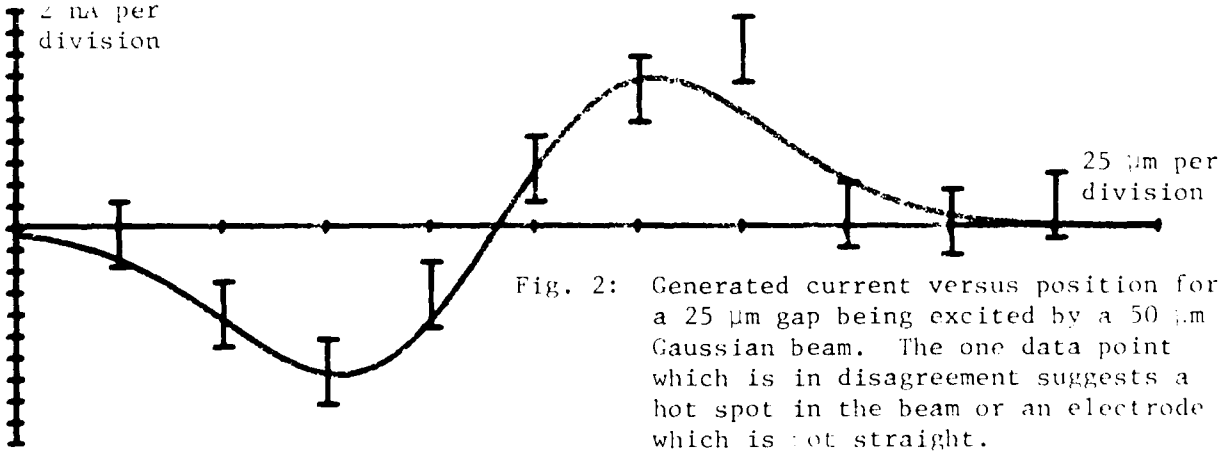

Fig. 2: Generated current versus position for a 25 μm gap being excited by a 50 μm Gaussian beam. The one data point which is in disagreement suggests a hot spot in the beam or an electrode which is not straight.

Optoelectronic Modulation of Millimeter-Waves in a Silicon-on-Sapphire Waveguide

Chi. H. Lee, Aileen M. Yurek, M. G. Li, E. Chauchard and R. Fischers,
Department of Electrical Engineering, University of Maryland,
College Park, MD 20742

Optically controlled millimeter-wave devices such as IMPATT [1] and TRAPATT[2] diode have been reported. Millimeter-wave phase shifter utilizing an electronically injected electron-hole plasma in a semiconductor waveguide has also been demonstrated.[3] None of these devices, however, can operate at high speed. In our laboratory, we have developed a family of optoelectronic devices at the millimeter-wave spectral region which have picosecond speed capability.[4,5] For example, the gating of millimeter-wave pulse with vasriable pulse duration ranging from a few nanoseconds to subnanoseconds has been reported. When the device is operated as a phase shifter, the phase shift as large as 1500°/cm has been observed.[5] In these previous studies, we have found that, in general, the carrier diffusion will cause large loss and less phase shift for the millimeter-waves. In this work, we will report on the performance of dielectric waveguide made of silicon-on-sapphire (SOS). It is expected that the optically induced electron-hole plasma will be confined in a thin layer of epitaxially grown silicon and thus a high density but thin thickness plasma layer may be maintained, resulting in a small dynamic insertion loss.

Millimeter-waves at 100 GHz have a period of 10 picoseconds. Therefore it is most convenient to manipulate the millimeter-wave signal by picosecond optoelectronic technique. Conversely, the performance of many picosecond electronic devices may be studied by picosecond optoelectronically modulated millimeter-wave signal. With the advent of picosecond optoelectronic technique, it is also anticipated that the individual electric pulse in a CW millimeter-wave pulse train may be manipulated with a high repetition rate. It is believed that such an electrical waveform may be quite suitable to study the response of a high speed electronic device.

Fig. 1 shows the modulation of a CW millimeter-wave signal by a frequency doubled mode-locked pulse train from a Nd:YAG laser. The experimental arrangement for generating such a signal has been discussed elsewhere.[5] It is clear that the millimeter-wave output (b) mimicking the incident optical pulse train (a). The rapid decay of the millimeter-wave is attributed to the short lifetime of free carriers in the silicon expitaxial layer. Strong surface recombination at the silicon-air and silicon-sapphire interfaces may also contribute to the rapid decay. Using a single picosecond optical pulse, we can also generate a single millimeter-wave pulse. The temperal profile of such a millimeter-wave pulse has to be measured by the standard excite-and-probe technique. We have also used the ultrashort millimeter-wave pulse thus generated to probe the behavior of diffusion of the optically induced carriers in a bulk silicon waveguide. The results of these studies will be presented at the meeting.

This work was supported in part by the U.S. Army Research Office, the Air Force Office of Scientific Research and the National Science Foundation.

References

(1) H. W. A. Gerlach and R. Wellman, Proc. IEEE. MTT-S International Microwave Symposium, pp. 70-72, 1983.

(2) R. A. Kiehl, IEEE Trans. Microwave Theory Tech. MTT-28, pp. 409-413, 1980.

(3) H. Jacobs and M. M. Chrepta, IEEE Trans. Microwave Theory Tech. MTT-22, pp. 411-417, 1974.

(4) Chi H. Lee, Aileen M. Yurek, M. G. Li and C. D. Striffler, 9th International Conference on Infrared and Millimeter-Waves, Osaka, Japan, Oct 22-26, 1984.

(5) Chi H. Lee, Chapter 5, in "Picosecond Optoelectronic Devices", edited by Chi H. Lee, Academic Press, 1984.

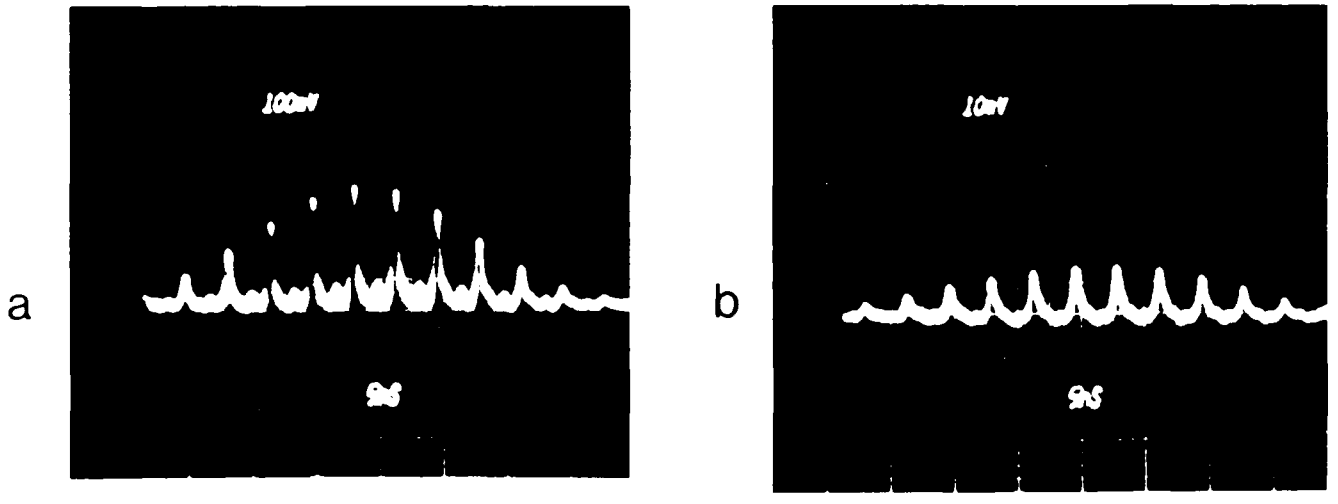

Fig. 1. Millimeter-wave pulse train (b) mimicking the incident optical pulse train (a) from a frequency doubled mode-locked Nd:YAG laser. The waveguide material is silicon on sapphire and the oscilloscope sweep speed is 5 ns per division. The traces shown here are bandwidth limited by the oscilloscope.

Kilovolt Sequential Waveform Generation by Picosecond Optoelectronic Switching in Silicon

C. S. Chang, M. J. Rhee, Chi H. Lee
University of Maryland, Department of Electrical Engineering; College Park, MD

A. Rosen, H. Davis
RCA Laboratories; Princeton, NJ

Several methods for generating the RF sequential waveform have been demonstrated [1,2]. A frozen wave generator, a simple and efficient device [2], consists of many segments of transmission lines connected by switches in series. When the switches in the generator are closed simultaneously, the "frozen waves" which are charged inside the segments of the transmission line will be brought out sequentially. We have demonstrated in the previous paper [3] the generation, using three silicon switches, of a sequential pulse of two and one half cycles (250 MHz) having a rise time in picoseconds region. However, due to the limited high voltage handling capability of the switches, previous experiments [1,2,3] are not easily extended to the kilovolt applications.

Intrinsic silicon has been widely used as an ultrafast optoeletronic switch for producing nanosecond square pulse. However, due to the thermal runaway phenomenon, silicon switch with a 2mm gap cannot maintain a DC bias in which the voltage across the gap is higher than several hundred volts [4,5]. Two methods were suggested to overcome this problem. The first method is to use a DC bias with the switches at cryogenic temperature [6]. The second method is to use a pulse bias [4,7]. In this report we describe the extension of the previous work [3] by using a pulse bias.

The schematic diagram of the frozen wave generator used in this work is shown in Fig. 1. It is composed of three charged line segments and three silicon switches. The three charged line segments have lengths of 42cm, 42cm, and 21cm, which correspond to pulse lengths of 2ns, 2ns, and 1ns respectively. This frozen wave generator produces a pulse of two and one half cycles with a period of 4ns. Three switches of 0.25mm gap were fabricated on a silicon wafer, and they were separated to prevent coupling between them. The surfaces of the switches were coated with a thin layer of clear epoxy. The pulsed power supply used in this experiment consists of a high voltage charged capacitor, a krytron switch, and an output transformer. The transformer has two secondary windings to produce both positive and negative polarity outputs. A typical output pulse has a $\sim$ 200ns pulse length and 500 to 3000 volts amplitude at 50 ohms load for both polarities.

The single optical pulse is generated from a mode-locked Nd:YAG laser of wavelength 1.06 μm. This picosecond excitation pulse is switched out from a pulse train by a Pockel cell. A photodiode and a variable delay unit were employed to synchronize the charging pulse and the single laser pulse.

An individual switch was tested with a charged line configuration. The pulse charging voltage was varied up to 1300 volts, and a square pulse of up to 600 volts was obtained. The upper limit of charging voltage was tentatively chosen not to exceed the surface breakdown electric field of 5×10^4 v/cm reported previously [7].

In the experiment of sequential wave generation, the switch surfaces were coated with a thin layer of clear epoxy. This improvement made it possible to increase the charging voltage up to $\pm$ 900 volts. A single picosecond laser pulse of $\sim$ 50 μJ was used

to activate the three switches simultaneously. The resultant output waveform, as shown in Fig. 2, has a pulse of two and one half cycles (250 MHz), a period of 4ns, and a peak-to-peak amplitude of 850 volts.

In conclusion, this experiment demonstrates a method to generate a kilovolt sequential waveform pulse by applying a pulse bias to the frozen wave generator. This method could possibly generate sequential waveform pulse of even higher voltage if the surfaces of the silicon switches were properly protected. However, the pulse bias which applied to the silicon switches can extend only to the intrinsic bulk breakdown region(E $\sim 3\times10^5$ v /cm). Therefore, it appears that in future experiments a design utilizing wider gaps in the switches will be necessary for the generation of a multikilovolt sequential waveform pulse.

References

(1) H.M. Cronson, "Picosecond-Pulse Sequential Waveform Generation," IEEE Trans. Microwave Theory Tech., Vol. MTT-23, pp. 1048-1049, 1975.
(2) J.M. Proud, Jr., and S.L. Norman, "High-Frequency Waveform Generation Using Optoelectronic Switching in Silicon," IEEE Trans. Microwave Theory Tech., Vol. MTT-26, pp. 137-140, 1978.
(3) C.S. Chang, M.C. Jeng, M.J. Rhee, Chi H. Lee, A. Rosen, and H. Davis, "Sequential Waveform Generation by Picosecond Optoelectronic Switching", Picosecond phenomena, June 1984.
(4) A. Antonetti, M.M. Malley, G. Mourou, and A. Orszag, "High-Power Switching with Picosecond Precision: Applications to High Speed Kerr Cell and Pockels Cell," Opt. commun., Vol.23, No.3, Dec. 1977.
(5) G. Mourou and W. Knox, "High Power Switching with Picosecond Precision," Appl. Phys. Lett., 35(7), Oct. 1979.
(6) M. Stavola, M.G. Sceats, and G. Mourou, "Picosecond Switching of a Multikilovolt DC Bias with Laser Activated Silicon at Low Temperatures," Opt. commun., Vol.32, pp. 485-488, Mar. 1980.
(7) P. Lefur and D.H. Auston, "A Kilovolt Picosecond Optoelectronic Switch and Pockel's Cell," Appl. Phys. Lett., Vol.28, No.1, Jan. 1976.

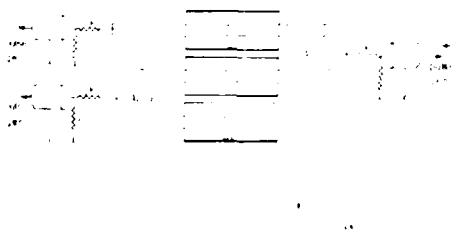

Fig. 1 The schematic of the frozen wave generator

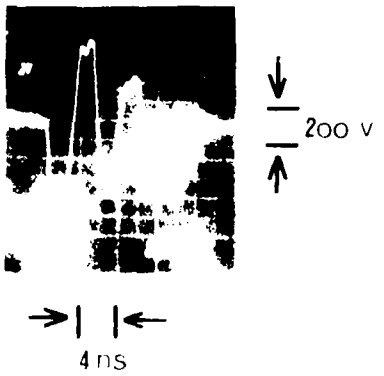

Fig. 2 The oscillogram of the RF waveform

Observation of Modulation Speed Enhancement and Phase Noise Reduction by Detuned Loading in a Coupled-Cavity Semiconductor Laser

Kerry Vahala, Joel Paslaski, Amnon Yariv
128-95 California Institute of Technology
Pasadena, CA 91125

Kam Lau and Nadav Bar Chaim
Ortel Corporation
Alhambra, CA

An understanding of the modulation dynamics and phase noise properties of semiconductor lasers will be essential in certain applications of these devices. In this regard two important quantities are the relaxation oscillation frequency ω_R which sets the useful direct modulation bandwidth of the device [1], and the field spectrum linewidth $\Delta\omega$ which gives a direct measure of phase noise in single mode operation [2,3]. In another paper two of us proposed a new method for control of the above properties [4]. This method, referred to as "detuned loading," was shown in that paper to simultaneously cause enhancement of modulation speed and reduction of phase noise (linewidth). In general, the method involves the introduction of a frequency dependent loss mechanism in the spectral proximity of the lasing frequency and relies upon the unique physics involved in lasing action in a semiconductor (a detuned gain spectrum leading to amplitude-phase coupling in the lasing field [2,3]). In this paper we present the first experimental observations of the detuned loading effect in semiconductor lasers. Specifically, we have observed enhancement of the modulation response with simultaneous reduction of linewidth resulting from application and control of detuned loading.

Our measurement employed a coupled-cavity device consisting of an active cavity loaded by a passive cavity. The active cavity was formed by an Ortel large optical cavity buried heterostructure GaAs/GaAlAs injection laser which lased predominantly in one mode and had a threshod current of 25.6 mA. The passive cavity was formed by one facet of the laser and a small gold coated concave mirror. Piezoelectric micropositioners controlled the mirror's position relative to the laser for tuning purposes.

In such a system modulation corner frequency and linewidth are given by [4],

$$\omega_R^2 = g'_{eff} P/\tau_{eff} \qquad (1)$$

$$\Delta\omega = \Delta\omega_{ST}(1+\alpha_{eff}^2) \qquad (2)$$

where the conventional uncoupled expressions are simply those without the "eff" subscripts. In these expressions P is the photon density and $\Delta\omega_{ST}$ is the modified Schawlow-Townes linewidth. g', α, and τ are the derivative of gain with respect to carrier density, the linewidth enhancement factor and the

unpumped photon lifetime of the lasing mode. Coupling to the passive resonator leads to the effective quantities in (1) and (2) which depend on tuning of the passive resonator.

In Fig. 2 we show the measured modulation response for this device taken at extremes of a tuning range for a single mode (i.e. A range of passive cavity length over which the combined resonator system will not mode jump). The output powers (and hence the photon densities) at these points were the same (Output Power = 1 mW). The effective photon lifetimes are also equal in the two cases as these are endpoints of a tuning range. The conclusion is that the observed corner frequency variation from 1.6 GHz to 2.5 GHz results solely from variation of the effective differential gain (see (3)) with tuning, that is from the detuned loading effect. In this case the net variation in g'_{eff} was roughly 2X. Linewidth measurements will also be presented which show variation of α_{eff} with tuning.

This work was supported by the NSF, ITT Corporation, and Rockwell International.

[1] K. Y. Lau, N. Bar Chaim, I. [illegible], Ch. Harder, A. Yariv, Appl. Phys. Lett., 43, pp. 1-3 (1983)
[2] C. H. Henry, IEEE J. Quant. Electron., QE-18, pp. 259-264 (1982)
[3] K. Vahala, A. Yariv, IEEE J. Quant. Electron., QE-19, pp. 1096-1101 (1983)
[4] K. Vahala, A. Yariv, Appl. Phys. Lett., 45, pp. 501-503 (1984)

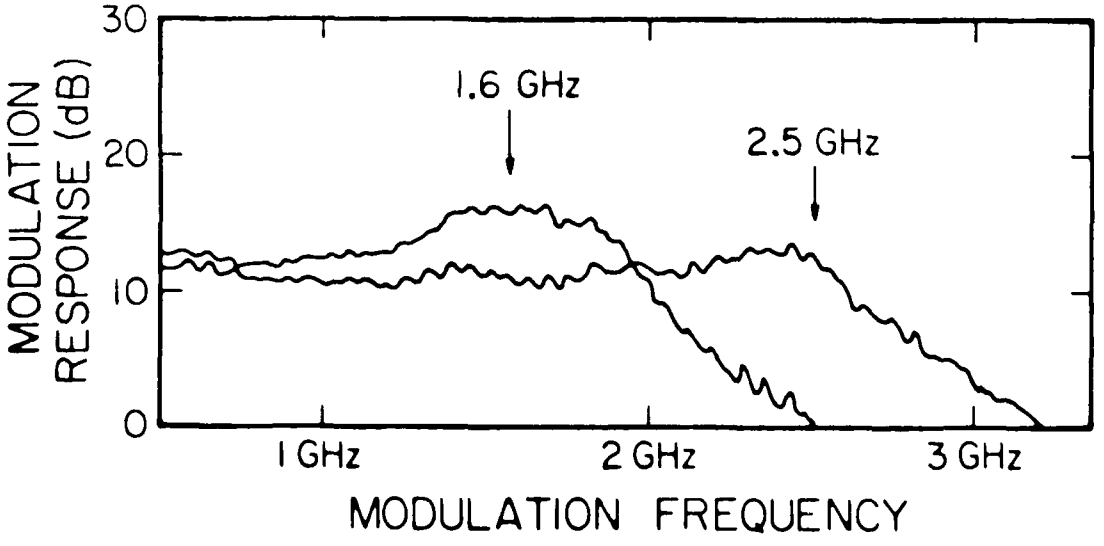

Hot Electron Diffusion in Superlattices

J. Ho and R. O. Grondin
Center for Solid State Electronic Research
College of Engineering and Applied Sciences
Arizona State University
Tempe, Arizona 85287

Hot electron diffusion in a lateral surface superlattice (LSSL) is studied by the Monte Carlo technique. The LSSL is a surface oriented, two-dimensional superlattice made from GaA1As and GaAs. Reich et al [1] have previously developed a Monte Carlo model of hot electron transport in a LSSL. They found that the structure should exhibit a negative differential mobility due to the onset of Bloch oscillations. This negative differential mobility may make this structure useful as a millimeter-wave negative resistance oscillator. To properly model its application as such an oscillator one needs to know the value of the electron diffusion coefficient as a function of field. We have used the Reich model and estimated values of the diffusion coefficient by Monte Carlo techniques.

The diffusion coefficient was estimated by observing an ensemble of electrons whose velocity and position are allowed to evolve in time. The ensemble is initially located at an arbitrary location in real space with initial k-vectors chosen in accordance with an equilibrium Maxwellian. The ensemble is then allowed to evolve through an initial transient into a steady state condition, which is identified by waiting for the drift velocity to settle. The ensemble electrons are all then assigned a real space position of zero, without altering their k-vector values. We then observed the spread of this initial delta function into an approximately gaussian shape and estimated the diffusion coefficient by using the standard time-of-flight estimate

$$D = \frac{\langle \Delta x^2 \rangle}{2t}$$

where D is the diffusion coefficient, Δx is the deviation of an electron real space position from the mean value, and t is the time of flight. The diffusion coefficient fell from a value of 130 cm^2/s at 1 kV/cm, to a value of 7 cm^2/s at 25 kV/cm. Statistical variance of order of 10% is associated with these values.

Reich et al [1] had demonstrated that the velocity fluctuation autocorrelation function exhibited significant peaks at periods corresponding to that of the Bloch oscillation. We also estimated this function, found identical peaks and integrated the function. This integral should also produce the diffusion coefficient [2]. This result of this integration differed by approximately 5% from the above values, a difference which we attribute to both numerical error and to the use of a finite integration time instead of the infinite integration time found in the formal theory. We attribute the low values of diffusion coefficient found at the high fields to the existence of Bloch oscillations. This can be visualized either as a consequence of their producing a damped, oscillatory autocorrelation function, or to the fact that an electron moves in a periodic fashion in real space when it undergoes a Bloch oscillation.

1. R. K. Reich, R. O. Grondin and D. K. Ferry, Physical Rev. B 27 3483 (1983)

2. J. P. Nougier in Nonlinear Transport in Semiconductors, ed. by D. K. Ferry, C. Jacoboni and J. R. Barker, Plenum, New York, 1980

Time-Resolved Photoluminescence of GaAs/$Al_xGa_{1-x}As$ Quantum Well Structures Grown by Metal-Organic Chemical Vapor Deposition

J.E. Fouquet and A.E. Siegman
Edward L. Ginzton Laboratory
Stanford University, Stanford, Ca. 94305

R.D. Burnham and T.L. Paoli
Xerox Palo Alto Research Center
Palo Alto, Ca. 94304

Previous studies of time-resolved photoluminescence from GaAs/$Al_xGa_{1-x}As$ quantum well structures have examined material grown by molecular beam epitaxy. The large differences in behavior seen by different groups suggests a strong dependence of carrier dynamics on material. Until now, time-resolved photoluminescence from GaAs/$Al_xGa_{1-x}As$ quantum wells grown by metal-organic chemical vapor deposition (MOCVD) has not been extensively studied. We report data taken at temperatures from 16K to 300K and over a wide range of excitation densities on MOCVD quantum well structures. These structures were grown in a reactor which routinely produces high quality laser material, and exhibit high photoluminescence efficiency at room temperature.

The photoluminescence decay rate at room temperature depends strongly on excitation energy density in the multiple quantum well sample (Figure 2). The increase in decay time with increasing excitation is characteristic of carriers falling into a limited number of traps. Ryan *et al.* [1] have observed such trapping at 4K in a modulation-doped GaAs/$Al_xGa_{1-x}As$ quantum well sample grown by molecular beam epitaxy. The results presented here are quite unusual, however, in that tens of nanoseconds after the establishment of an initial slow exponential decay rate, the rate increases. This behavior has not been previously observed in bulk GaAs or GaAs/$Al_xGa_{1-x}As$ quantum wells, to the best of our knowledge. This increase in decay rate may be due to carriers falling out of traps with relatively short lifetimes. Considering the enhanced role of interfaces in quantum well structures, these traps may be associated with the interfaces. At the lowest temperatures, exciton dynamics become important. Initial decays are faster than at room temperature and are followed by slower decays. Comparison of time-resolved photoluminescence at different temperatures and excitation levels allows evaluation of the relative roles of bimolecular free carrier recombination, exciton recombination, and trapping.

Room temper.. ure time-resolved photoluminescence using photon energies above (647 nm) and below (752 nm) the barrier bandgap of a single quantum well verifies that the collection time into the well from the continuum is not slow, confirming our expectations. Furthermore, the similar trapping behavior at both wavelengths suggests that the trapping mechanism is not a shallow *n*-type impurity in the $Al_xGa_{1-x}As$ barriers.

References

1. J.F. Ryan, R.A. Taylor, A.J. Turberfield, A. Maciel, J.M. Worlock, A.C. Gossard, and W. Wiegmann, *Phys. Rev. Lett.* **53**, 1841 (1984).

Time-integrated (Figs 1 and 3) and time-resolved (Figs 2 and 4) photoluminescence from the multiple quantum well structure. Excitation wavelength is 647 nm. Resolution is 4 nm. The relative scaling of the different time-resolved photoluminescence curves is only approximate, but each curve follows a consistent scale.

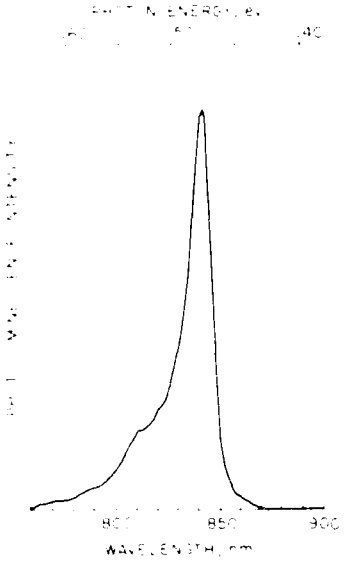

Fig. 1 - Room temperature photoluminescence spectrum

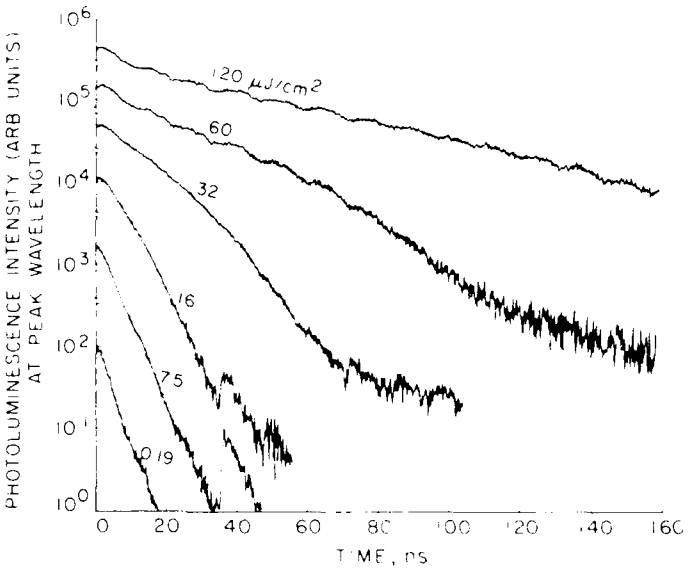

Fig. 2 - Room temperature time-resolved photoluminescence

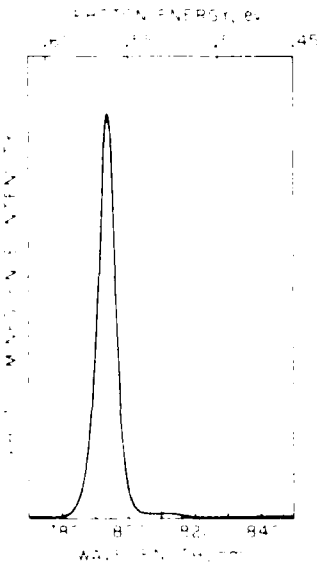

Fig. 3 - 57K photoluminescence spectrum (note scale)

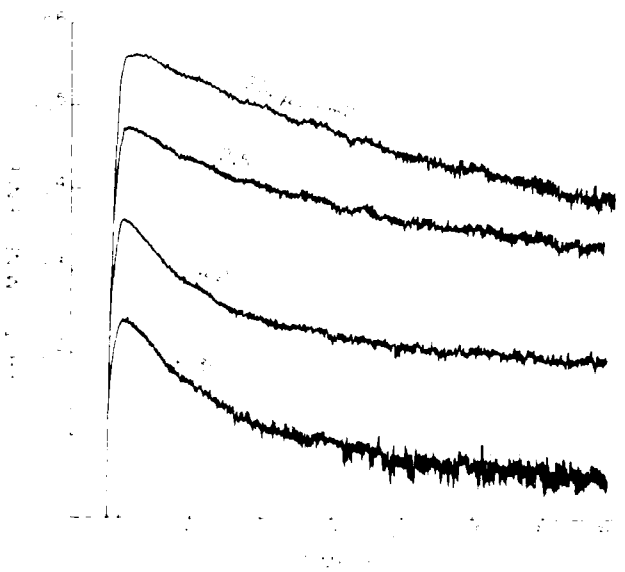

Fig. 4 - 57K time-resolved photoluminescence (note time scale)

PICOSECOND PULSE PRODUCTION IN THE SEMICONDUCTOR LASER WITH A 100 GHz REPETITION RATE

J. McLean, D. Haas, J. Wurl, and
T. K. Gustafson†
Department of Electrical Engineering and Computer Sciences
and the Electronics Research Laboratory
University of California, Berkeley, CA 94720 U.S.A.

(415)642-3139

We present the possibility of optical phase modulation of the semiconductor laser to produce mode locked pulses. By the external injection of two laser lines we show that it is possible to modulate the index of refraction of GaAs through $\chi^{(3)}$ strongly enough to produce pulses in the 5 to 10 psec range. The main advantage of this technique is that repetition rates as high as 100 GHz should be possible.

If the difference frequency of the two external laser lines has a wavelength equal to the semiconductor laser cavity length, then conditions will be favorable for the creation of mode locked pulses with a repetition rate equal to the roundtrip cavity time. The analysis is as follows:

We start with the basic pulse propagation equation [1]

$$[\,i(\beta(\omega_0)-k_0) + (\frac{\partial}{\partial z} + k_1\frac{\partial}{\partial t})]E(t,z) = k_2 i\frac{\partial^2 E}{\partial t^2} - \frac{i}{2k_0}\left\{\frac{\omega_0}{c}\right\}^2 \frac{P_{NL}(z,t)}{\varepsilon_0} \qquad (1)$$

here $P_{NL}(z,t)$ is the nonlinear polarization amplitude corresponding to the difference frequencies of the two external lasers. $P_{NL}(z,t)$ then has the form

$$\frac{\omega_0^2}{c^2}\ \frac{1}{2k_0}\ \frac{P_{NL}(z,t)}{\varepsilon_0} = \alpha_m(1-\cos(\omega_m t - (\beta_1-\beta_2)z))E(z,t) \qquad (2)$$

where α_m is proportional to the third order nonlinear susceptibility and the injected laser intensity. $\beta(\omega_0)$ is the modal propagation constant for the semiconductor laser frequency ω_0. β_1 and β_2 are those of the two injected lasers (assumed real), and ω_m is the modulation frequency $(\omega_1 - \omega_2)$.

†Research sponsored by the National Science Foundation Grant ECS-8318682.

After several standard approximations we find the solutions of eq. (1) to be of the form

$$E(\eta) = e^{-\frac{1}{2}\omega_p^2\eta^2} e^{\frac{1}{2}(\frac{1}{v} - k_1)\frac{1}{\alpha_g T_2^2}\eta} \tag{3a}$$

with

$$\omega_p = (\frac{i\,\alpha_m}{2\alpha_g})^{1/4}(\frac{\omega_m}{T_2})^{1/2} \tag{3b}$$

and

$$1 - \frac{\alpha_l}{\alpha_g} - \frac{1}{4}\frac{1}{(\alpha_g T_2)^2}\left[k_1 - \frac{1}{v}\right]^2 = (\omega_p T_2)^2 \tag{3c}$$

Here α_l is the linear loss and α_g is the peak gain due to stimulated emission. $(T_2)^{-1}$ is the half-width gain. The $(k_1 - \frac{1}{v})$ term is the velocity mismatch which shifts the pulses from the peak of the modulating wave. Also $\eta = t - z/v$, and α_g = gain coefficient. ω_p determines the pulse width and the chirp.

To obtain numerical estimates of the output pulse characteristics we chose a real $\chi^{(3)} = 1.4 \times 10^{-19}(m/v)^2$ which appears pessimistic. For 5 psec pulses Eqs. (3) predicts that roughly 5 watts CW power would provide sufficient modulation. At the present time we are experimentally investigating this approach to ultra-high repetition rate optical pulse generation while numerically calculating pulse characteristics as a function velocity of mismatch, $\chi^{(3)}$, and more detailed representations of the gain medium. More generally the theoretical approach, which generalizes the Kuizinga Siegman theory[2] to semiconductor laser pulse generation, can be used to discuss pulse generation through a complex $\chi^{(3)}$ either by parametric or fully-nonlinear self-excitation. The possibility and limitations upon the latter will be discussed. It is anticipated that by utilizing various techniques to enhance the nonlinearity such modulation schemes will be useful for a wide range of optical signal processing devices.

References

[1]T. K. Gustafson, J. P. Taran, H. A. Haus, J. R. Lifsitz, and P. L. Kelley, Phys. Rev. **177**, 306 (1969).

[2]D. J. Kuizenga and A. E. Siegman, IEEE J. Quantum Electron., **QE-6**, 694 (1970).

Measurements of the Temperature and Intensity Dependence of Transient Photoconductivity in InP:Fe*

D. R. Kania and R. J. Bartlett
Physics Division
Los Alamos National Laboratory
Los Alamos, New Mexico 87545

and

R. B. Hammond and D. L. Smith
Electronics Division
Los Alamos National Laboratory
Los Alamos, New Mexico 87545

Recent applications of photoconductors as radiation detectors[1] has increased interest in a deeper understanding of the operation of these devices and the physical processes affecting their operation. Specifically, a more complete understanding of transient recombination of photoproduced carriers in intrinsic semiconductors is required. Here, we report our measurements of the temperature and photon intensity dependence of transient photoconductivity in InP:Fe photoconductors.

Samples of InP:Fe were mounted in 50 Ohm striplines. The detectors had impulse response FWHM of 150 - 1500 ps as measured with a 90 ps laser diode pulse. A semiconductor diode laser pulser was configured to produce 1 - 1000 ns long light pulses (830 nm) with rise and fall times of less than one nanosecond. The maximum power was 5 mW and was constant ± 3% for the duration of the pulse. The light intensity exciting the detector was controlled with neutral density filters. The detectors were mounted in a cryogenic cooler and the temperature was varied from 77 to 300 K.

Tests performed on room temperature detectors show nonlinearities in the photoresponse. We have developed a theoretical model which predicts the observed nonlinear phenomena. The model includes trapping and recombination of electrons and holes at Fe sites in the InP crystal. In an attempt to further our understanding of these phenomena and to facilitate the production of linear devices, we have measured the intensity and time dependence of photoconductivity as a function of the temperature in InP:Fe photoconductors. This information yields an indirect measurement of the temperature dependence of the electron and hole recombination rates and indicates how the linearity of these photoconductors may be increased for detector applications.

*Work performed under auspices USDOE.

[1]D. R. Kania, et. al., Appl. Phys. Lett. 44(11), 1059 (1984).

Pulse Waveform Standards for Electro-Optic Sampling

Dr. Robert A. Lawton

Electromagnetic Fields Division
National Bureau of Standards
325 Broadway
Boulder, Colorado 80303

Summary

The maturing of the semiconductor industry has resulted in the need for faster methods for the measurement of pulse waveforms. The measurement requirements are fast outstripping the capability of integrated circuit testers. The fastest commercial sampling oscilloscope today has a step response transition duration (risetime) of 20 picoseconds. For the measurement of single transients, available time resolution is somewhat less. This time resolution is not adequate to support the measurement of the faster semiconductor devices being developed such as gallium arsenide logic gates whose switching times have been estimated to be 12 picoseconds (1). Measurement of such transitions requires a significant advance in measurement technology. A prime candidate for making the required quantum leap in time measurement resolution is the electro-optic sampler (2). This sampler has a demonstrated resolution of 0.4 picoseconds and theoretical resolution limit much shorter than that.

Much work remains to be done, however, to make this an accurate means of measuring pulse parameters. An important step in that direction would be the development of a reference waveform standard by means of which the pulse waveform measurement accuracy of the Automatic Pulse Measurement System (3) (APMS) at the National Bureau of Standards (NBS) can be applied to the electro-optic sampler. This talk will trace the development of reference waveform standards at NBS and will describe measurements made with electro-optic samplers on three commercial pulse generators to test their viability as reference waveform standards for electro-optics. These generators are: a tunnel diode; a complete pulse generator with variable pulse duration, repetition rate etc.; and a comb generator.

1. G. Nuzillat, "GaAs IC Technology for Ultra-High Speed Digital systems", URSI XXIst General Assembly digest and lecture, Florence, Italy, Aug. 28 - Sept. 5, 1984, p. 496.

2. J.A. Valdmanis, G. Mourou, and C.W. Gabel, "Subpicosecond Electrical Sampling" Proceedings of the SPIE, Vol. 439, Aug. 24-26, 1983, p. 142.

3. N.S. Nahman, J.R. Andrews, W.L. Gans, M.E. Guillaume, R.A. Lawton, A.R. Ondrejka and M. Young, "Application of Time Domain Methods to Microwave Measurements", IEE Proc., Vol. 127, Pt. H, No. 2, April, 1980, p.

Monte Carlo Investigation of Hot Carriers Generated by Subpicosecond Laser Pulses in Schottky Barrier Diodes*

M.A. Osman, U. Ravaioli and D.K. Ferry

Center for Solid State Electronics Research
Arizona State University
Tempe, Arizona 85287

The self-consistent Ensemble Monte Carlo (E.M.C.) method is used to study the dynamics of carriers generated by subpicosecond laser pulses in a Silicon n+/n/metal submicron Schottky diode. The E.M.C. model for the Schottky diode is the same presented in [1]. In this model the Poisson's equation is solved using an accurate collocation method [2], which gives a very precise solution for the electric field E on the ohmic contact boundary. This allows us to determine the current injected through the ohmic contact using the relation $J=n^{+}\mu_{o}E(0)$, where μ_{o} is the low field mobility in an n^{+} contact region. This is justified if the width of the n^{+} region is at least a few Debye lengths, so that we can consider the carriers at the ohmic contact boundary to be in equilibrium with the lattice. In this way we can model the depletion of carriers and fully account for the non charge neutral behavior of the Schottky barrier diode, keeping track of the carriers exiting the device and allocating the ones which are not reinjected on the metal side.

Tunnelling current from the semiconductor to the metal is included by a WKB approach as in [1], with an improved formulation of the tunnelling probability, which takes into account nonparabolicity and the effect of finite bandgap.

The photoexcitation of carriers is made by simulating a laser pulse with subpicosecond duration. For Silicon the useful wavelengths which we can investigate span between 0.5 and 1.2 μm [3].

The excess energy of the photoexcited electrons has been evaluated including nonparabolicity of the conduction band, and the dependence on whether the generated hole is light or heavy. In the random excitation process of our model we therefore take into account the generation probability of light and heavy holes which, for Silicon, is found to be respectively 16% and 84% . Parabolic, spherical valence bands are considered to compute the excess energy of the photogenerated holes.

In our approach we neglect the energy spread due to the phonons, so that the transition between valence and conduction band is treated as a direct one. This is justified for our purposes since the excess energy of the generated carriers is much greater than the phonon energy. Moreover, we have to consider that soon after generation the carriers relax to the bottom of the conduction band by emitting successive optical phonons, and during this particular process the equilibrium state of the crystal lattice is basically unaltered.

Using the E.M.C. simulation for the carrier dynamics, we do not have to make any simplified assumption on the electron transport [3] to estimate the transit time across the device, since all the scattering and nonlinear transport effects are naturally included in the E.M.C. model. Carrier-carrier interaction, energy-gap narrowing and state filling effects [4], which are effective at high excitation and/or doping levels are neglected in this study.

The transport of holes will also be included in our results. Energy dependent electron-hole recombination can also be considered. However, since we simulate a submicron diode, the recombination rate across the device turns out to be very small, for the doping levels in our model, and is therefore neglected in the present approach.

* Supported by the Army Research Office and the Office of Naval Research

[1] P. Lugli, U. Ravaioli and D.K. Ferry: "Monte Carlo simulation of contacts in submicron devices", to be published in Proceedings of VLSI Satellite Conference, Palo Alto, 1984.

[2] U. Ravaioli, P. Lugli, M. Osman and D.K. Ferry: "Advantages of collocation methods over finite differences in one-dimensional Monte Carlo simulation of submicron devices", II Conference on Numerical Simulation of VLSI Devices, Boston, 1984, to be published.

[3] B.J. Thelan, L.R. Larson, N.V. Frederick and D.L. Franzen: "Subnanometer interdigital silicon detectors for the measurement of picosecond optical pulses", Proceedings of SPIE, Picosecond [illegible], Vol. 439, p. 92, 1983.

[4] S.D. Ferris: "Energy gap narrowing and state filling effects in [illegible] high intensity laser irradiation", Phys. Rev. B, Vol.18, p. [illegible], 1978.

Hertzian Dipole Measurements with InP and InGaAs Photoconductors

P. M. Downey and J. R. Karin
AT&T Bell Laboratories
Holmdel, N. J. 07733

Research in the use of radiation damaged semiconductors[1] as picosecond photoconducting pulse generators and sampling gates has led to the identification of material systems where subpicosecond[2] free carrier relaxation times along with reasonably high free carrier mobilities and material dark resistivities can be realized. However, on such small time scales these optoelectronic autocorrelation measurements are limited by the speed of response of the microstrip circuits used[3]. A recently described measurement scheme[4] overcomes such circuit limitations to the response speed by utilizing picosecond photoconductors as radiating and receiving dipole antennas. In such Hertzian dipole experiments no transmission line structures are used to couple the electrical pulse generator to the sampling gate; instead, the picosecond electromagnetic pulse from the pulse generator is radiated freely through a bulk dielectric medium to the receiving photoconductor, which acts as a picosecond sampling gate. This results in a high pass coupling scheme, as opposed to the low pass transfer characteristics of microstrip interconnections.

In this paper we will discuss and compare Hertzian dipole measurements of the picosecond photoresponse in radiation damaged InP and InGaAs photoconductors in two different configurations: the back-to-back geometry described previously[4], and a face-to-face geometry. For our measurements in the back-to-back geometry, the photoconductors were separated by two 250 micron thick semi-insulating InP substrates ($\epsilon_r = 12$) sandwiching an Al foil aperture. In the face-to-face geometry, the photoconductors were spaced ~ 7 mm apart on opposite sides of an Al foil aperture (diameter ~ 1 mm). The aperture limits the field of view of the receiving photoconductor and serves as a high pass filter on the radiated field from the pulse generating photoconductor.

The results obtained from correlating the photoresponse of two $^3He^+$ bombarded InP photoconductors in the face-to-face geometry are shown in Fig. 1. The correlation trace has a FWHM of 1.7 ps and a 10-90 percent risetime of 1.8 ps on the reflection-free (left) side. This risetime can be attributed primarily to the rapid decay of the photoresponse in the receiving photoconductor. The rapid decay on the right hand side of the correlation trace, however, cannot be directly attributed to the speed of response of the pulse generator. This is graphically demonstrated in Fig. 2, which shows a Hertzian dipole measurement obtained with the same setup and sampling gate as for Fig. 1 but with a Be bombarded InGaAs photoconductor as the pulse generator. Although Fig. 2 indicates a decay time for the radiated pulse of several picoseconds, simultaneous sampling oscilloscope measurements of the InGaAs photoconductive response exhibited a 1/e decay time of 400 ps[5]. This discrepancy between the speed of response of the pulse generator as determined by Hertzian dipole measurements and by sampling oscilloscope measurements can be attributed to the high pass transfer characteristics of the aperture. We conclude then that the aperture makes a major contribution to the speed of the Hertzian dipole measurements.

REFERENCES

[1] P. R. Smith, D. H. Auston, A. M. Johnson, and W. M. Augustyniak, Appl. Phys. Lett. 38, 47 (1981).

[2] P. M. Downey and B. Tell, to be published in J. Appl. Phys.

[3] P. M. Downey and B. Schwartz, Appl. Phys. Lett. 44, 207 (1984).

[4] D. H. Auston, K. P. Cheung and P. R. Smith, Appl. Phys. Lett. 45, 284, (1984).

[5] P. M. Downey, R. J. Martin, R. E. Nahory and O. G. Lorimor, submitted to Appl. Phys. Lett.

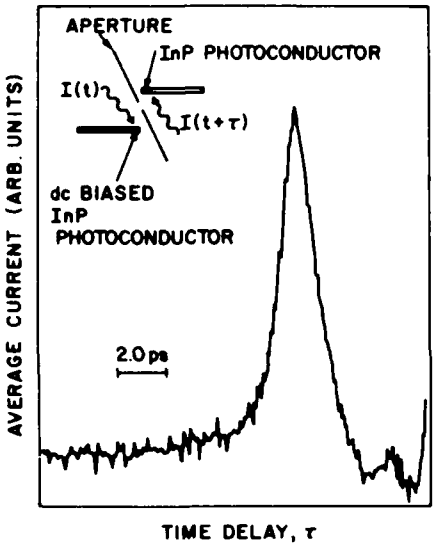

Fig. 1 Correlated photoresponse of two ion bombarded InP photoconductors, configured in a face-to-face geometry as illustrated in the inset. The plotted curve shows the average current through the receiving dipole (upper right) vs. relative delay in the optical excitation of the two photoconductors. The transmitting (dc biased) and receiving photoconductors received radiation doses of $4x10^{14}$ and $1x10^{14}$ $^3He^+/cm^2$ respectively.

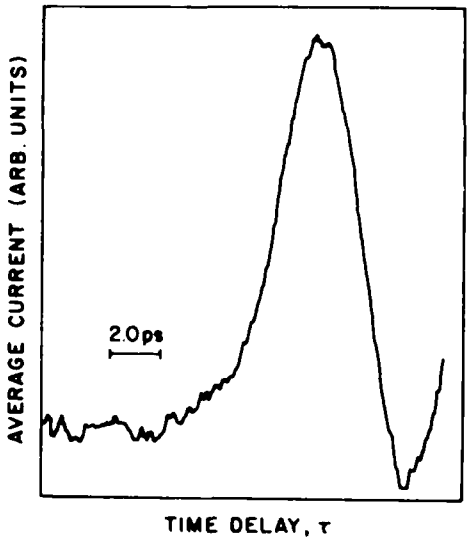

Fig. 2 Correlated photoresponse observed with the same setup used for Fig. 1 except that the transmitting dipole is now a radiation damaged InGaAs photoconductor characterized by a free carrier lifetime of 400 ps.

Modeling of Picosecond-Pulse Propagation in Silicon Integrated-Circuits

K. W. Goossen
Electrical Engineering Department, Princeton University, Princeton, NJ 08544

R. B. Hammond
Electronics Division, Los Alamos National Laboratory, Los Alamos, NM 87545

We have made theoretical time-domain analyses of the dispersion and loss of both square-wave and exponential pulses on microstrip transmission line interconnections on silicon integrated-circuit substrates. Geometric dispersion and conductor linewidth, as well as losses from conductor resistance, conductor skin effect, and substrate conductance are considered over the frequency range from 100 MHz to 100 GHz. Results show the enormous significance of the substrate losses, and demonstrate the need for substrate resistivities >10 Ω-cm for high performance circuits. The results also show the effects of geometric dispersion for frequencies above 10 GHz (which increase with decreasing linewidth), the transition from the high-frequency quasi-TEM regime to the "slow-wave" regime, and the unimportance of conductor skin-effect losses for frequencies up to 100 GHz. Qualitatively similar phenomena are seen for Al, W, and WSi_2 lines. The differences in resistivity of these materials do not significantly alter their pulse propagation properties. Surprisingly, however, slow-wave velocity is increased for either increasing conductor resistivity, decreasing conductor linewidth, or both. Poly-Si, with its significantly greater loss, shows qualitatively different frequency-dependent behavior. High phase velocity and high loss can coexist in poly-Si lines.

We present model calculations of picosecond pulse propagation for various conductor linewidths and conductor materials on 10 and 100 Ω-cm silicon substrates.

Femtosecond nonlinearities of standard transparent optical glasses

J. Etchepare, I. Thomazeau, G. Grillon, A. Migus and A. Antonetti

Laboratoire d'Optique Appliquée. Ecole Polytechnique. ENSTA. 91120-Palaiseau

Several standard silicate glasses have been shown to present large third order susceptibilities ($\chi^{(3)} \simeq 10^{-14}$ esu)[1]. We report here kinetics of induced anisotropies resolved on a femtosecond time scale. For all the studied glasses, we find responses always limited by the pulsewidth which implies that the processes involved are of electronic origin. A correlation is verified between the nonlinearities and the linear indices of refraction and spectral dispersion.

The technique of measurement is based on the optical Kerr effect. Gigawatt peak power pulses of 100 fs. FWHM at 620 nm are used for excitation; the probe pulse wavelength is selected at a specific value from a continuum of light. The several materials investigated are readily available optical glasses from Schott, Corning France and Hoya industries; they all are transparent in the whole visible wavelength range.

For binary lead silicate glasses, the nonlinearity increases with lead concentration; lead is present in glass as cation network modifier and its nonlinear character is fully explained by the high polarizability of Pb^{2+} ions. Other glasses, with more complex and not well known exact composition, have been studied. We report results on TiO_2 doped glasses showing that for equivalent content in modifier ion, those media are more efficient nonlinear materials than lead glasses. We attribute this effect to the known high nonlinearities of TiO_2.

As a comparison, we present in a last step kinetics of color glasses which have been shown[2] to exhibit third order nonlinearities of $\simeq 10^{-9}$ esu.

We have detected in these glasses a two step process : an instantaneous one, and an other one, most efficient, and characterized by a relaxation time in the range of several tens of picoseconds.

1. I. Thomazeau, J. Etchepare, G. Grillon and A. Migus
Submitted for publication

2. R.K. Jain and R.C. Lind,
J. Opt. Soc. Am. 73, 647 (1983).

THURSDAY, MARCH 14, 1985

ThA, OPTOELECTRONICS

John Whinnery, UC-Berkeley, *Presider*

Picosecond Integrated Optics

R. C. Alferness, S. K. Korotky, G. Eisenstein, R. S. Tucker
AT&T Bell Laboratories
Crawford Hill Laboratory
Holmdel, NJ 07733

We review the principles, current status, and potential applications of high-speed Ti:LiNbO optical waveguide switch/modulators as well as the use of such devices as intracvity elements for semiconductor laser mode locking.

A Study of Exciton and Carrier Dynamics and a Demonstration of One-Picosecond Optical NOR Gate Operation of a GaAs-AlGaAs Device

N. Peyghambarian, H. M. Gibbs and J. L. Jewell*
Optical Sciences Center
University of Arizona
Tucson, AZ 85721

A. Migus and A. Antonetti
Laboratoire d'Optique Appliqué
Ecole Polytechnique-ENSTA
F-91120 Palaiseau, France

D. Hulin and A. Mysyrowicz
Group de physique des solids
Ecole Normale supérieure
2 Place Jussieu, F-75005
Paris, France

We report the first time-resolved observation of a GaAs-AlGaAs multiple-quantum-well (MQW) optical NOR gate. The ≈ 1-ps speed of this room-temperature nonlinear etalon is the fastest for such a low-power optical logic device. About 100-fJ/μm² energy per unit area was used for the logic operation.

The device consists of alternating layers of 152-Å GaAs and 104-Å AlGaAs (≈ 1.5 μm total GaAs thickness) grown by molecular beam epitaxy on a GaAs substrate. The substrate was etched away and the remaining flake sandwiched between two dielectric coated glass slides with ≈ 90% reflectivities. The amplified output of a cw mode-locked ring dye laser[1] (pulses of ≈ 100-fs duration at 620 nm) was divided into two parts, each focused on a 2-cm-long water cell to generate white-light-continuum pulses (also of ≈ 100-fs duration). One of the continuum pulses was used as a broad-band probe; and a narrow-band interference filter was inserted in the second continuum beam to generate a pump beam with frequency above the band gap of GaAs (wavelength ≈ 760 nm). The pump frequency was below the band gap of AlGaAs, so only GaAs layers were excited. The probe beam was focused to a 50 to 100 μm spot. The pump beam overlapped the probe and was focused to a much larger spot. The focal spot was magnified by a factor of 40, and a 200-μm pinhole was scanned across this image to probe small areas of the device (effective sample size ≈ 5 μm). The probe light was detected either by a combination of optical multichannel analyzer, spectrometer, and photodiode array or by a single photodiode and spectrometer.

The origin of the optical nonlinearity in our device is the presence of an exciton resonance below the band gap of GaAs at room temperature. The device is adjusted in the absence of the pump beam such that one of the Fabry-Perot transmission peaks is on the low-frequency side of the exciton resonance. The pump beam creates carriers, screening the Coulomb interaction between electron and hole in the exciton orbit and causing saturation of the exciton absorption. If the device is originally transmitting, the application of the pump shifts the Fabry-Perot peak away from the laser wavelength causing the transmission to decrease. This is the physical mechanism for the operation of our optical NOR gate.

*Presently at AT&T Bell Laboratories, Holmdel, NJ 07733

Dynamical measurements of exciton screening either by injecting carriers or additional excitons give information about the saturation time of the exciton resonance, its recovery time, dissociation time of excitons into free carriers and the formation time of excitons from free carriers. The exciton screening in MQW samples is instantaneous within the resolution of the measuring system of ≈ 150 fs. Since the index change occurs as fast as the exciton saturates, the speed of the optical gate should be limited by the cavity buildup time of $(2n\ell/((1-R)c) \approx 300$ fs (assuming an effective mirror reflectivity of 0.6 from the measured finesse of ≈ 6). However, the data suggest[3] that the shift of the Fabry-Perot peak lasts for ≤ 3 ps. This sluggishness in the response might be attributed to the induced absorption occurring on the tail of the exciton resonance. The measurements of the exciton dynamics suggest that this absorption lasts for a few picoseconds. The index change due to the induced absorption might partially cancel that caused by the exciton saturation until the induced absorption decreases. In fact, the next Fabry-Perot order at about 200 Å longer wavelength, where the exciton absorption has dropped considerably, shows a faster response of ≈ 1 ps. (The NOR-gate contrast for this transmission peak was poor because of its greater detuning from the exciton resonance.)

In conclusion, we have performed measurements of exciton and carrier dynamics and demonstrated for the first time ≈ 1-ps operation of an optical NOR gate using a GaAs-AℓGaAs nonlinear etalon at room temperature and a femtosecond laser system. These measurement show that an etalon peak can be shifted in ≈ 1 ps. The NOR gate contrast is only ≈ 2.5 because our probe pulses are shorter than the cavity response time of the etalon, but we have observed recently a contrast of more than 4 to 1 in a similar device with less than 3 PJ of energy incident. The measured speed of this gate also suggests that similar MQW bistable switches should have the same switch-on times (the fastest measured switch-on time previously reported for a bistable device is detector-limited 200ps[2]). An array of such devices might allow parallel logic operations and may also be used as an all-optical addressable spatial light modulator.

The Arizona portion of this research has been supported by grants from NSF, AFOSR, ARO and NATO 882/83. The authors would like to thank A. C. Gossard and W. Wiegmann for the MQW crystals.

References

1. A. Migus, J. L. Martin, R. Astier, A. Antonetti and A. Orszag in Picosecond Phenomena III (Springer, New York, 1982) p. 6.

2. S. S. Tarng, K. Tai, J. L Jewell, H. M. Gibbs, A. C. Gossard, S. L. McCall, A. Passner, T. N. C. Venkatesan and W. Wiegmann, Appl. Phys. Lett. 40, 205 (1982).

3. A. Migus, A. Antonetti, D. Hulin, A. Mysyrowicz, H. M. Gibbs, N. Peyghambarian and J. L. Jewell, to be published in Appl. Phys. Lett. Jan. 15, 1985.

22-GHz Bandwidth InGaAs/InP PIN Photodiodes

by

J. E. Bowers*, C. A. Burrus** and R. S. Tucker**

Holmdel* and Crawford Hill** Laboratories
AT&T Bell Laboratories
Holmdel, NJ 07733

Fast GaAs Schottky photodetectors for visible and near-infrared applications have been demonstrated [1], and high-speed PIN structures using InGaAs/InP for the emerging lightwave communications wavelengths ($1.3 - 1.6\ \mu m$) have been reported [2,3]. We describe here the fabrication and characterization of an improved InGaAs/InP PIN photodiode with a measured 3 dB bandwidth of 22 GHz.

The structure of the improved detector (Fig. 1(a)) is similar to detectors described previously [2]. It is a $25-\mu m$ diameter mesa utilizing a $2-\mu m$ thick layer of zinc-diffused p^+ InGaAs on a $1.5-\mu m$ thick layer of n-InGaAs grown on a (100) n^+InP substrate. The structure is back-illuminated, and a $25-\mu m$ diameter wire contact is epoxied to the top of the metalized mesa. The capacitance of the junction at -10 V bias is about 0.05 pF. A commercial package for microwave detectors (HP 3330C) was modified to accept the back-illuminated detectors. The biasing circuit is shown in Fig. 1(b).

The frequency response of the detectors was determined by illuminating the diode with a 100-MHz train of 10-ps (FWHM) pulses at $1.5-\mu m$ wavelength (from a mode-locked color-center laser [4]) and measuring the rolloff with a spectrum analyzer connected directly to the detector package (Fig. 1(b)). The result is shown in Fig. 2 for optical pulses with a peak power of 10 mW. The response rolls off by just 3 dB at 22 GHz. Using the measured pulsewidth of 10 ps, we calculate that 2 dB of the rolloff is probably due to the finite frequency content of the laser source. This was confirmed by observing the degradation in the measured frequency response which accompanied a slight detuning of the laser. Three detectors from this wafer were measured and all had -3 dB frequencies in excess of 21 GHz. The -3 dB frequency did not decrease when the optical beam was laterally misaligned or defocused. The frequency response did degrade for peak optical powers greater than 20 mW. The bias dependence of the -3 dB frequency is shown in Fig. 3. The response to constant at 22 GHz from 10 to 20 V.

The improved frequency response (22 GHz versus 12 GHz [2]) is due to (1) shorter hole and electron transit times resulting from the thinner (1.5 μm) n-layer in this detector, (2) lower doping in the n-layer, and (3) improved packaging.

We wish to thank L. F. Mollenauer for allowing us to use the color-center laser, S. Lorimer and A. Dentai for providing LPE wafers, and J. C. Campbell, S. K. Korotky, and D. M. Bloom for useful discussions.

References

[1] S. Y. Wang and D. M. Bloom, Electron Lett. *19*, 554 (1983).

[2] T. P. Li, C. A. Burrus, K. Ogawa, and A. G. Dentai, Electron Lett. 17, 431 (1981).

[3] K. Li, E. Rezek and H. D. Law, Electron Lett. *20*, 196 (1984).

[4] L. F. Mollenauer and D. M. Bloom, Optics Lett. *4*, 297 (1979).

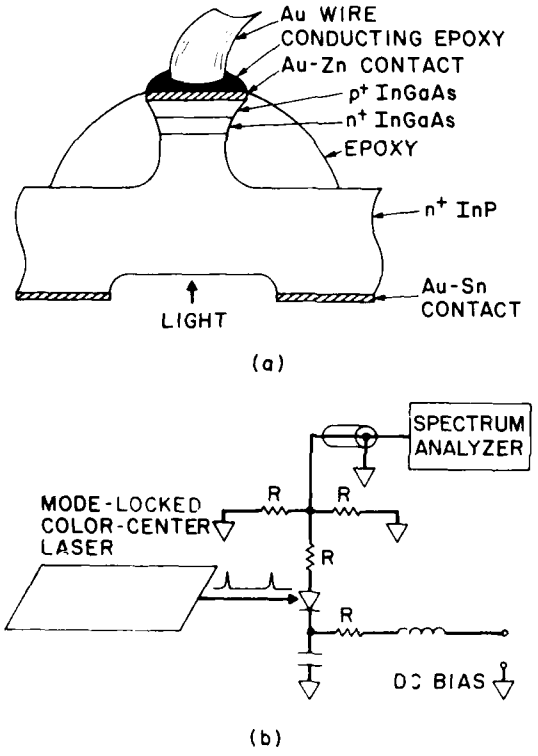

1. (a) Schematic diagram of back-illuminated PIN InGaAs/InP photodetector. (b) Experimental set-up and diagram of biasing network.

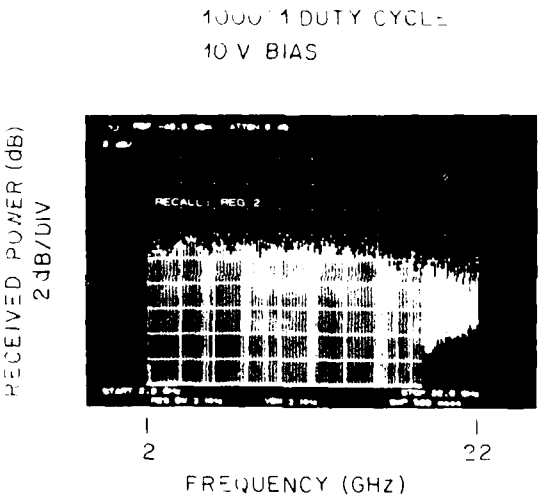

2. Frequency response of photodetector for excitation with 10-mW peak power, 10-ps FWHM pulses at 1.5 μm.

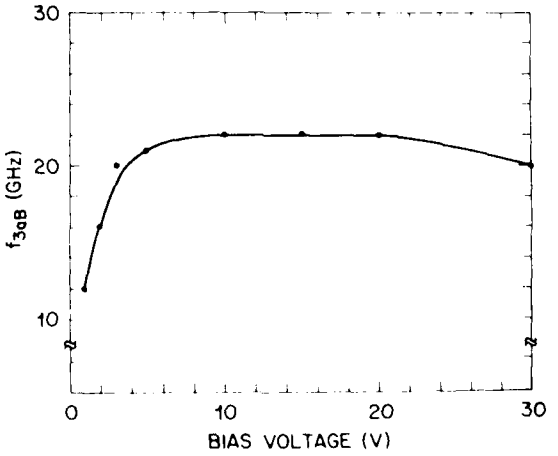

3. Bias dependence of -3 dB frequency.

ULTRAFAST TRAVELING-WAVE LIGHT MODULATORS WITH REDUCED VELOCITY MISMATCH

Masayuki IZUTSU, Hiroshi HAGA, and Tadasi SUETA

Faculty of Engineering Science, Osaka University
Toyonaka, Osaka 560, Japan

For the high-speed and wideband operation, the traveling-wave structure has been developed for guided-wave modulators. Applying the asymmetric stripline as electrodes, the frequency response of the $LiNbO_3$ waveguide modulators has been smoothed over. The operation bandwidth has been expanded up to 18 GHz[1] and a temporal pulse waveform less than 50 ps created by the modulator has already been observed by the streak camera[2].

The bandwidth of the traveling-wave modulator is inversely proportional to the velocity difference of light and modulating waves[3]. For a $LiNbO_3$ waveguide modulator with the coplanar parallel strip electrode, the guided lightwave travels two times faster than the modulating microwave, so that the 3dB bandwidth becomes 6.6 GHz (for 1 cm long electrode) which is three times broader than that of the conventional lumped type modulator of the same size.

To realize wider bandwidth or faster time response, it is important to reduce the velocity mismatch between light and modulating waves. If the velocity of the modulating microwave can be increased about 15 %, nearly 50 % broadening of the bandwidth is expected for the $LiNbO_3$ traveling-wave modulator.

For the reduction of velocity mismatch, several methods have already been proposed to modify the electrode structure[4-6]. These can be grouped into two types. In the first type, discontinuities along with the electrode are introduced periodically to readjust the phase relation between two waves which changes during their propagation. The discontinuities yields an unevenness of the frequency response which results to the complicated time response of the modulator. The second type uses a modified electrode cross section. A material of low dielectric constant is placed close proximity to the electrodes to decrease the effective refractive index for the microwave.

We have considered to use the double-layer substrate as shown in Fig. 1. The waveguide is in a thin layer of the high index crystal of which thickness d is in the same order to the electrode separation s. A portion of the modulating field energy spreads to the low index bottom layer to decrease the effective index. The calculated effective index for the modulating wave versus the thickness of the high index film is also shown in the figure.

The change of the effective index was measured experimentally. The $LiNbO_3$ film was supported by the glass block which had a long hole just below the optical and microwave waveguides on the crystal film so that the underlayer was air. For a 28 μm wide electrode of 13 μm separation on a 20 μm thick crystal film, measured characteristic impedance of the line was between 45 and 55 ohms. The effective index for the microwave was measured as 3.2 which implys the bandwidth is doubled. Modulation experiment is remained for the future work.

Fig. 2 shows our another model to reduce the velocity mismatch. A hollow channel is made on the crystal surface between two electrodes, so that the effective index for the microwave is decreased. At the same time, unwanted coupling of the light beams in parallel waveguides is suppressed by the groove to achieve high extinction ratio with shortened waveguide separation. The device employs the Mach-Zehender interferometer structure with the asymmetric X junction as the output coupler to have two complementary outputs.

The 6 μm wide groove was made by the reactive ion etching to 4.3 μm deep. Aluminium electrode 3 μm thick was fabricated with 80 nm SiO_2 buffer layer. The 6 mm long strip electrode was 20 μm wide and 10 μm apart from the ground plane. The effective index for the microwave decreased to 3.8 from the conventional value 4.2, so that the 20 % broadening of the bandwidth is expected. The half-wave voltage was 3 V for 630 nm TM mode and the extinction ratio was −18 dB. The modulation frequency response at the microwave region is also shown in Fig. 2. The 3 dB bandwidth is 12 GHz and, consequently, the P/Δf figure is 4.2 mW/GHz for 88 % intensity modulation.

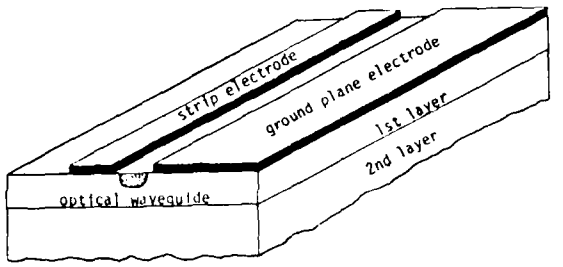

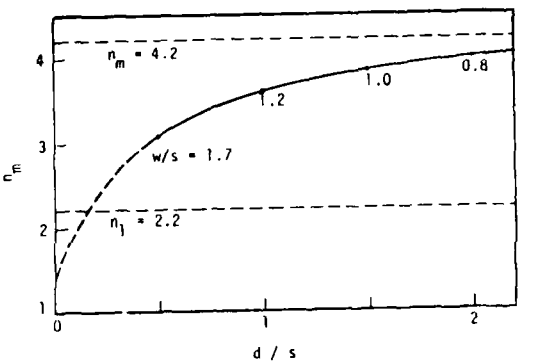

Fig. 1 Traveling-wave modulator with double-layer substrate

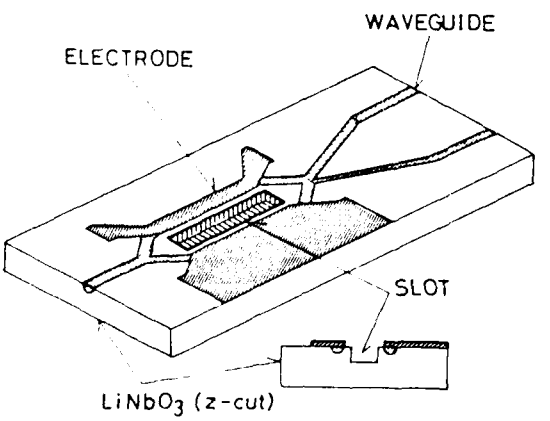

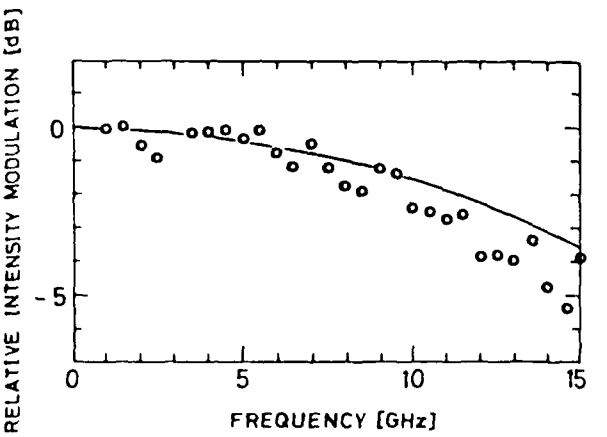

Fig. 2 Traveling-wave modulator with grooved substrate

REFERENCES
[1]M. Izutsu, T. Sueta: Trans. IECE Japan, J64-c, 264/271, 1981.
[2]M. Izutsu, T. Sueta: IEEE J.Q.E., 19, 668/674, 1983.
[3]M. Izutsu, T. Sueta: Appl. Phys., 5, 307/315, 1975.
[4]E.A.J. Marcatili: Appl. Opt., 19, 1468/1476, 1980.
[5]P.L. Liu: J. Opt. Commun, 2, 2/6, 1981.
[6]R.C. Alferness, S.K. Korotky, E.A.J. Marcatili: IEEE J.Q.E., 20, 301/309, 1984.

Direct DC to RF Conversion by Impulse Excitation of a Resonant Cavity

Ming G. Li, Chi H. Lee, A Caroglanian and E. A. Greene+
Department of Electrical Engineering
University of Maryland
College Park, MD 20742

C. Y. She* and P. Polak-Dingles
Laboratory for Physical Sciences
4928 College Avenue
College Park, MD 20742

A. Rosen
RCA Laboratories
Princeton, NJ 08549

Direct DC to RF conversion with an optoelectronically switchable frozen-wave generator has recently been demonstrated.[1,2] Using picosecond optical pulses. A sequential waveform consisting of two and one half cycles has been obtained with a voltage conversion efficiency better than 90%.[2] However, there are some drawbacks associated with the frozen-wave generator device. One of them is that a large number of switches must be simultaneously activated and each switch must operate at close to 100% efficiency in order to form a good pulse sequence. These requirements are rather difficult to meet, because each switch may have somewhat different characteristics owing to the fabrication process. The simultaneous closure of several switches also demands a large amount of laser energy.

In this paper, we report on our recent study of DC to RF conversion using a single optoelectronic switch and a coaxial resonant cavity. The basic principle is described below. (Fig. 1) The electrical impulse generated by an optoelectronic switch is coupled via an antenna to a coxial structure cavity. This pulse will reflect back and forth inside the resonant cavity which is shorted at one end and opened at the other end. At the shorted end of the cavity, the resultant electrical field has to be zero to meet the boundary condition. Thus the reflected electrical field must have the same amplitude but opposite parity of the incident pulse. At the open end, the total current must be zero. Thus the reflected current pulse has opposite polarity. The pulse bouncing back and forth inside the coaxial cavity forms a series of pulses of alternative polarities. If one uses another antenna inside the cavity to couple these pulses out, the output signal will consist of a damped periodic pulse train. The frequency of this oscillation equals to the cavity resonant frequency. The damping rate depends on the coupling coefficiency of the cavity or the loaded quality factor (Q). The higher the quality factor (Q), the slower the damping rate.

For efficient conversion, the number of RF output pulses in the train may be limited, since the total energy of the entire RF output pulse train should be less than the energy of the single exciting impulse. For low conversion efficiency, we can also analyze this problem in the frequency domain. A narrow pulse contains many frequency components. The cavity here acts as a narrow bandpass filter. The passed signal, according to the inverse Fourier transform, will form a damped RF oscillation. A narrow band signal corresponds to a slowly damped oscillation.

In our experiment, a piece of Cr doped GaAs or Fe doped InP was used as a single pulse switch. GaAs or InP switch is essential since it will generate an electrical impulse with duration much shorter than the period of the RF signals. It can also withstand higher DC bias voltage than Si switch. Fig. 2 shows the output waveform from such a device. More than one hundred cycles of 300 MHz oscillation was generated by a single pulse of green light produced by a frequency doubled mode-locked Nd:YAG laser (30 ps, 20 μj). Note the fast build up of the oscillation. We have also used the whole pulse train of the Q-switched and mode-locked pulses as the exciting light source. In this case, we generally obtained at the output of the device an RF pulse train with high amplitude and more total energy provided that the electrical length of the coaxial resonator was tuned to a sub-multiple of the optical cavity length. With strong input and output coupling to the resonator, we were able to convert a single electrical pulse to a string of RF pulses with a total energy efficiency better than 50%.

This technique can also be extended to generate a CW RF oscillation if the exciting light source is a CW mode-locked laser. The RF oscillation is sustained by the periodic excitation of optical pulses. Using a frequency doubled CW mode-locked Nd:YAG laser at 100 MHz, we were able to generate microwaves at 1.6 GHz. Fig. 3 shows the oscillogram of such an oscillation. To obtain an oscillation with a near constant amplitude we had to: (1) tune the frequency of the resonating cavity to an integer multiple of the repetition frequency of the mode-locked laser pulses, (2) match the length of the transmission line between the semiconductor switch and the input coupler with that of the optical cavity, and (3) maintain a high Q for the electrical resonator which means that both the input and output coupling coefficients must be reduced.

In conclusion, we have demonstrated the experiments of a picosecond laser pulse triggered DC to RF conversion in a coaxial resonant cavity. A comparison of this device with a frozen-wave generator and its advantages are also discussed. This work was supported in part by the National Science Foundation, the Air Force Office of Scientific Research and the Laboratory for Physical Sciences.

References

1. J. M. Proud, Jr., and S. L. Norman, "High-Frequency Waveform Generation Using Optoelectronic Switching in Silicon", IEEE Trans. Microwave Theory Tech., Vol. MTT-26, pp. 137-140, 1978.

2. C. S. Chang, M. C. Jeng, M. J. Rhee and Chi H. Lee, A. Rosen and H. Davis, "Direct DC to RF Conversion by Picosecond Optoelectronic Switch", 1984 IEEE MTT-S International Microwave Symposium Digest, pp. 540-541, also in the Proceedings of SPIE - The International Society for Optical Engineering on "Optical Technology for Microwave Applications", Vol. 477, pp. 101-104, 1984.

+ Mailing address: Department of Physics, University of Maryland, College Park, MD 20742.

* On leave from Colorado State University, Ft. Collins, Colorado 80523

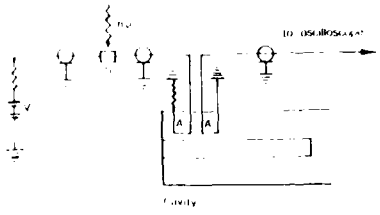

Fig. 1 Experimental arrangement, S is the semiconductor switch, A_1 and A_2 are loop antennas and the cavity is a coaxial structure.

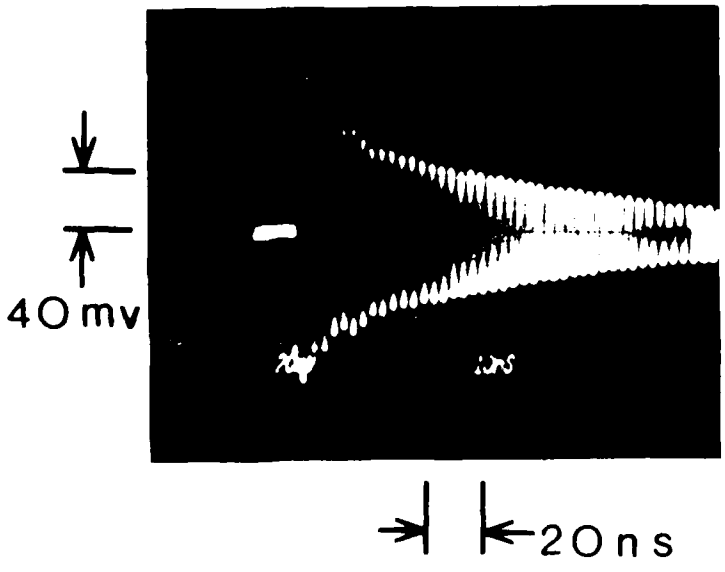

Fig. 2 The oscillogram of the RF output pulse train excited by a single electric impulse from a Cr:GaAs switch.

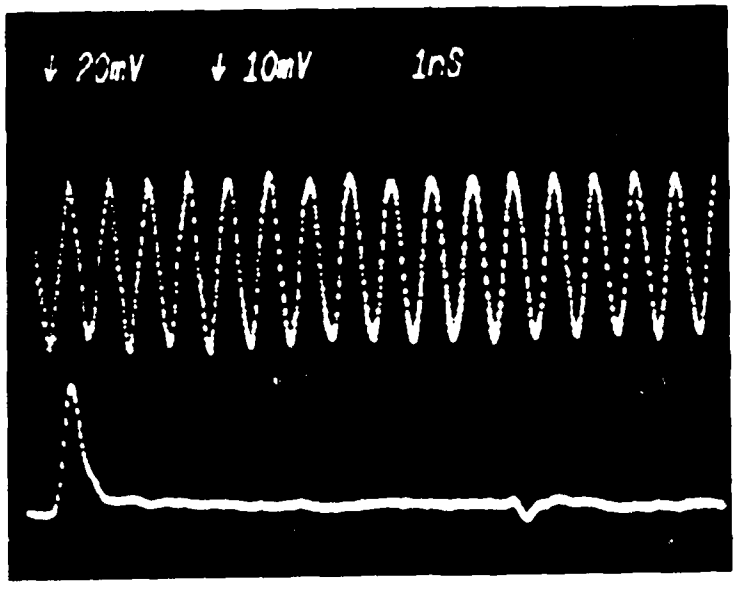

Fig. 3 The oscillograms of (a) (lower trace) the mode locked laser pulse and, (b) (upper trace) the CW RF pulse train actuated by the optical pulse train from the CW mode-locked laser.

SUBPICOSECOND RESPONSE TIMES FROM ION BOMBARDED InP

P. M. Downey
AT&T Bell Laboratories
Holmdel, New Jersey 07733

Picosecond photoconductivity studies of $^3He^+$ bombarded Fe-doped InP have demonstrated free carrier lifetimes and mobilities of 6 ps and 600 cm^2/Vs , respectively[1]. This result compares very favorably with the 10 ps response time and mobility less than 20 cm^2/Vs observed in oxygen irradiated silicon-on-sapphire[2]. Even when compared to proton irradiated GaAs sampling gates[3] the He bombarded InP photoconductors demonstrate over an order of magnitude higher peak electrical transmission with comparable sampling apertures and optical pulse energies. Radiation damaged InP appears then to be the more promising material for achieving ultrashort response times and optimum photoconducting sensitivity. In this paper we explore the extent to which the free carrier response time can be reduced by increasing the radiation dose in ion bombarded InP photoconductors. Subpicosecond response times are demonstrated for InP photoconducting sampling gates, but the required radiation doses are found to severely compromise the device sensitivity.

With the exception of protons, light ion ($^3He^+$, $^4He^+$, and Be^+) bombardment produces very similar damage in Fe-doped InP. For low and moderate radiation doses a monotonic decrease in free carrier lifetime is observed with increasing radiation dose, whereas the dark resistivity and free carrier mobility remain relatively constant. In other words the effect of moderate ion bombarding doses is to increase the density of recombinations centers without significantly changing the number of momentum scattering sites in the crystal. The dark resistivity of the damaged layers bombarded with moderate doses was consistently found to be ~3000 ohm-cm, suggesting that even at low doses a defect level was introduced which pinned the Fermi level ~.3 eV below the conduction band. For all three light ions investigated, however, a critical or threshold dose was identified[4] above which the dark resistivity also decreased with increasing dose and the free carrier mobility plummeted by more than a factor of 30 to <10 cm^2/Vs .

The autocorrelated photoresponse of an InP sample bombarded below the threshold dose is shown in Fig. 1. It is characterized by a 10-90 percent risetime of 2.4 ps corresponding to a 1/e relaxation time of 1.1 ps. Similar autocorrelation traces were obtained from samples irradiated with doses closer to the threshold dose, indicating that our measurements were limited by the response speed of the microstrip circuit. The same sample used to collect the data for Fig. 1 was also used as a sampling gate in a back-to-back Hertzian dipole[5] configuration with another radiation damaged InP photoconductor. In such an experiment the speed of response of the sampling gate is no longer limited by the charging time of the device capacitance. We were thus able to directly resolve a free carrier relaxation time of 0.9 ps for the sample from Fig. 1 when observed in the Hertzian dipole configuration.

We also carried out Hertzian dipole measurements on a series of samples bombarded with $^3He^+$ ions at 300 keV at doses near the threshold dose. The shortest 1/e response time observed from such an InP sample was 0.45 ps; the device had received a bombarding dose of $4x10^{14}/cm^2$ and exhibited a dark resistivity of 500 ohm-cm. By irradiating the sample above the threshold dose we were thus able to improve the response speed of the InP photoconductor by a factor of two at the expense of a four-fold decrease in dark resistivity and an order of magnitude decrease in free carrier mobility. This is in contrast to the rapid decrease in free carrier response time observed with increasing dose below the threshold dose which is accomplished with minimal loss in free carrier mobility or dark

resistivity.

We conclude therefore that from the point of view of making picosecond optoelectronic pulse generators and sampling gates from radiation damaged InP photoconductors there exists an optimum radiation dose for which one achieves one picosecond response times. Slight improvements in response speed can be attained with higher doses, but only at great expense to the device sensitivity.

REFERENCES

[1] P. M. Downey and B. Schwartz, Proc. SPIE Vol. 439, 30 (1983).

[2] P. R. Smith, D. H. Auston, A. M. Johnson, and W. M. Augustyniak, Appl. Phys. Lett. 38, 47 (1981).

[3] D. H. Auston and P. R. Smith, Appl. Phys. Lett. 41, 599 (1982).

[4] P. M. Downey and B. Tell, to be published in J. Appl. Phys.

[5] D. H. Auston, K. P. Cheung, and P. R. Smith, Appl. Phys. Lett. 45, 284 (1984).

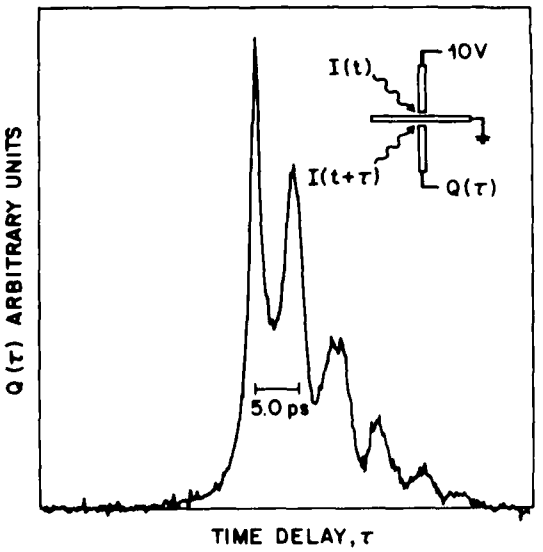

Fig. 1 The autocorrelation trace of an InP sample bombarded with a dose of 10^{14} $^4He^+/cm^2$ at 300 keV; it has a full width at half-maximum (FWHM) of 1.8 ps and a 10-90 percent risetime of 2.4 ps. Shown in the inset is the autocorrelation circuit used, consisting of 200 micron wide microstriplines on a 250 micron thick semi-insulating InP substrate. The reflections observed on the right-hand side of the correlation trace are due to an electromagnetic pulse which is radiated by the picosecond photocurrent and undergoes multiple reflections between the top and bottom surfaces of the InP substrate.

THURSDAY, MARCH 14, 1985

ThB, CRYOELECTRONICS

Tushar Gheewala, Gigabit Logic, *Presider*

High-Speed Analog Signal Processing with Superconductive Circuits*

Richard W. Ralston

Lincoln Laboratory, Massachusetts Institute of Technology
Lexington, MA 02173-0073

A new technology utilizing superconductive components for pulse compressors and convolvers that are capable of processing analog signals having bandwidths from 2-20 GHz will be described. The technology has two key features: low-loss and low-dispersion electromagnetic striplines which provide tapped delay on compact substrates; and superconductive tunnel junctions which provide efficient low-noise mixing and high-speed sampling circuits. A pulse expander/compressor pair (1) and a convolver (2) with respective time-bandwidth products of 86 and 21 have been demonstrated.

The basic tapped-delay-line structure is shown in Fig. 1. The two adjacent striplines are coupled by a cascaded array of quarter-wavelength-long backward-wave couplers; a chirp filter with a linear group-delay-vs-frequency relationship is synthesized by adjusting the length and spacing of each coupler. Filters of this type have been fabricated in a spiral configuration using 3-m-long niobium lines on 5-cm-dia. silicon wafers. The fidelity of the phase and amplitude characteristics of such filters is evidenced by the clean compressed pulse shown in Fig. 2. In this pulse expander/compressor demonstration of two filters, a Hamming-weighted compressed pulse response with -25-dB side lobes and a 2.3-GHz bandwidth was observed.

The response of a chirp filter is fixed, as it is determined by the geometry of the coupled striplines. In advanced communication and radar systems, there is often a need for a filter with a rapidly reprogrammable response. The performance characteristics of a preliminary convolver which is being developed for this purpose will be described.

As a demonstration of the utility of this new class of superconductive devices in high-speed signal processing, an ultrawideband chirp-Fourier spectrum analyzer (1) has been developed. The circuit architecture is shown in Fig. 3. The wideband input time function is analyzed by multiplying with a chirp followed by convolving the product with a chirp of opposite slope. The circuit transforms the spectral channels into time bins, as is seen in Fig. 4 where seven tones equally spaced by 100 MHz are well resolved. The circuit provides a 60-channel analysis of a 2.4-GHz band in 40 ns.

Projections based on these results indicate that superconductive technology should support analog device time-bandwidth products of at least 1000 and thereby provide substantial processing gains at very wide bandwidths. Such devices will provide real-time signal-processing functions with the digital equivalent of up to 10^{12} operations/sec. In addition to pure analog structures, superconductive technology offers the potential for hybrid analog/digital signal processors of great efficiency and speed.

*This work was sponsored by the Department of the Army, the Defense Advanced Research Projects Agency, and the Department of the Air Force, in part under a specific program for the Air Force Office of Scientific Research.

References

1. R. S. Withers, A. C. Anderson, J. B. Green and S. A. Reible, "Superconductive Delay-Line Technology and Applications", 1984 Applied Superconductivity Conference, San Diego. Proceedings to be published in IEEE Trans. Magnetics, 1985.

2. S. A. Reible, "Superconductive Convolver with Junction Ring Mixers", 1984 Applied Superconductivity Conference, San Diego. Proceedings to be published in IEEE Trans. Magnetics, 1985.

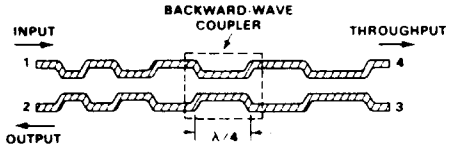

Fig. 1. Chirp filter formed by adjacent electromagnetic delay lines.

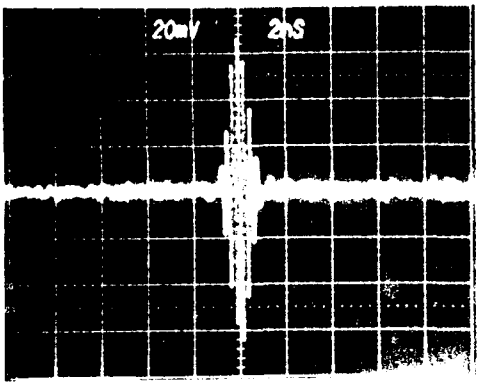

Fig. 2. Compressed-pulse response of a pair of complementary chirp filters.

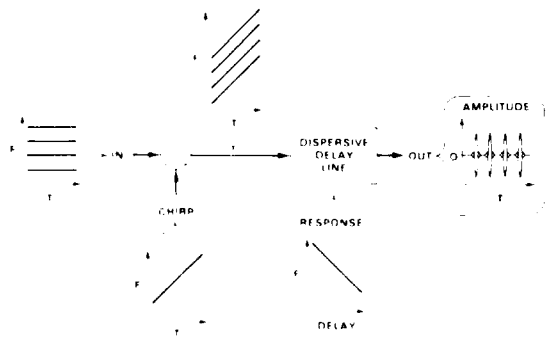

Fig. 3. Chirp-Fourier spectrum analyzer architecture.

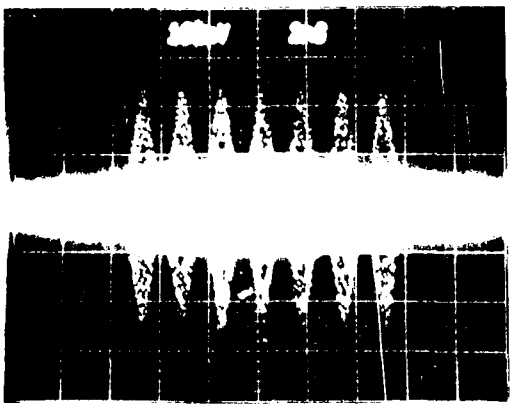

Fig. 4. Analyzer output in response to 7 CW tones from 3.4 to 4.0 GHz.

AD-A168 685 PICOSECOND ELECTRONICS AND OPTOELECTRONICS HELD AT INCLINE VILLAGE NEVADA..(U) OPTICAL SOCIETY OF AMERICA WASHINGTON D C J W QUINN 04 FEB 86 AFOSR-TR-86-0157 2/2

UNCLASSIFIED AFOSR-85-0105 F/G 9/3 NL

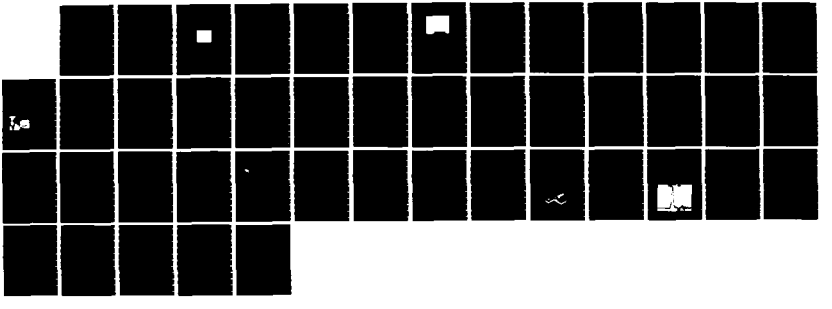

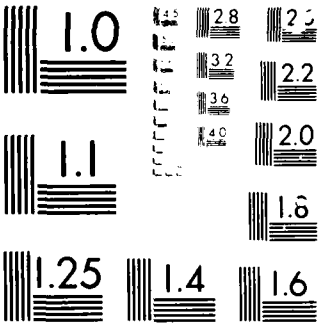
1.0
1.1
1.25
1.4
1.6
2.8
3.2
3.6
4.0
2.2
2.0
1.8

PICOSECOND SAMPLING WITH JOSEPHSON JUNCTIONS

Peter Wolf

IBM Zurich Research Laboratory, Säumerstr. 4, CH-8803 Rüschlikon, Switzerland

SUMMARY

A Josephson sampler basically consists of a sampling gate and a sampling-pulse generator. As Fig. 1 shows, the sampling gate is a Josephson junction to which the signal, the sampling pulse and a dc bias are coupled either directly, as in the figure, or via control lines. The dc bias is adjusted such that the sum of the three inputs just reaches the threshold of the gate, the switching of which is detected by an external voltage dector. The dc bias is adjusted automatically with an external feedback loop. If the sampling pulse is moved along the signal by means of a variable time delay, then the dc bias current as a function of the delay will yield a replica of the signal.

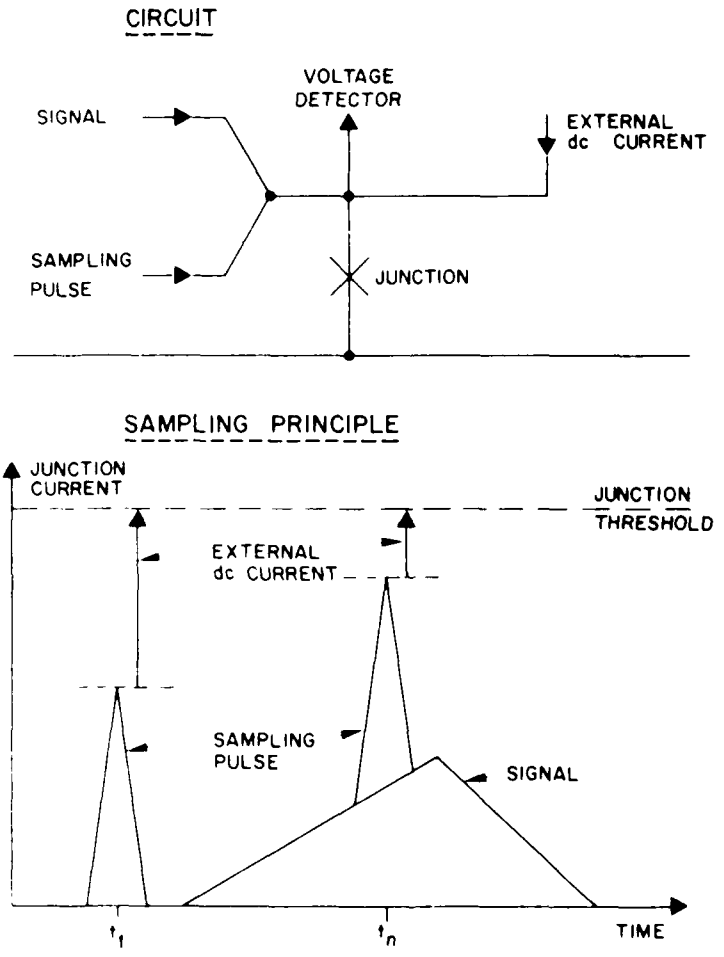

Fig. 1: Principle of operation of a Josephson sampler.

The spike-like sampling pulse is produced by a simple circuit first proposed by Faris, which basically consists of two junctions and a resistor. This pulser is triggered by an external pulse generator which in addition should also provide a voltage-controllable delay for moving the pulse time-wise along the signal. This delay can either be achieved with a motor-driven variable delay line or by electronic methods. With electronic delay methods, high sampling rates of 1 MHz or more have been achieved which allow a flicker-free display on an oscilloscope.

The cryogenic part of these sampling systems can be very simple, since it needs only three Josephson junctions and one resistor. The same is true of the room-temperature part which does not require very fast or elaborate electronics. The best resolution obtained is 2.1 ps, as shown in Fig. 2. Here, the oscillogram of a switching Josephson junction is given. It is a double exposure with one waveform shifted by 10 ps with an external airline for time calibration.

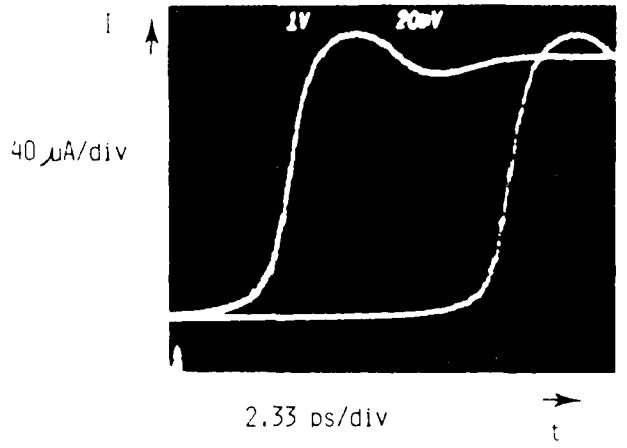

Fig. 2: Oscillogram of a switching Josephson junction. Double exposure with one waveform shifted by 10 ps with an external delay line. The 10%-90% rise-time displayed is 2.1 ps.

The present sampling systems have not reached the limit of their time resolution which basically depends on the plasma frequency of the sampling gates. The plasma frequency is proportional to the square root of the ratio Josephson current to junction capacitance. Here, considerable improvements are possible so that a resolution of less than 1 ps should be realizable in the future.

Josephson junctions operate only at low temperatures, typically liquid-helium temperature. Therefore, mostly phenomena at the same temperature and even on the same chip as the sampler have been investigated. For other temperatures, especially room temperature, transmission lines are required which lead the signals from and to the cryogenic environment. This is not easy and has not been investigated extensively. However, designs seem possible which avoid an excessive decrease in time resolution. If this could be achieved, then Josephson samplers would be a fairly cheap and general method to investigate picosecond signals.

Transmission Line Designs With a Measured Step Response of 3ps Per Centimeter.

Charles J. Kryzak, Sadeg M. Faris
Hypres, Inc. 175 Clearbrook Rd., Elmsford, N.Y. 10523
914 592-1190

Kevin E. Meyer, Gerard A. Mourou
Laboratory for Laser Energetics, University of Rochester
250 East River Rd., Rochester, N.Y. 14623
716 275-4412

In order to effectively exploit the speed-high and high sensitivity potential of both superconducting and electro-optics technologies, proper generation, coupling and propagation of signals with bandwidths in excess of 100 Gigahertz is required. We report on extensive theoretical and experimental investigations of transmission lines of various configuration that was undertaken in order to find an optimum transmission medium which satisfies the ultra-wide bandwidth requirements. The investigation included various substrate thickness and dielectric constants as well as conductor material. We concluded that it is possible to realize transmission line designs capable of supporting bandwidths in excess of 100 Gigahertz if careful attention is paid to the generation and coupling of the ultra-wide bandwidth waveforms, i.e., taking into consideration the radiation and polarization of the fields set up by the generator as well as impedance matching between the generator and the line.

To verify the theoretical predictions we designed experiments based on a new variation of an electro-optical sampling technique [1], which is proven to have subpicosecond resolution. The experimental investigation consisted of the generation of picosecond electrical pulses, an impedance matching coupling configuration, and the propagation of pulses down the transmission line. Our technique allows the measurement of the waveforms at any point along the transmission line, thereby allowing an accurate determination of pulse degradation and step response per unit length of our transmission line designs.

Illustrated below are measured waveforms which verify that a step response of 3ps per centimeter is indeed possible. This is the fastest waveform that has been generated, coupled, and propagated up to 3.3 centimeters which is known to have been reported. With this we believe it is possible to design and construct transmission lines capable of step responses less than 1ps per centimeter.

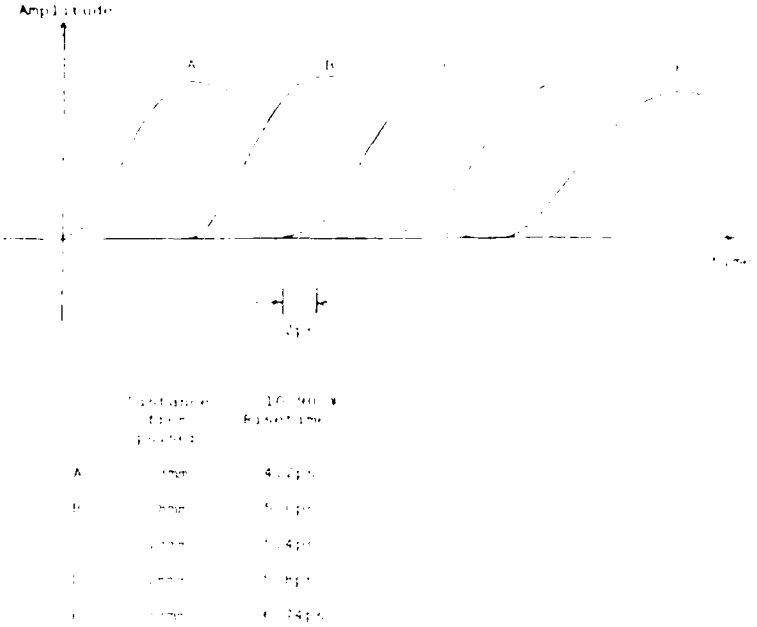

1. G.A. Mourou, K.E. Meyer, Applied Physics Letters Vol. 45, pp492, 1984

Development of a Picosecond Cryo-Sampler Using Electro-Optic Techniques*

D.R. Dykaar, T.Y. Hsiang
The University of Rochester
Dept. of Electrical Engineering
Rochester, New York 14627

G.A. Mourou
The University of Rochester
Laboratory for Laser Energetics
Rochester, New York 14623

Previously we reported on a picosecond electro-optic sampling system used to characterize superconducting Josephson devices.[1] A block diagram is shown in Figure 1. The sampler was driven by a colliding-pulse mode-locked laser which produced two 120 fs FWHM pulses at 100 MHz. One pulse was used to generate an electrical signal of adjustable height and width, via a photoconductive switch. This signal was used to excite the test device placed in the cryogenic environment. The resultant electrical transient was then sampled with the second optical pulse using a birefringent lithium tantalate crystal. By changing the relative delay between the optical excitation and sampling pulses, the temporal development of the electrical transient was recorded using conventional slow speed electronics. The limitations on system response were found to be due to the long cables required to move signals into, and out of, the cryogenic environment.

We report here our attempt to eliminate the various cables and connections by placing the sampler directly in the cryogens. In the initial version, only the lithium tantalate detector was directly cooled. An electrical pulse generated at room temperature and detected by the cryogenic crystal is shown in Figure 2. The risetime was measured to be 16.4 picoseconds, which is dominated by the long coaxial cable required for input signal transmission. A room temperture version of this sytem has demonstrated a risetime of < 500 fs.[2]

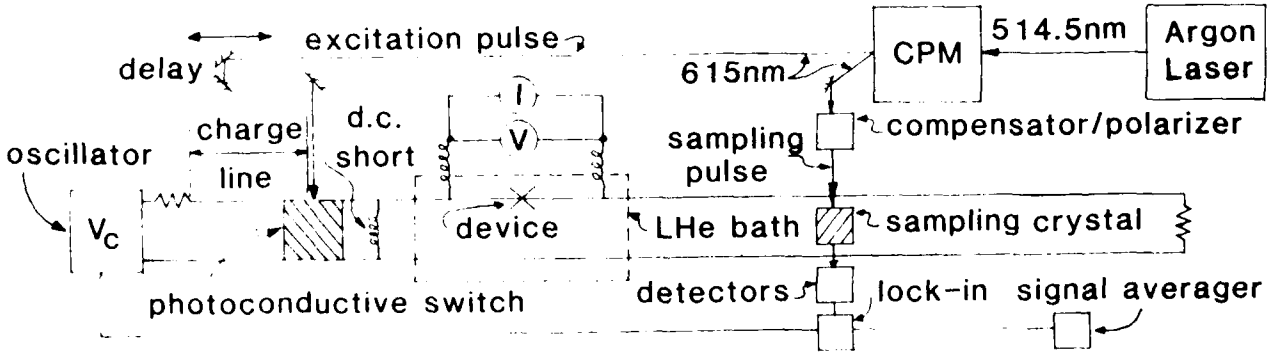

Figure 1 - Schematic diagram of experimental set-up

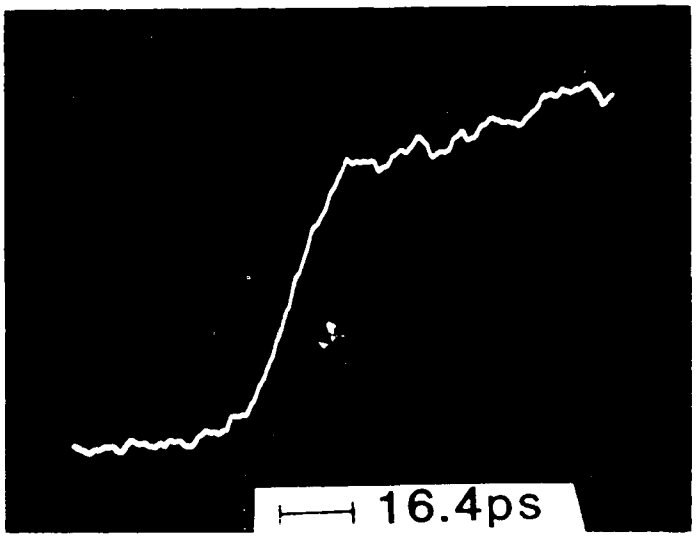

Figure 2 - Output signal from the sampler (placed in cryogenic environment)

[1]D.R. Dykaar, T.Y. Hsiang, G.A. Mourou, "An Application of Picosecond Electro-Optical Sampling to Superconducting Electronics," submitted to IEEE Trans. Magn., 1984.

[2]G.A. Mourou, K.E. Meyer, "Subpicosecond Electro-Optic Sampling Using Coplanar Strip Transmission Lines," Applied Physics Letters, Vol. 45, No. 5, pp. 492-494, September 1984.

*This work was supported by National Science Foundation Grant ECS-8306607 and Sponsors of The Laboratory for Laser Energetics. One of us (D.R.D.) acknowledges support from an IBM Pre-doctoral Fellowship.

Picosecond Josephson Logic Gates for Degital LSIs

Jun-ich Sone, Jaw-Shen Tsai, and Hiroyuki Abe

NEC Corporation
1-1 Miyazaki Yonchome, Miyamae-ku
Kawasaki 213 Japan

Introduction

This paper will discuss the realized and projected picosecond logic speed of Resistor Coupled Josephson Logic for LSI applications. The 4b x 4b parallel multiplier, developed very recently by using 5-μm lead alloy technology, demonstrates a multiplication time as small as 280 picoseconds. The averaged logic delay per gate is 21 picoseconds in this multiplier. The advancement in Josephson IC fabrication technology, on the other hand, has shown the possibility for fabricating 1-μm minimum line width Josephson LSI. The projested logic delay per gate of densely packed 1-μm RCJL LSI will be less than 10 picoseconds.

Medium Scale Integration

Figure 1 shows a 4b x 4b parallel multiplier chips's microphotograph. The multiplier, implemented in 5-μm RCJL gates, employs dual rail logic aiming at high-speed operation. The circuit contains 249 gates consisting of 862 Josephson junctions. The gate are laid out in an array configuration. The critical (longest) path for 4b x 4b multiplication contains 13 gates. The 21 picoseconds logic delay per gate contains 6 picoseconds signal propagation time along the 500-μm transmission line interconnecting the gates. The 280-picoseconds 4b x 4b multiplication time is one order of magnitude faster than semiconductor multipliers, such as GaAs MESFET multipliers.

Projected RCJL Performances

The essential factors for logic circuit performances are summarized in Tab.1. The main interest in this paper is the projected logic delay in the future large scale integrated circuit chips, which depends on the fan-in and fan-out condition and on the averaged interconnection line length.

The performances of RCJL LSI are discussed employing standard logic cell configuration. The standard cells are

laid out on an LSI in an array and are interconnected by superconducting transmission lines as shown in Fig.2. The cell contains a gate unit, consisting of two OR gates and one AND gate, and an area to install n interconnection lines on X and Y directions. Each gate unit's output drives [illegible] other gates. The averaged distance between the driving gate unit and driven gate unit is m times as long as the unit cell size.

Using the standard cell layout, the gate performance are projected along with the minimum feature size reduction. The RCJL logic delay is the sum of the turn-on delay τ_t, the voltage rise time τ_r and the signal propagation time τ_p. The junction size reduction results in τ_r reduction. The propagation time τ_p is in proporation to the unit cell size, which decreases proporationally with the minimum feature size. The logic delay for highly miniaturized RCJL gates is essentially determined by the quantum mechanical time constant $\tau = h/2eV_g \sim 1$ picosecond and the velocity of light in the superconducting transmission line. Table 2 shows the results of RCJL performance projection.

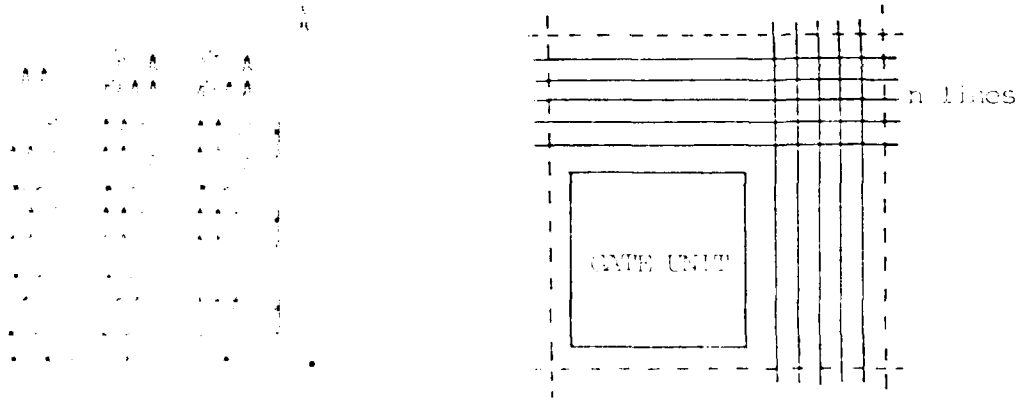

GATE UNIT = 2 OR + 1 AND

Fig. Standard Cell Layout

[illegible] performance

NOTES

THURSDAY, MARCH 14, 1985

ThC, ULTRAFAST ELECTRONICS

James Harris, Stanford University, *Presider*

Picosecond Switching Speed GaAs Circuits

Raymond Dingle
Pivot III-V Corporation
PO Box 795
New York, NY 10003

The speed performance of simple integrated circuits made from III-V materials in general, now rivals Josephson junction devices for all time speed records. In particular, the most developed technology is that involving GaAs (as a MESFET) or GaAs and (AlGa)As in combinations such as the selectively doped heterostructure transistor (SDHT, sometimes called HEMT, TEGFET, MODFET) and the heterojunction bipolar transistor. This talk will compare and contrast the performance of these GaAs based approaches. Speculation about the near future will be attempted.

Characterization of TEGFETs and MESFETs Using the Electro-Optic Sampling Technique

K.E. Meyer, D.R. Dykaar, and G.A. Mourou
Laboratory for Laser Energetics, University of Rochester, 250 East River Road, Rochester, New York 14623-1299

It has been demonstrated that the electro-optic sampling technique can be used to characterize electrical signals with rise times as short as .46 ps.[1] In this report we show the application of this sampling technique to the measurement of the transient response of GaAs TEGFETs and MESFETs.

The experimental configuration is shown in Fig. 1. Two synchronized trains of short (1 ps) optical pulses are provided by a CPM laser. The two electrodes on the GaAs serve as the gate bias and input signal line; when the gap is illuminated and biased a fast electrical signal is injected into the FET gate. The response of the FET is a current pulse out of the drain. The TEGFET has been tested using a microstrip sampler, while the MESFET results were obtained with a coplanar geometry. The electro-optic birefringence is detected by a probe pulse focused between the sampler electrodes.[1,2]

Experimental results are shown in Fig. 2. With the FET biased "off" some of the pulse is coupled through the device. With the FET biased "on", the ouput is amplified and gain is apparent. The measured TEGFET rise time is 16 ps; this agrees well with the calculated cutoff frequency of 23 GHz. The observed MESFET rise time is 25 ps, which corresponds approximately with the 20 GHz current-gain cutoff obtained with S-parameter measurements. This technique will be used to study transient effects in high-speed devices.

Acknowledgment

This work was supported by the Laser Fusion Feasibility Project at the Laboratory for Laser Energetics which has the following sponsors: Empire State Electric Energy Research Corporation, General Electric Company, New York State Energy Research and Development Authority, Northeast Utilities Service Company, Ontario Hydro, Southern California Edison Company, The Standard Oil Company, the University of Rochester, and the United States Air Force Office of Scientific Research. Such support does not imply endorsement of the content by any of the above parties. Additional support for the work was provided by NSF Grant Number ECS-8306607. GaAs FETs were provided by S. Cammitz of the Electrical Engineering Department of Cornell University. TEGFETs were provided by Thomson C.S.F. One of us (D.R.D.) was a NSF Graduate Fellowship.

References

1. D.H. Auston and K.E. Meyer, Appl. Phys. Lett. 45, 292 (1984).
2. D.H. Auston, A.M. Johnson, P.R. Smith, and J.C. Bean, IEEE J. Quantum Electron. QE-16, 1016-1022 (1980).

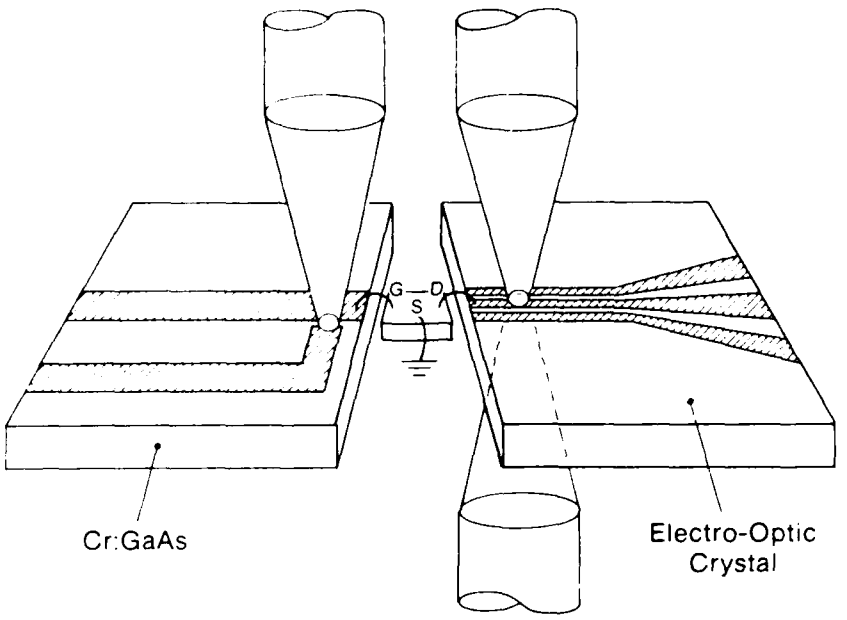

Fig. 1 Sampling geometry used to characterize TEGFETs and MESFETs. The optical beam on the left generates the fast input pulse; the beam on the right detects the output response of the device.

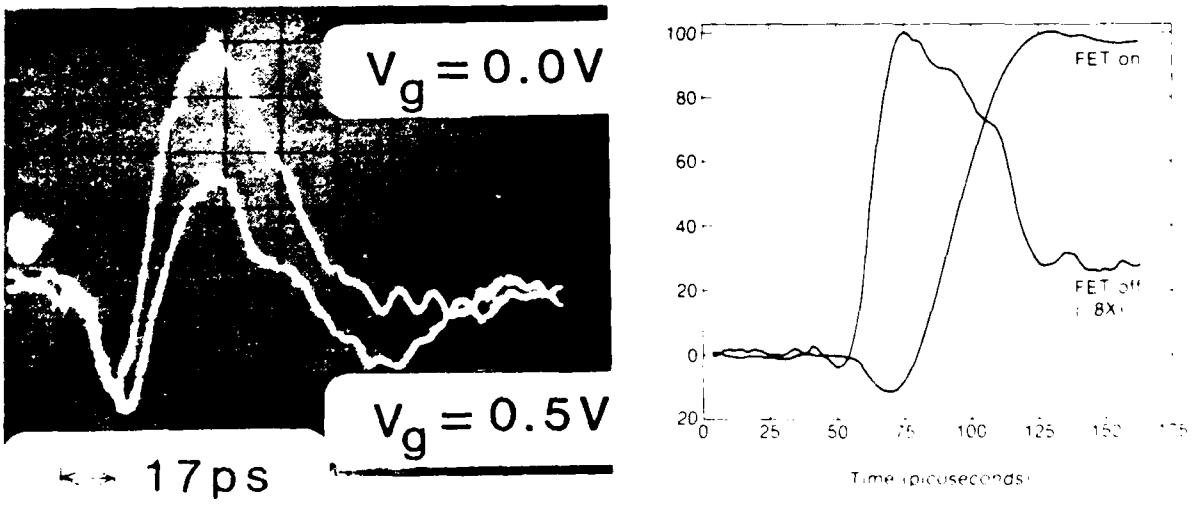

Fig. 2 (a) TEGFET response with the gate on (τ = 16 ps) and with the gate pinched off; (b) MESFET response with the drain bias on (τ = 25 ps) and off.

Picosecond Optoelectronic Diagnostics of Field Effect Transistors

Donald E. Cooper

Chemistry and Physics Laboratory
The Aerospace Corporation
Mail Stop: M2-253
P.O. Box 92957
Los Angeles, CA 90009

Picosecond optoelectronics provides the capability to measure the frequency response of solidstate devices with much greater bandwidth than conventional techniques.[1] Short electrical pulses are fed into device terminals, and the output is optoelectronically sampled to measure the device impulse response function. The Fourier transform of this data yields the frequency response curve. All elements of the scattering matrix (S matrix) can be obtained through the use of various combinations of device terminals as input and output ports. Thus all information obtained from conventional CW network analyzer techniques is available from the time-domain picosecond optoelectronic data, with excellent bandwidth capability and electronic simplicity. Here we present impulse response measurements of a submicron field effect transistor.

Optoelectronic switches are fabricated in microstrip circuits deposited on silicon-on-sapphire wafers. The wafers are ion implanted with Si^+ to shorten the photoconductive response to below 10 picoseconds. For these experiments the electrical pulse durations and the sampling apertures were about 7 picoseconds. For measurement of the impulse response of a FET a microstrip with a pair of optoelectronic switches is connected to both the gate and the drain, and the source is connected to the microstrip ground plane. Gate and drain bias voltages are applied to the microstrips. Impulse response data to generate the S matrix element S_{11} is obtained by creating an electrical pulse at the gate with one switch and sampling the reflected waveform with the other switch. The other S parameters are measured in similar fashions, using the gate and the drain in all four permutations as input and output ports. To eliminate packaging effects the microstrip circuits were wire-bound directly to chip devices. To our knowledge these are the first published impulse response measurements on unpackaged FETs.

The impulse response functions for an Avantek AT-8041 FET (0.5 μm gate) are shown in Figure 1 a-d. For the operating conditions used for these measurements (V_{DS} = 3V, V_{GS} = 0.9V) the drain current is 30 mA. Figure 1a shows the result of pulsing and sampling the gate terminal, and Fig. 1d shows the same data for the drain terminal. These data are dominated by the large peak produced by the sampling of the input pulse as it is generated. The reflected pulse is found at later times to the right of the large peak. A shoulder on the main

peak corresponds to reflection at the wire bond on the microstrip, and the broad peak on the left is the reflection from the device itself. The scattering parameters S_{11} and S_{22} are derived from the Fourier transform of these reflected peaks.

Figure 1b shows the result of pulsing the drain and sampling the gate terminals. This signal has a negligible DC component, as would be expected from a circuit with only capacitative coupling between drain and gate. As the FET bias conditions are varied this signal shows a significant change in shape indicative of a shift in the phase of the transmitted signal. Finally, Figure 1c shows the result of pulsing the gate terminal while sampling the drain output. This pulse represents the amplified input pulse, and shows the broadening effect due to the FET gain bandwidth being less than the bandwidth of the input pulse. The Fourier transform of this signal gives the frequency response curve for the insertion gain S_{21}. Digital Fourier transform calculations have been performed on this data, and the resulting frequency spectrum shows the expected f^{-2} dependence.

In summary, we hve performed impulse response measurements on fast unpackaged FETs using picosecond optoelectronic techniques. These measurements permit the extraction of scattering matrix parameters in the millimeter wave regime without the use of frequency mixing techniques.

References

1. P. R. Smith, D. H. Auston, and W. M. Angustiniak, Appl. Phys. Lett, 39, 739(1981).

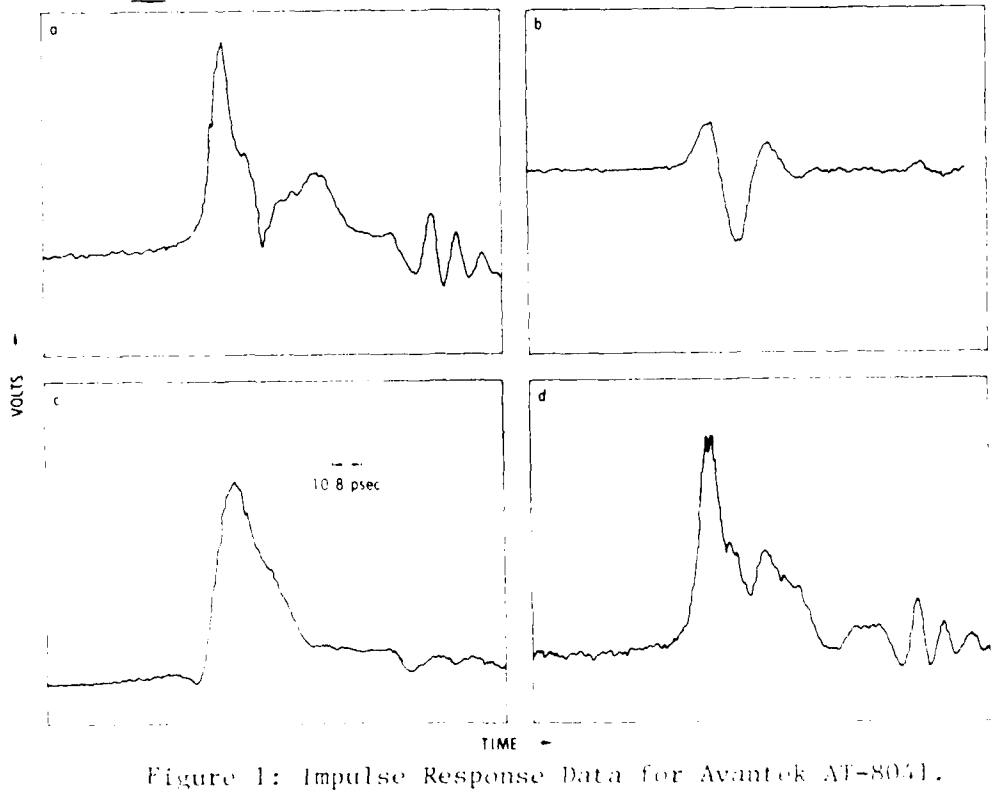

Figure 1: Impulse Response Data for Avantek AT-8031.

High Electron Mobility Transistors - Their Evolution and Ultimate Speed

H. Sakaki
Tokyo University
Institute of Industrial Science
22-1 Roppongi 7 Chome
Minato-ku, Tokyo 106
Japan

Physical mechanisms governing the ultimate speed of high-purity heterojunction FETs (HEMTS) are discussed together with a preliminary experiment on a novel velocity modulation transistor.

Time-domain Measurements for Silicon Integrated Circuit Testing Using Photoconductors

W. R. Eisenstadt
Electrical Engineering Department, University of Florida, Gainesville, FL 08544

R. B. Hammond
Electronics Division, Los Alamos National Laboratory, Los Alamos, NM 87545

D. Bowman and R. W. Dutton
Integrated Circuits Laboratory, Stanford University, Stanford, CA 94302

Picosecond time-domain measurements of silicon integrated circuit interconnects were successfully performed using photoconductors integrated on-chip. Both bulk silicon and thin-film polycrystalline silicon photoconductors were studied. Standard integrated circuit fabrication techniques followed by shadow-masked, ion-beam irradiation were used to create photoconductor/interconnect structures. Starting materials used were 70 Ω-cm n-type wafers and 16 Ω-cm p-type wafers. A subpicosecond pulsed laser system excited the photoconductors to produce and sample picosecond pulses on the Si substrate.

Optoelectronic correlation measurements with photoconductor pulsers and photoconductor sampling gates were performed to characterize both the photoconductors and interconnections. Photoconductors processed as pulsers have produced electrical pulses with ∿2 ps risetime, ∿200-mV peak amplitude and full-width at half-maxima (FWHM) of <10 ps. Photoconductors processed as sampling gates have demonstrated 3-dB measurement bandwidths of 20 GHz. Due to the absence of jitter, on-chip signal delays were measured with subpicosecond precision.

MOLECULAR BEAM EPITAXY MATERIALS FOR HIGH SPEED DIGITAL HETEROSTRUCTURE DEVICES

D.L. Miller
Rockwell International Corporation
Microelectronics Research and Development Center
1049 Camino Dos Rios, Thousand Oaks, CA 91360

Introduction

Molecular beam epitaxy (MBE) has made many important contributions to research and development of III-V compound semiconductor devices. For example, MBE has become the predominant technique of epitaxial material growth for digital heterostructure circuits employing heterojunction bipolar transistors (HBTs) and high electron mobility transistors (HEMTs). This has occurred despite the relatively high cost of MBE apparatus, and the reputation of MBE as an esoteric technology. Since high speed heterostructure devices appear to be moving rapidly toward the production line, it is important to consider the status of MBE in device research and development, and the future of MBE in the transition to production.

MBE in HEMT and HBT Research and Development

All of the recent impressive highspeed digital circuit performance demonstrations by HEMT and HBT devices have been accomplished using MBE material. HEMT ring oscillators, with propagation delays as low as 12.2 pS at 300K[1] and 11.0 pS at 77K,[2] are the fastest semiconductor digital switching circuits ever reported, and HEMT dividers operating at 10.1 GHz at 77K[2] are the fastest semiconductor dividers ever achieved. HBT devices operating with cutoff frequencies f_t up to 40 GHz,[3] and frequency dividers operating up to 8.5 GHz at room temperature[3] are the fastest bipolar devices ever reported.

MBE material has been used for these impressive results primarily because of its unequalled control and versatility in making structures which contain multiple thin layers of high quality material. MBE is basically a simple process, a carefully controlled vacuum co-evaporation of elements onto a heated substrate. The growth rate is relatively slow, three to four Angstroms per second. The vacuum environment allows simple shutters to be used to interrupt the beams used for growth in times which correspond to submonolayer deposition. A low substrate temperature of about 600°C during the growth of GaAs minimizes interdiffusion of deposited materials. This results in relative ease in controlling the placement of dopants and interfaces. Furthermore, well-engineered commercial MBE apparatus is available from several manufacturers.

A basic HEMT device consists of an undoped GaAs buffer layer, an undoped $Al_{.3}Ga_{.7}As$ spacer layer, typically 50A thick, followed by about 300A of n-type $Al_{.3}Ga_{.7}As$. The threshold voltage and the

current-carrying capacity of a HEMT device is a very sensitive function of these thicknesses and of the doping density in the AlGaAs. Also, the channel mobility of a HEMT device relies on an abrupt heterointerface and high purity material. With MBE, the thin layers of these devices are extremely simple to make, and thicknesses and doping may be modified in a straightforward manner to optimize device performance.

HBTs also benefit from the ability of MBE to accurately control doping and composition on a small thickness scale. The low growth temperature reduces dopant diffusion from the heavily doped base region, while the ability to reproducibly provide compositional grading in the emitter-base junction region and reduce base transit times.

Further gains in HEMT and HBT performance are being realized by using MBE for "bandgap engineering" in the AlGaAs/GaAs system. The use of superlattices to improve the characteristics of both HBTs and HEMTs is an important example of this.

The Future of MBE

The foreseeable future of MBE as a research and development tool for III-V devices and circuits seems assured, because of its control and versatility, and the resultant device performance. The usefulness of MBE as a production tool, however, must still be demonstrated. For production of circuits, the high speed performance demonstrated in the laboratory must be achieved at an acceptable cost per wafer. This cost will be determined by equipment and labor costs, and the throughput, and yield of good wafers. The present cost per MBE wafer may be acceptable for pilot production, if yield limitations imposed by oval defects and the need for frequent equipment recalibration can be reduced or removed. This will require a joint effort between MBE researchers and manufacturers of MBE equipment.

References

1) C.P. Lee, D. Hou, S.J. Lee, D.L. Miller, and R.J. Anderson, Proc. IEEE Gallium Arsenide Integrated Circuit Symposium, Oct., 1983, p.152.

2) S.S. Pei, N.J. Shah, R.H. Hendel, C.W. Tu, and R. Dingle, Proc. IEEE Gallium Arsenide Integrated Circuit Symposium, Oct., 1984, p.129

3) P.M. Asbeck, D.L. Miller, R.J. Anderson, R.N. Deming, R.T. Chen, C.A. Leichti, and F.H. Eisen, Proc. IEEE Gallium Arsenide Integrated Circuit Symposium, Oct. 1984, p.133.

FRIDAY, MARCH 15, 1985

FA, QUANTUM STRUCTURES

Claude Weisbuch, Thomson-CSF, *Presider*

New high-speed Optoelectronic and electron superlattice and heterojunction devices

Federico Capasso
AT&T Bell Laboratories
Murray Hill, NJ 07974

In this talk very recent advances in heterojunction and superlattice structures for high-speed optoelectronic and electron device applications are discussed.

(1) *Interface Engineering via doping-interface-dipoles: tunable heterojunction barrier heights and band-edge discontinuities.*

We have succeeded for the first time in artificially tuning the conduction and valence band barrier heights at an abrupt intrinsic semiconductor-semiconductor heterojunction via a doping interface dipole (DID). This is achieved by means of ultrathin ionized donor and acceptor sheets in situ grown within $\lesssim 100$ Å from the hetero-interface by molecular beam epitaxy. In the limit of a few atomic layers separation between the charge sheets this amounts to modifying the band-edge discontinuities. A barrier lowering of $\simeq 0.10$ eV has been achieved at an AlGaAs/GaAs heterojunction interface leading to a one order of magnitude enhancement in the heterojunction photocollection efficiency. The doping interface dipole concept, as a band-gap engineering technique, has far-reaching implications for both the physics of interfaces and the design of novel heterostructure devices. Application to high speed detectors, staircase APDs, lasers and FETs will be discussed.

(2) *Pseudo-Quaternary GaInAsP Semiconductors: a new high-speed avalanche photodiode with graded gap superlattice.*

We have demonstrated for the first time a pseudo-quaternary GaInAsP semiconductor consisting of a graded gap $Ga_{0.47}In_{0.53}As/InP$ superlattice. The average composition and the band gap of this structure is spatially varied by gradually changing the thicknesses of the InP and $Ga_{0.47}In_{0.53}As$ layers between 5 and 55 Å while keeping constant the period of the superlattice (=60 Å). This graded gap superlattice has been used to eliminate the interface pile-up effect of holes (which is detrimental to device speed) in a new "high-low" $InP/Ga_{0.47}In_{0.53}As$ avalanche photodiode, without requiring the growth of a separately lattice-matched $Ga_{1-x}In_xAs_{1-y}P_y$ layer. High speed operation at 1.7 Gb/sec and $\lambda = 1.55$ μm has been achieved. Pseudo-quaternary semiconductors represent a new technique of growing GaInAsP and can conveniently replace conventional $Ga_{1-x}In_xAs_{1-y}P_y$ alloys in a variety of device applications.

(3) *New ultrahigh speed negative differential resistance quantum well devices for microwave and multiple valued logic applications.*

A new class of quantum well device concepts which have potential for high frequency oscillators has been introduced. In addition these functional devices have potential for many signal processing and logic applications, allowing tremendous simplification in circuitry and increase in speed. In one configuration the device provides a binary digital output for an analog or multiple valued digital input, acting as threshold logic gate. This can be used as a parity generator in error detection circuits and in novel A to D converters. In another configuration the device has a multiple valued negative differential resistance characteristic. When connected to a resistive load a device having N stable states ($2 \leq N \leq 8$) is produced, which can be used in multiple valued logic applications.

SEMICONDUCTOR QUANTUM WELLS : PHYSICS AND APPLICATIONS

by
D. S. Chemla
AT&T Bell Laboratories, Holmdel

The nonlinear optical effects utilized in various optoelectronics devices are the variations of the refractive index (n) or of the absorption coefficient (α) induced by an optical or by a static electromagnetic field. In semiconductors these nonlinearities exhibit large enhancements close to the excitonic resonances that are observed at low temperature near the band gap in bulk materials. Recently, modern techniques of crystal growth have permitted the fabrication of ultra-thin semiconductor layers ($L_z \sim 100$Å) with atomically smooth interfaces and perfectly controlled composition. One important effect of the confinement of carriers in ultra-thin layers is to stabilized excitonic resonances which become consequently observable at room temperature. In quantum wells it is therefore possible to observed and utilize enhanced nonlinear optical effects in very convenient conditions for applications. In addition excitons at room temperature exhibit interesting new specific properties not observed at low temperature. In our laboratory multiple quantum well structures (MQWS) of high enough quality to exhibit excitonic resonances at room temperature have been grown in the GaAs/AlGaAs and in the GaInAs/AlInAs systems (1,2). The excitonic resonances occur at 0.85 μm and 1.6 μm for the two systems respectively.

The dynamics of the excitonic absorption saturation has been studied using *cw*, psec and fsec lasers (3,4). Extremely large optical nonlinearities have been observed. They consist of two components, one which is due to phase-space filling and one due to free carrier screening. The first one has a very fast recovery time ~300 fsec limited by the thermal LO-phonon ionization of room temperature excitons and has a cross section about twice as large as than that due to screening. Theoretical model in good agreement with experiment have been developed. Applications to diode laser four wave mixing (5) and diode laser mode locking have been demonstrated (6). Stable operation and generation of pulses as short as 1.6 psec have been obtained (6).

Strong electro-absorption can be seen when static electric fields are applied to MQWS parallel or perpendicular to the layers. These effects are intrinsically very fast because they are

related to the speed at which the electronic envelope functions can follow the applied field. When the field is perpendicular to the layers one observes large red shifts of the exciton resonances which remain well resolved up to fields > 50 times the classical ionization field (7). This new Quantum-Confined Stark effect (QCSE) has been applied to high speed optical modulation (8,9), gates for optical logic (10), linearized optical modulators (11) and optical level shifters (11). When the field is parallel to the layers the usual Stark effect of the quasi two-dimensional exciton produces a broadening and loss of oscillator strength due to the field ionization. Although the changes in absorption observed in this geometry are less contrasted than for the QCSE the two dimensional Stark effect is very sensitive and can be exploited in extremely fast devices owing to the very small capacitance associated with this geometry (12). Application to high speed/high sensitivity sampling has recently been demonstrated (13). For both geometries excellent agreement has been obtained between experiment and theory (7,12).

REFERENCES

[1] D. A. B. Miller, D. S. Chemla, P. W. Smith, A. C. Gossard, W. T. Tsang, Appl. Phys., B28 96 (1982).

[2] J. S. Weiner, D. S. Chemla, D. A. B. Miller, T. H. Wood, D. Sivco A. Y. Cho, to be published.

[3] D. S. Chemla, D. A. B. Miller, P. W. Smith, A. C. Gossard, W. Wiegmann, IEEE QE-20 265 (1984).

[4] W. H. Knox, R. L. Fork, M. C. Downer, D. A. B. Miller, D. S. Chemla, C. V. Shank, A. C. Gossard, W. Wiegmann to be published.

[5] D. A. B. Miller, D. S. Chemla, P. W. Smith, A. C. Gossard, W. Wiegmann, Optic. Lett. 8 477 (1983).

[6] Y. Silberberg, P. W. Smith, D. J. Eilenberger, D. A. B. Miller, A. C. Gossard, W. Wiegmann to be published in Optics Letters.

[7] D. A. B. Miller, D. S. Chemla, T. C. Damen, A. C. Gossard, W. Wiegmann, T. H. Wood, C. A. Burrus to be published.

[8] T. H. Wood, C. A. Burrus, D. A. B. Miller, D. S. Chemla, T. C. Damen, A. C. Gossard, W. Wiegmann, Appl. Phys. Lett. 44 16 (1984).

[9] T. H. Wood, C. A. Burrus, D. A. B. Miller, D. S. Chemla, T. C. Damen, A. C. Gossard, W. Wiegmann to be published.

[10] D. A. B. Miller, D. S. Chemla, T. C. Damen, A. C. Gossard, W. Wiegmann, T. H. Wood, C. A. Burrus, Appl. Phys. Lett. 45 13 (1984).

[11] D. A. B. Miller, D. S. Chemla, T. C. Damen, A. C. Gossard, W. Wiegmann, T. H. Wood, C. A. Burrus, Optic. Lett. 9 (1984).

[12] D. A. B. Miller, D. S. Chemla, T. C. Damen, A. C. Gossard, W. Wiegmann, T. H. Wood, C. A. Burrus, to be published.

[13] W. H. Knox, D. A. B. Miller, P. M. Downey, T. C. Damen, D. S. Chemla, A. C. Gossard, W. Wiegmann, to be published.

Electric Field-induced Decrease of Exciton Lifetime in GaAs Quantum Wells

J.A. Kash and E.E. Mendez
IBM Thomas J. Watson Research Center, Yorktown Heights, NY 10598
and H. Morkoc
University of Illinois at Urbana-Champaign,Urbana, IL 61801

Previously[1], it has been shown that c.w. photoluminescence (PL) at helium temperatures for excitons confined in quantum wells decreases sharply (i.e. is quenched) when an electric field is applied perpendicular to the layers. It was suggested there that the decrease might be due to spatial separation of the electrons and holes under the influence of the electric field. This separation would reduce the electron-hole spatial overlap, thus increasing the exciton radiative lifetime. In order to examine the luminescence quenching in more detail, we have measured the exciton PL decay directly.

We used MBE grown quantum wells consisting of six $Ga_{0.65}Al_{0.35}As$ - GaAs quantum wells. Well thickness was ~30Å, with a barrier thickness of 100Å. The wells were clad between a 1μm GaAs buffer layer and a 0.1μm $Ga_{0.65}Al_{0.35}As$ layer on top. An electric field perpendicular to the layers was applied by means of a Schottky diode configuration, formed by evaporating a 60Å thick semitransparent Ni film on the heterostructures. The quantum wells were inside the space-charge region, estimated to be ~0.8μm, where the built-in field was ~10^4 V/cm. With an applied voltage V_{ext}=-1.0 V, we estimate the total electric field to be ~5×10^4 V/cm.

The samples, held at T=8K, were excited with a synchronously-pumped cavity-dumped dye laser producing 10 psec pulses at a 700 kHz repetition rate. The laser wavelength was 5820Å, and the maximum pulse energy incident of the sample was 1 njoule. The PL was analyzed with a double-pass 0.75m monochromator and detected with a cooled photomultiplier tube. The time decay was measured by time-resolved photon counting, as described more fully elsewhere[2]. The system resolution was 200 psec (FWHM); decay times as short as 50 psec were inferred from deconvolution techniques.

Figure 1 shows the PL decay of the intrinsic n=1 exciton at several values of externally applied voltage V_{ext}. Note the substantial decrease in lifetime with applied field. The fastest decay is approaching the system resolution limit. The time-integrated PL spectra also decreases sharply[1]. Similar results are seen in other quantum well samples. In fig. 2, the luminescence decay time τ vs. V_{ext} is shown for several average laser pump powers for the same sample. We see that the lifetime quenching is reduced at high laser intensities.

The carrier separation proposed in Ref. 1 to explain the c.w. data does not explain the time-resolved data presented here, as this model predicts an increase in τ. We propose two mechanisms which could be responsible for the observed decrease. First, the carriers, which are strongly polarized within the wells by the external field, can leave the wells by Fowler-Nordheim tunneling. The tunneling probability depends[3] exponentially on the combination $-(m^*)^{1/2}\phi^{3/2}/\mathcal{E}$, where m^* is the effective mass, ϕ is the potential barrier with respect to the quantum level, and $\mathcal{E}$ is the electric field. Times of order 10^{-13} sec can be obtained for $\mathcal{E}=5\times10^5$ V/cm and reasonable values of ϕ (e.g. ϕ_e = 0.06 eV, ϕ_h = 0.03 eV). Unfortunately, the [illegible] time for carriers in the well is very sensitive to ϕ and $\mathcal{E}$, so

that a more quantitative analysis could not be made. The second explanation is field-induced leakage of the wave functions into the $Ga_{1-x}Al_xAs$ barriers. A variational calculation, similar to the one described elsewhere[4], shows that this leakage will reduce the exciton lifetime, but the reduction is too small to account for our data. Thus Fowler-Nordheim tunneling is the principle cause of the lifetime quenching.

Exciton screening can account for the observed dependence on laser power. The photo-created excitons in the wells will be polarized by the electric field, and the net exciton polarization (which depends upon the exciton density) can in turn screen out the electric field. We estimate that the screening will be important at exciton concentrations comparable to the highest ($\sim 3\times10^{18}$ cm^{-3}) used in these experiments.

The work at IBM has been sponsored in part by the U.S. Army Resarch Office. The work at the University of Illinois has been sponsored by the Joint Services Electronics Program.

REFERENCES

1. E.E. Mendez, G. Bastard, L.L. Chang, L. Esaki, H. Morkoc, and R. Fischer, Phys. Rev. B26, 7101 (1982).
2. J.A. Kash, J.H. Collet, D.J. Wolford, and J. Thompson, Phys. Rev. B27, 2294 (1983).
3. R.A. Smith, *Wave Mechanics of Crystalline Solids, Second Edition*, (Chapman and Hall, London, 1969), p. 60.
4. G. Bastard, E.E. Mendez, L.L. Chang, and L. Esaki, Phys. Rev. B28, 3241 (1983).

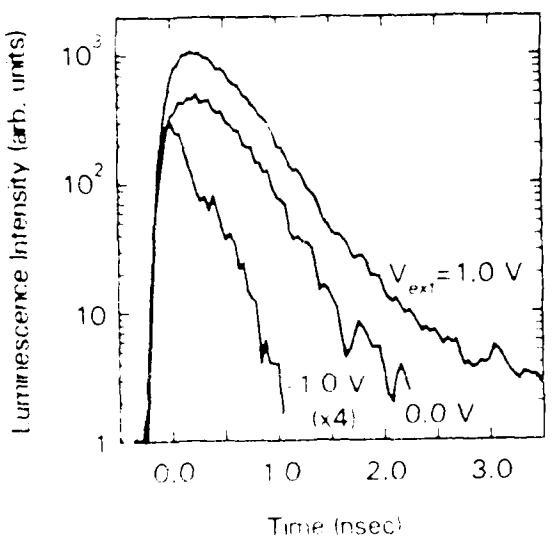

Figure 1. Photoluminescence decay of the intrinsic n=1 exciton at 7570nm for several values of externally applied voltage V_{ext}. The average laser power here was four watts.

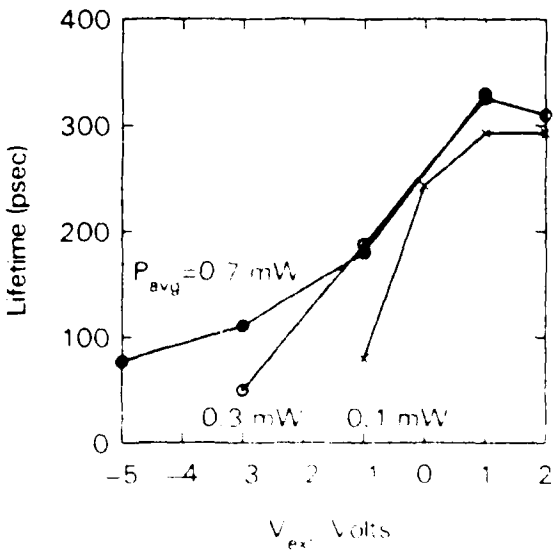

Figure 2. Luminescence decay times vs V_{ext} for several average laser pump powers for the same sample as in Fig. 1. The highest power corresponds to a peak exciton density of about 3×10^{18} cm^{-3}.

Reduction of Electron-Phonon Scattering Rates by Total Spatial Quantization

M.A.Reed, R.T.Bate, W.M.Duncan, W.R.Frensley, and H.D.Shih

Central Research Laboratories
Texas Instruments Incorporated
P.O.Box 225936, M S 134
Dallas, Texas 75265

The physics of spatially quantized systems has been the subject of intense investigation since the introduction of MBE and MOCVD. Quantum wells have been exhaustively examined since the seminal works of Dingle et al[1]. More recently, studies on quantum wires[2] have yielded interesting new properties. Here, we present data on a completely spatial quantized system that shows unique photoluminescence structure resulting from an electron or hole phonon scattering bottleneck.

The dimensionally confined structures studied were reactive ion etched GaAs-AlGaAs multiple quantum well samples. The photoluminescence from quantum wells (2 degrees of freedom, or "2 DOF") were compared to that from quantum wires (1 DOF) and found to be essentially the same. However, photoluminescence from "quantum dots" (0 DOF) was strikingly different, exhibiting enhanced electron - light hole recombination. The enhanced light hole population is explained by a reduction in the interbranch hole phonon scattering rate that produces a bottleneck near the zone center. Similar results demonstrated that the bottleneck can also occur for electrons. These results are uniquely observable in quantum well samples due to the reduction in the radiative recombination

time[3].The imposition of total spatial quantization on a semiconductor system turns the quasi-continuous dispersion relations of the 2- or 1- DOF structures into a series of discrete energetic levels for the 0 DOF quantum dot case. Thermalization rates down these branches as well as the interbranch scattering rates are slowed due to a decrease in the density of final states and modification of the phonon spectra. We believe that the observation of this bottleneck is the first experimental evidence for discrete electronic levels in a total spatially quantized semiconductor system.

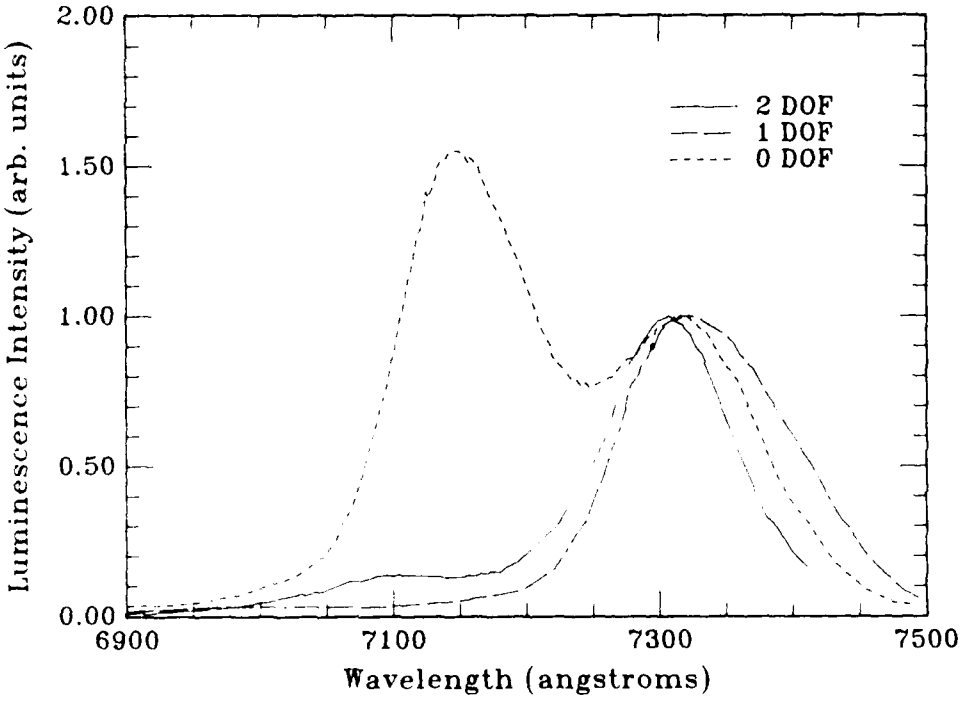

[1]R.Dingle, A.C.Gossard, and W.Wiegmann, *Phys. Rev. Lett.* 34, 1327(1975).

[2]W.J.Skocpol, L.D.Jackel, E.L.Hu, R.E.Howard, and L.A.Fetter, *Phys. Rev. Lett.* 49, 951(1982).

[3]J.Christen, D.Bimberg, A.Steckenborn, and G.Weimann, *Appl. Phys. Lett.* 44, 84(1984).

High Speed Phenomena in Resonant Tunneling*

T. C. L. G. Sollner, H. Q. Le†, C. A. Correa,
P. E. Tannenwald and W. D.Goodhue

Lincoln Laboratory, Massachusetts Institute of Technology
Lexington, Massachusetts 02173

Resonant tunneling devices have recently been used as detectors and mixers to demonstrate that the nonlinearities and negative resistance persist even up to 2.5 THz(1), and that oscillations at microwave frequencies are possible using the negative resistance(2). This presents a unique opportunity to explore the physics and device possibilities in semiconductors on time scales of 100 fs. During our investigations of fast processes, additional phenomena with other time constants were observed. One effect which has been studied in detail is attributed to persistent photoconductivity which involves ionization of DX centers(3) in the AlGaAs barriers. Another effect is observed by mixing two optical beams of above-band-gap radiation with a high difference frequency.

The double-barrier tunneling structures (quantum-well resonators) studied here are reviewed in Figure 1. Resonant tunneling requires the coherent interaction of an electron wavefunction over the double-barrier structure. The very thin layers of $Al_{0.35}Ga_{0.65}As$, because of their higher bandgap, act as partially transparent mirrors to electrons incident from the GaAs regions, the transmission taking place by tunneling. Just as in a Fabry-Perot resonator, there are peaks in the transmission, i.e. in the current, when incident electrons have the resonant energy. This produces current-voltage curves also shown in Figure 1.

In the persistent photoconduction experiments, the well-barrier region was illuminated from a grating monochromator through an electronic shutter. Figure 2 shows experimental I-V curves for several different exposures. Note that as the number of photons increases, the current peak increases and shifts to lower voltages. This is explained by the model illustrated in Fig. 3, which shows modifications to the conduction band of the double barrier structure due to positive charges in the barrier. These positive charges arise from ionization of DX centers which are known to exist in Si doped AlGaAs(3). Calculations of I-V curves using essentially the method of Tsu and Esaki(4) agree well with the observed I-V curves shown in Fig. 2. The relationship between peak current and number of ionized centers (deduced from the exposure required for saturation) is found to be linear both theoretically and experimentally, and the derived DX center density is found to agree with estimates from material growth parameters.

The high-speed photoconductive mixing effects mentioned above are currently under investigation to establish the limiting process. Response on the order of 100 fs is likely.

*This work was supported by the U.S. Army Research Office.

†Francis Bitter National Magnet Laboratory, Massachusetts Institute of Technology, Cambridge, Massachusetts 02139

REFERENCES

1. T. C. L. G. Sollner, W. D. Goodhue, P. E. Tannenwald, C. D. Parker, and D. D. Peck, Appl. Phys. Lett. 43, 588 (1983).
2. T. C. L. G. Sollner, P. E. Tannenwald, D. D. Peck, and W. D. Goodhue, to be published, Appl. Phys. Lett. 15 Dec. 1984.
3. D. V. Lang and R. A. Logan, Inst. Phys. Conf. Ser. 43, 433 (1979).
4. R. Tsu and L. Esaki, Appl. Phys. Lett. 22, 562 (1973).

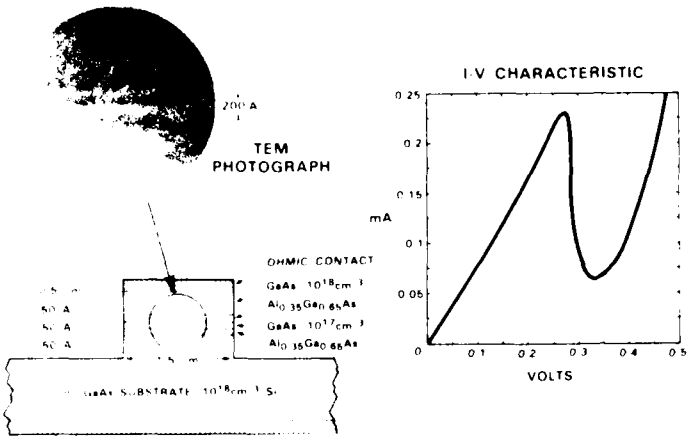

Figure 1. Resonant tunneling structure and resulting I-V curve. The Si doping in the GaAs regions diffuses into the barriers to produce DX centers.

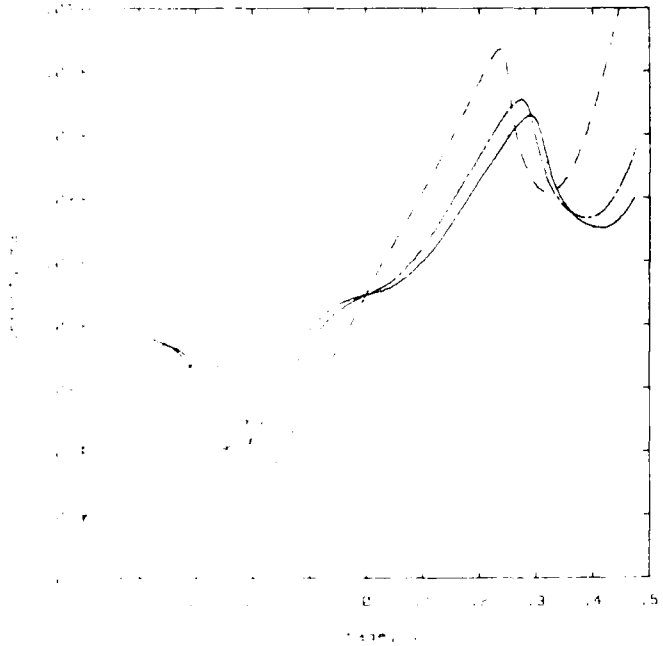

Figure 2. Current-voltage curves of quantum well resonator with increasing exposure. The solid curve is unexposed, the broken curve has integrated flux N, the dashed curve is 10N, the dotted curve is 100N.

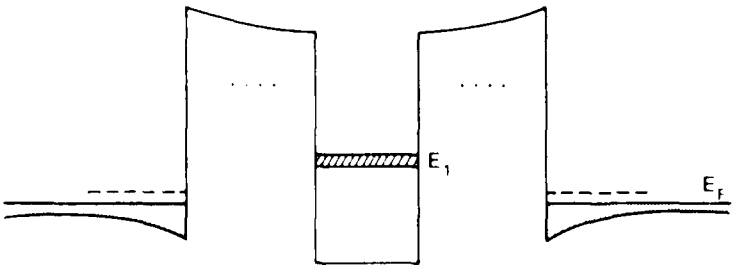

Figure 3. Conduction band including positive charges in the barriers and electrons in the contact regions. These cause the parabolic band bending.

FRIDAY, MARCH 15, 1985

FB, ELECTRONICS AND OPTOELECTRONICS

Gerald Witt, Air Force Office of Scientific Research,
Presider

[illegible] HETEROJUNCTION BIPOLAR TRANSISTOR TECHNOLOGY FOR HIGH SPEED INTEGRATED CIRCUITS

P.M. Asbeck
Rockwell International Corporation
1049 Camino Dos Rios, Thousand Oaks, CA 91360

A bipolar [illegible] provides many potential benefits for picosecond electronic circuits: (a) current flow is vertical, through epitaxial layers whose thickness is only a few tenths of a micron, decreasing carrier transit times; (b) large amounts of current can be carried by modest size transistors, enabling rapid charging of interconnect capacitances; and (c) threshold voltages are tied to built-in potentials of pn junctions, which are easy to reproduce device-to-device, enabling low-rate logic voltages to be established. Added advantages [illegible] using III-V heterojunctions rather than Si: (a) high electron mobility; (b) pronounced transient electron velocity overshoot effects; (c) ability to incorporate quasi-electric fields into the devices by semiconductor composition variations; and (d) ability to insure adequate emitter efficiency with wide gap emitters. As a result of these advantages, HBTs offer prospects for switching time delays in the sub 10 ps regime, with a robust, manufacturable fabrication process.

A [illegible] GaAs/GaAlAs single-heterojunction HBTs is shown in Fig. 1. An abrupt emitter-base heterojunction gives rise to a conduction-band [illegible] discontinuity that may act as a "ballistic launching ramp" to inject high velocity electrons into the base. With a graded emitter-base heterojunction this spike disappears, and the full bandgap difference contributes to reducing hole injection into the emitter. High gain, high speed devices have so far been made with both approaches. Grading the aluminum composition, and hence bandgap, across the base can provide a quasi-electric field to drive electrons to the collector more rapidly than by diffusion alone. Other possibilities include the insertion of a wide bandgap collector (in order to minimize hole storage during transistor saturation), as well as the [illegible] superlattice regions in the emitter and collector [illegible] GaAs material combinations.

[illegible] HBT performance has been carried out at several levels of [illegible]. Figure 2 shows the short circuit frequency [illegible] dimensional [illegible] ad-hoc way only. The [illegible] GHz as well as [illegible] Monte-Carlo calculations with [illegible] electron effects [illegible] for f_t is the collector depletion [illegible] in accordance with the base- [illegible] current-dependent [illegible].

To replace [illegible] MBE epitaxial [illegible] have been utilized. [illegible] process which uses [illegible] isolation between devices [illegible] is used to avoid [illegible] produce a [illegible] between extrinsic base [illegible]

Experimental device characteristics show current gain adequate for digital integrated circuits (30-50 in devices with 1.6 μm emitters), high current handling capability (up to 10^5 A/cm^2), high transconductance (6000 mS/mm) and high threshold voltage uniformity (standard deviation of 4 mV across a wafer). Data of current gain vs frequency calculated from S parameter measurements are displayed in Fig. 4, indicating a cutoff frequency f_t of 40 GHz.

Prototype digital integrated circuits have been fabricated with these HBTs. In nonthreshold logic (NTL) ring-oscillators, propagation delays down to 30 pS per gate have been demonstrated (at 4 mW per gate, with devices whose emitters were 1.2 μm wide). Current-mode logic (CML), a simplified form of ECL, has been used to implement frequency dividers which to date have operated up to 8.5 GHz. Applications in very high speed digital integrated circuits at various levels of complexity, gate arrays, A/D converters, as well as in microwave and mm wave discrete devices may be envisioned. For microwave applications, HBTs benefit from having much lower 1/f noise than FETs.

HBT technology is presently in its infancy. Significant performance advances are expected from device scaling and introduction of self-aligned fabrication methods. Added benefits may result from the use of new materials systems.

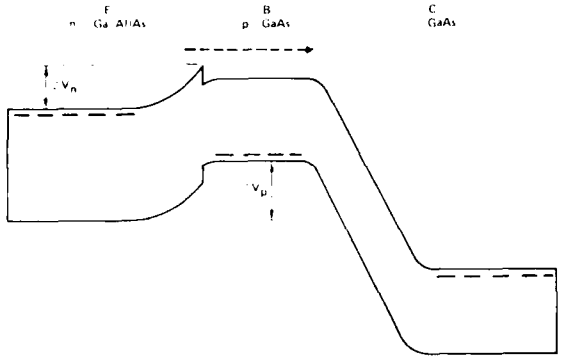

Fig. 1 Schematic band diagram of HBT.

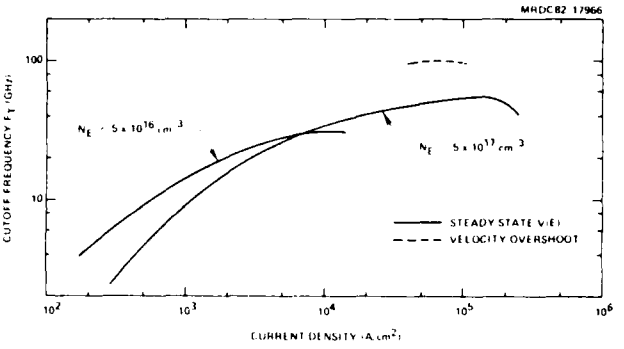

Fig. 2 Calculated cutoff frequency vs collector current density.

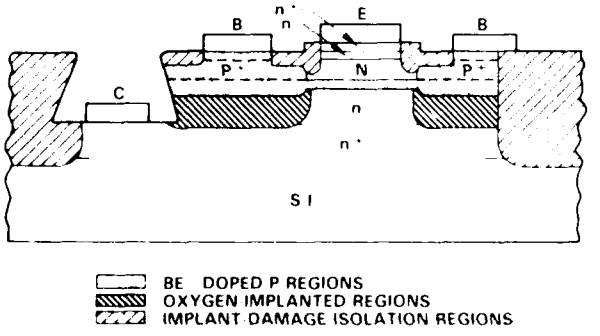

Fig. 3 Schematic cross-section of HBTs fabricated at Rockwell.

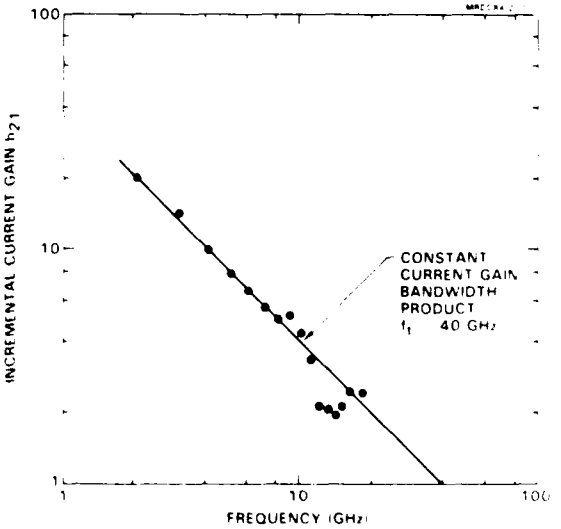

Fig. 4 Current gain, h_{21}, vs frequency from S parameter measurements.

The Permeable Base Transistor*

R. A. Murphy

Lincoln Laboratory, Massachusetts Institute of Technology
Lexington, Massachusetts 02173

The permeable base transistor (PBT) was conceived in 1979[1] and the first devices were fabricated shortly thereafter[2]. Numerical simulations predicted usable gains in the EHF frequency range[3] and high speed performance in a logic circuit[4]. A three-dimensional drawing of a GaAs PBT showing a cutaway region is shown in Figure 1. The unique feature of a PBT is the thin tungsten grating of submicrometer periodicity (3200 Angstroms in the devices we have fabricated) embedded in the single-crystal GaAs. The tungsten grating separates the emitter layer from the collector layer and forms the base of the transistor. Because the tungsten forms a Schottky barrier with the GaAs, the voltage on the metal can be used to control the current flowing from the collector the emitter. The critical length of the control region is determined by the metallization thickness and the depletion width around the tungsten. Hence it can be made quite short, giving rise to the PBT's high frequency and high speed properties. In the device of Figure 1 proton bombardment is used to isolate and define the device and to provide insulating regions on which to fabricate contact pads.

An intensive effort to develop the complex technology necessary to fabricate PBTs has taken place in the past five years. We have fabricated both silicon and GaAs PBTs. This effort has included the development of x-ray lithographic techniques for base patterning, base metallization techniques, contact fabrication techniques, and techniques for GaAs overgrowth. The best result achieved with the GaAs PBT are devices with an extrapolated maximum frequency of oscillation (f_{max}) exceeding 100 GHz[5], and that achieved with a silicon PBT is an f_{max} of 20 GHz. Both of these results are comparable with the best results obtained with any high frequency transistor.

The achievement of high quality and controllable GaAs epitaxial overgrowths has proved to be a particularly difficult problem. We have investigated a number of overgrowth techniques, including vapor phase epitaxy (VPE), molecular beam epitaxy (MBE) and organometallic chemical vapor deposition (OMCVD). We have also recently conducted a comprehensive investigation of the overgrowth process using secondary-ion mass spectrometry (SIMS). These results have indicated that OMCVD and MBE may be fundamentally superior to VPE for the overgrowth process. In addition, we have obtained very encouraging device results with OMCVD-overgrown and MBE-overgrown PBTs, and are currently concentrating on PBTs fabricated with these techniques.

The PBT faces strong competition from other high speed devices, such as AlGaAs/GaAs transistors, heterojunction bipolar transistors, and conventional FETs. Perhaps the ultimate high speed device of the future will combine the best elements of all of these devices. However, the experimental results we

*This work was sponsored by the Defense Advanced Research Projects Agency and the Department of the Air Force.

have obtained demonstrate excellent high speed capability of the PBT. Although the manufacturability of the PBT remains to be demonstrated, we believe that the technological problems involved can be solved and that the PBT will find many analog, digital, and electrooptical applications.

References

1. C. O. Bozler, G. D. Alley, R. A. Murphy, D. C. Flanders, and W. T. Lindley, "Permeable Base Transistor," in Proc. 7th Bien. Cornell Conf. on Active Microwave Semiconductor Devices, p. 33, August 1979.

2. C. O. Bozler and G. D. Alley, "Fabrication and Numerical Simulation of the Permeable Base Transistor," IEEE Trans. Electron Devices, vol. ED-27, p. 1128, June 1980.

3. C. O. Bozler, G. D. Alley, R. A. Murphy, D. C. Flanders and W. T. Lindley, "Fabrication and Microwave Performance of the Permeable Base Transistor," in IEEE Int. Electron Devices Mt. Tech. Dig., p. 384, December 1979.

4. C. O. Bozler and C. D. Alley, "The Permeable Base Transistor and Its Application to Logic Circuits," Proc. IEEE, vol. 70, p. 46, January 1982.

5. G. D. Alley, C. O. Bozler, N. P. Economou, D. C. Flanders, M. W. Geis, G. A. Lincoln, W. T. Lindley, R. W. McClelland, R. A. Murphy, K. B. Nichols, W. J. Piacentini, S. Rabe, J. P. Salerno and B. A. Vojak, "Millimeter-Wavelength GaAs Permeable Base Transistors," 1982 Device Research Conference, Ft. Collins, CO.

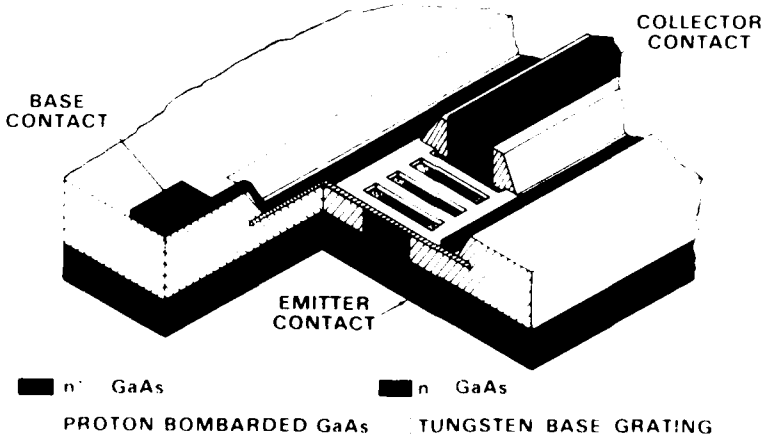

Figure 1. Cross-sectional drawing of a GaAs PBT.

Picosecond Photoconductivity In Polycrystalline CdTe Films Prepared By UV Enhanced OMCVD

A. M. Johnson, D. W. Kisker, and W. M. Simpson

AT&T Bell Laboratories
Holmdel, New Jersey 07733

Picosecond photocurrent transients have been reported in thin films of amorphous[1] and radiation-damaged[2] semiconductors. We report the first measurements of picosecond photoconductivity in 1800 Å thick films of polycrystalline CdTe grown by organometallic chemical vapor deposition (OMCVD) with a grain size of approximately 200 Å. We have made high-speed photodetectors with a sampling oscilloscope limited response time of 35 psec (FWHM) with an average drift mobility of $\mu \geq 11 cm^2/Vsec$. The variation of the grain size as a means of varying the carrier relaxation time and drift mobility will be discussed.

The CdTe film was grown by a modified OMCVD technique. Normally, the low temperature limit of thermal deposition for these materials is about 380-410 °C due to the stability of the starting compounds, diethyltellurium and dimethylcadmium[3]. Using uv light to enhance the reaction, we are able to deposit polycrystalline CdTe and $Hg_{1-x}Cd_xTe$ with a grain size of about 200 Å, at a temperature of 250°C. This material can be grown on a variety of substrates such as GaAs, Si, and fused silica, and by varying the deposition temperature the grain size can be changed.

The 1800 Å thick CdTe film was deposited onto a 250 μm thick fused silica substrate and incorporated into a standard 50 Ω microstrip transmission line configuration[1]. In this gap cell configuration a 12 μm gap between the aluminum electrodes served as the active area of the photodetector. The sampling oscilloscope limited response of this detector to a picosecond excitation source[4] at 600 nm is displayed in Fig. 1. A peak photovoltage of 267 mV resulted when the detector was photoexcited by an absorbed average power of 3.3 mW (not corrected for electrode reflection) and a bias of 50V. The absorptance of the sample was 44%. With these operating parameters the detector had a responsivity of 5.6mA/W and a $\mu\tau$ product of 3.4×10^{-10} cm^2/V. A conservative estimate of the response time of the detector of 30 psec results in a lower limit of the average drift mobility of $\mu \geq 11 cm^2/Vsec$. This detector is comparable in both speed and sensitivity to 1-μm thick radiation-damaged silicon-on-sapphire photodetectors[2]. The dark resistance

of the detector at 50V bias was 3.3×10^{10} Ω for a resistivity of 2.6×10^{7} Ω-cm. High speed correlation measurements[5] will be performed to determine the true speed of response of the device. Experiments are in progress to study the electronic transport as a function of grain size and to determine the nature of the trapping and or recombination centers at the grain boundaries. We will describe the variation of detector properties with changes in substrate and Hg composition.

1. D. H. Auston, P. Lavallard, N. Sol, and D. Kaplan, Appl. Phys. Lett 36, 66 (1980).
2. P. R. Smith, D. H. Auston, A. M. Johnson, and W. M. Augustyniak, Appl. Phys. Lett. 38, 47 (1981).
3. J. B. Mullin, S. J. C. Irvine, and D. J. Ashen, J. Cryst. Growth 55, 92 (1981).
4. A. M. Johnson and W. M. Simpson, Opt. Lett. 8, 554 (1983).
5. D. H. Auston, A. M. Johnson, P. R. Smith, and J. C. Bean, Appl. Phys. Lett. 37, 371 (1980).

Figure 1: Response of the photodetector to 1 psec pulses from a synchronously modelocked Rh6G dye laser operating at a repetition rate of 100.498 MHz.

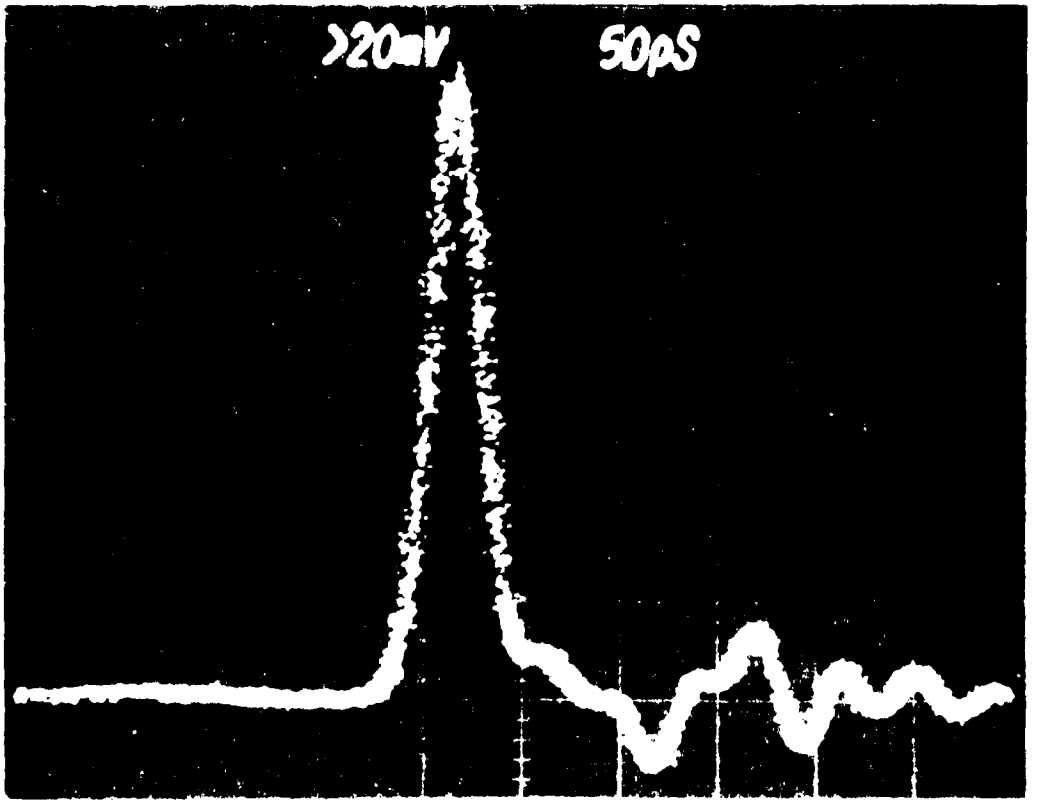

of ~ 10 ps without any loss in responsivity. These experiments are currently in progress and results will be reported.

These techniques are also applicable to a number of other Schottky barrier systems such as metal-GaAs and metal-Si. For the GaAs case, this will result in a fast detector, sensitive to near-infrared wavelengths, which can be simply fabricated on bulk material and can be integrated with additional GaAs circuits. For all of these systems the ability to tailor the spectral response by adjusting the grating parameters will provide enhanced capabilities, particularly for the detection of spectrally narrow sources.

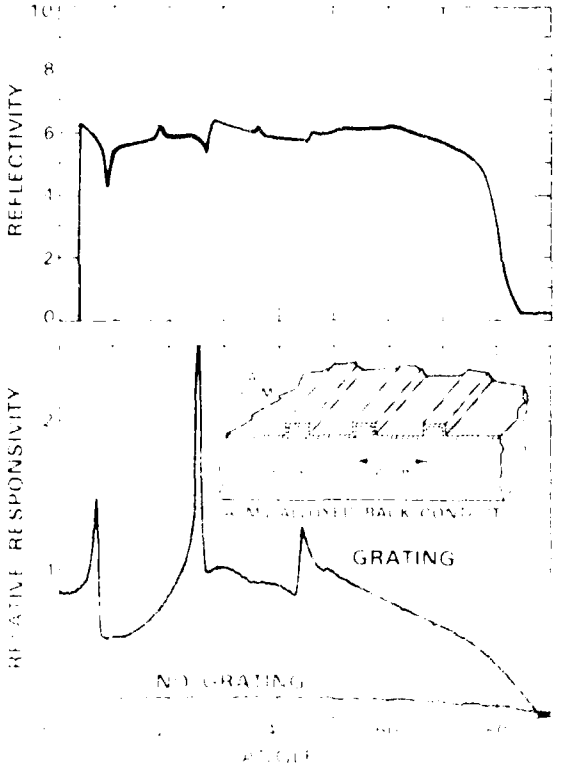

[illegible] the incident [illegible] on a $Al_xGa_{1-x}As$ [illegible] surface (see [illegible].

Submicron-gap Photoconductive Switching in Silicon

G.G. Shahidi, E.P. Ippen and J. Melngailis

Department of Electrical Engineering and Computer Science
and Research Laboratory of Electronics
Massachusetts Institute of Technology
Cambridge, MA 02139

The most common approach to increasing the speed of photoconductive switches has been to reduce the carrier lifetime, either by bombardment with high-energy ions [1] or by the use of disordered materials [2]. In either case, the material defects, which act as centers for recombination, may also reduce the free-carrier mobility before recombination and thus unnecessarily lower the sensitivity of the photoconductor. An alternative approach to increasing the speed of response is to sweep the photoinduced carriers out of the gap with the applied voltage in a time short compared to their lifetime [3]. Here we describe the application of this technique to photoconductive switching in high mobility silicon. With sub-micron photoconductive gaps and carrier sweep-out the response time has been reduced from 700 psec to 27 psec. Electrical pulses of more than 1 volt have been switched with optical pulse energies of less than a nanojoule.

The photoconducting samples used in our work were commercially available, intrinsic polysilicon films on sapphire. They were 1 μm thick, had a dark resistivity of 1.09×10^9 ohms/square, and had a measured (sum of electron and hole) mobility of about 470 $cm^2/V.sec$. Sub-micron gaps in aluminum strip-lines were fabricated by first using reactive ion etching to produce a sharp, straight-walled step in the silicon film and then evaporating at an angle to create a gap in the shadow of the silicon step.

Measurements of response times were performed, as a function of gap dimension and applied voltage, both by direct electrical detection with a sampling oscilloscope and by the correlation of two different gaps. Figure 1 shows the experimental, two-gap geometry. Optical pulses of about 4 psec (FHWM) from a synchronously pumped Rhodamine 6G dye laser were focused on the two gaps with variable relative delay. Figure 2 shows the response correlations obtained for two different bias voltages when one of the gaps, 0.8 μm in width, is operated in the sweep-out regime. For a 3 volt bias the rapid response indicates generation of an electrical pulse of 27 psec FWHM.

REFERENCES

1) P.R. Smith, D.H. Auston, A.M. Johnson and W.M. Augustyniak, Appl. Phys. Lett., 38, 47 (1981).

2) D.H. Auston, P. Cavalieri, A. Dienes, and J. Shah, Appl. Phys. Lett., 39, 66 (1981).

3) J. Degani, R.B. James, M.E. Nadler, M.A. Pollack, J.P. Heritage and J.C. Dewhurst, Appl. Phys. Lett., 39, 77 (1981).

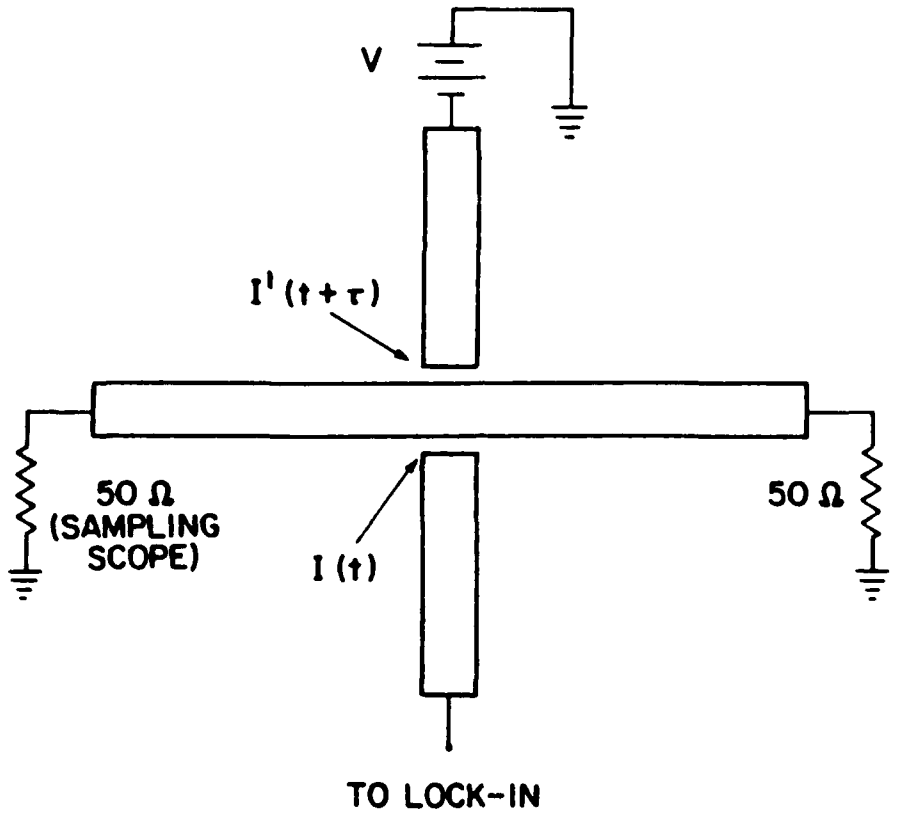

Figure 1

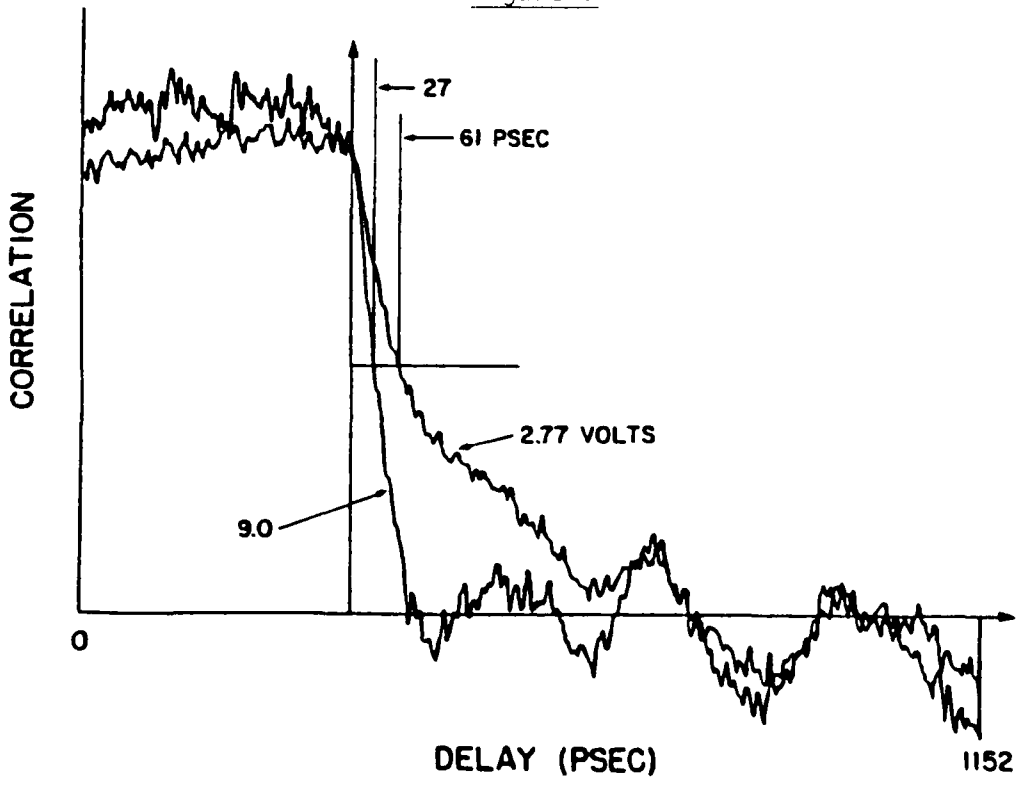

Figure 2

KEY TO AUTHORS AND PAPERS

KEY TO AUTHORS AND PAPERS—Continued

END

DTIC

7-86